Optimizing Nickel-based Hydrocyanation Catalysts

Zur Erlangung des akademischen Grades eines

Dr.rer.nat

von der Fakultät Bio- und Chemieingenieurwesen
der Technischen Universität Dortmund

genehmigte Dissertation

vorgelegt von

M. Sc. Till Köhler

aus

Datteln

Tag der mündlichen Prüfung: 20.11.2024

1. Gutachter: Prof. Dr. Dieter Vogt

2. Gutachter: Prof. Dr. Jörg Tiller

Dortmund 2024

Danksagung

Herrn Prof. Dr. Dieter Vogt danke ich besonders für die Betreuung und Möglichkeit diese Arbeit in seinem Arbeitskreis anfertigen zu können. Herrn Prof. Dr. Jörg Tiller danke ich sehr für die Übernahme des Zweitgutachtens zu dieser Arbeit.

Darüber hinaus möchte ich Dr. Thomas Seidensticker für die inspirierenden und fruchtbaren Gedankenanstöße danken.

Dank gilt in besonderem Maße auch Bernd Rienhoff für die gute Zusammenarbeit und die praktische Unterstützung auf diesem Gebiet, vor allem über seine Masterarbeit hinaus.

Den weiteren Mitgliedern des Arbeitskreises danke ich für die überdurchschnittlich gute Arbeitsatmosphäre.

Ein besonders großer Dank geht an meine Mutter, meine Großmutter und meinen Bruder, die mich während der zurückliegenden 4 Jahre durch alle Höhen und Tiefen dieser Arbeit begleitet und großartig unterstützt haben.

Ebenfalls ganz besonders danken möchte ich Dr. Volker Wagner und posthum Robert Riemer, die meine Leidenschaft für Chemie während meiner Schulzeit stets gefördert und mich während meiner Studienzeit freundschaftlich begleitet haben.

Theo Sombek danke ich ganz besonders dafür, dass er mit seinem persönlichen großen Engagement als Chemielehrer mein besonderes Interesse für Chemie entdeckt und mich stets gefördert, wie gefordert hat. Ohne ihn hätte ich womöglich nie eine derartige Begeisterung für dieses Fach entwickelt.

Mein Dank gilt natürlich auch allen weiteren Personen, die mich darüber hinaus unterstützt haben.

Table of contents

Abstract

Nitriles are versatile and highly desired chemical intermediates for a broad range of products. Thus, their economic large-scale production requires highly efficient and selective synthesis. The nickel-catalyzed hydrocyanation of C=C double bonds provides such selective and 100% atom-economical access to nitriles. Nevertheless, the catalysts hitherto lack activity and longevity.

The catalytic activity can be increased slightly by using $AlCl_3$ as the Lewis acid, still the overall activity remains unsatisfactory. As there is no literature focused on increasing the cooperativity between the Nickel catalyst and the Lewis acid cocatalyst, first in depth studies are conducted in this thesis. It was found, that adding acetonitrile as a promotor enhances the nickel-Lewis acid cooperation, boosting activity further. Furthermore, it was found that the Lewis acid $AlCl_3$ deactivates the nickel-catalyst reducing catalyst productivity. To increase the catalysts productivity and activity further, the catalyst stability needed investigation. It was found that the extremely oxygen sensitive catalyst requires an optimized experimental procedure to exclude oxygen contamination persisting of septum usage, HCN-addition as a solution and GC-standard addition after the reaction. That way, the full catalytic potential was utilized, resulting in a TOF_{20} of more than 300,000 h^{-1}. These findings also provide a beneficial insight and help to develop a deeper understanding of current limitations caused by deactivation of the highly sensitive catalyst in nickel-catalyzed hydrocyanations.

Conclusively, this catalytic system is applied in hydrocyanation of the renewable C10 1,3-diene β-myrcene under the optimized procedure, yielding C11-nitriles with excellent selectivity not described in literature to date. It was found that three major products can be formed depending on the choice of ligand, which marks an important step towards the synthetic accessibility of mid-chain nitriles based on renewable resources.

Zusammenfassung

Nitrile sind vielseitige und sehr attraktive chemische Zwischenprodukte für eine breite Produktpalette. Ihre wirtschaftliche Herstellung im großen Maßstab erfordert daher eine hocheffiziente und selektive Synthese. Die nickel-katalysierte Hydrocyanierung von C=C-Doppelbindungen bietet einen solchen selektiven und 100% atomökonomischen Syntheseweg zu Nitrilen. Bisher mangelt es den Katalysatoren jedoch an Aktivität und Langlebigkeit.

Die katalytische Aktivität kann zwar durch die Verwendung von $AlCl_3$ als Lewis-Säure leicht erhöht werden, dennoch bleibt die Gesamtaktivität unbefriedigend. Da es keine wissenschaftliche Literatur gibt, die sich mit der Erhöhung der Kooperativität zwischen dem Nickelkatalysator und dem Lewis-Säure-Cokatalysator befasst, werden in dieser Arbeit erste Untersuchungen diesbezüglich durchgeführt. Es wurde festgestellt, dass die Zugabe von Acetonitril als Promotor die Kooperation zwischen Nickel und Lewis-Säure verstärkt und die Aktivität weiter erhöht. Darüber hinaus wurde festgestellt, dass die Lewis-Säure $AlCl_3$ den Nickel-Katalysator deaktiviert und die Produktivität des Katalysators herabsetzt. Um die Produktivität und Aktivität des Katalysators weiter zu steigern, musste die Stabilität des Katalysators untersucht werden. Es wurde festgestellt, dass der extrem sauerstoffempfindliche Katalysator ein optimiertes experimentelles Vorgehen erfordert, um Sauerstoffverunreinigungen durch die Verwendung eines Septums, HCN-Zugabe als Lösung und GC-Standardzugabe nach der Reaktion auszuschließen. Auf diese Weise konnte das volle katalytische Potenzial genutzt werden, was zu einem TOF_{20} von mehr als 300.000 h^{-1} führte.

Abschließend wird dieses katalytische System bei der Hydrocyanierung des erneuerbaren C10 1,3-Dien β-Myrcens unter dem optimierten experimentellen Vorgehen eingesetzt, wobei C11-Nitrile mit ausgezeichneter Selektivität entstehen, die in der Literatur bisher nicht beschrieben wurden. Es wurde festgestellt, dass je nach Wahl des Liganden drei Hauptprodukte gebildet werden können, was einen wichtigen Schritt in Richtung der synthetischen Zugänglichkeit von mittelkettigen Nitrilen auf Basis von erneuerbaren Ressourcen darstellt.

Physical quantities

physical quantities	***symbol***	**unit**
chemical shift	δ	ppm
coupling constant	J	Hz
energy	E	J
frequency	ω	Hz
mass	m	g
molar mass	M	$g \cdot mol^{-1}$
molecular amount	n	mol
natural biteangle	$ß_N$	°
pressure	p	bar, atm
space	A	m_2
temperature	T	°C
time	t	s
Tolmans cone angle	θ	°
Tolmans electronic Parameter	TEP	cm^{-1}
turnover frequency	TOF	h^{-1}
turnover number	TON	-
volume	V	m^3

List of abbreviations

2M3BN	2-methyl-3-butenenitrile
3PN	3-pentennitrile
Ac	acetyl
acac	acetylTMSsas
ACH	acetone cyanohydrine
ADN	adiponitrile
BiPhePhos	6,6′-[(3,3′-Di-tert-butyl-5,5′-dimethoxy-[1,1′-biphenyl]-2,2′-diyl)bis(oxy)]bis(6H-dibenzo[d,f][1,3,2]dioxaphosphepine)
bippp	binaphthyl-isopropylphenyl-diphosphite
Bu	butyl
COD	1,5-cyclooctadiene
DMSO	dimethylsulfoxide
d	doublet
DoE	design of experiments
DPEPhos	6,6′-[(3,3′-Di-*tert*-butyl-5,5′-dimethoxy-[1,1′-biphenyl]-2,2′-diyl)bis(oxy)]bis(6*H*-dibenzo[*d*,*f*][1,3,2]dioxaphosphepine)
DPPE	1,2-bis(diphenylphosphino)-ethane
DPPP	1,3-bis(diphenylphosphino)-propane
eq.	equivalents
Et	ethyl
FID	flame ionization detector

GC	gas chromatography
LUMO	lowest unoccupied molecular orbital
m	multiplett
Me	methyl
MS	mass spectrometry
NMR	nuclear magnetic resonance
Ph	phenyl
s	singlet
r.t.	room temperature (22.5±2 °C)
t	triplet
TEP	tolmans electronic parameter
Tf	triflyl
THF	tetrahydrofurane
Thixantphos	(2,8-dimethyl-4,6-phenoxathiinediyl)-bis(diphenylphosphine)
TMEDA	*N,N,N',N'*-tetramethylethylenediamine
TMS	trimethylsilyl
TOF	turnover-frequency
TON	turnover-number
Xantphos	4,5-bis(diphenylphosphino)-9,9-dimethylxanthen

1 Preface

In times of increasing scarcity of raw materials and climate change, a rethinking is taking place in industry and society. Concepts for waste avoidance are increasingly coming into focus. Catalysis as a general concept in chemistry plays a special role here, as it—especially homogeneous catalysis—can carry out reactions selectively under mild conditions. Homogeneous catalytic reactions can also be used to replace several reaction steps of classic synthesis routes with an atom-economical reaction sequence and thus avoid waste.

One example of this is the synthesis of nitriles, as they are important chemical intermediates due to their diverse follow-up chemistry. They can be converted into their corresponding amines, amides, carboxylic acids, esters, aldehydes or even ketones (Figure 1).

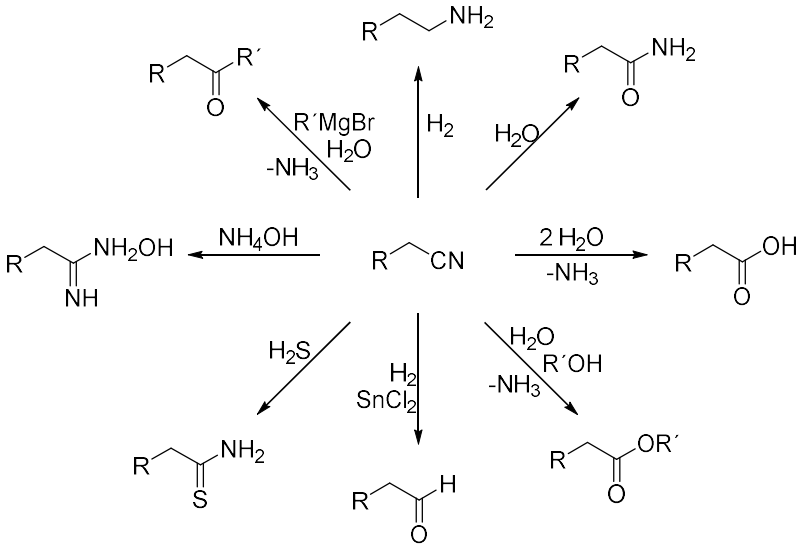

Figure 1: Follow-up chemistry of nitriles.[1]

Nitriles are traditionally accessible through KOLBE synthesis, the nucleophilic substitution of halides with metal cyanides. Unfortunately, this produces stoichiometric quantities of metal salts as waste.[2] This traditional synthetic route can be replaced by the hydrocyanation of C=C-double bonds, which is typically nickel-catalyzed. In this process, nitriles can be obtained in a 100% atom-economical manner.[3,4]

This reaction is already established on industrial scale in the production of adiponitrile, a precursor for nylon 66, since hydrocyanation of butadiene can be carried out efficiently, as the catalytic activity of the nickel complex towards 1,3-dienes and vinylarenes (activated alkenes) is high. Nevertheless, this is the only example of large-scale hydrogenation due to major drawbacks in catalytic activity in hydrocyanation of non-activated alkenes like 1-octene—these simple alkenes are unable to from η^3-complexes during the catalytic cycle making efficient catalysis difficult.

Since the nickel-catalyzed hydrocyanation offers key advantages, the production of other nitriles based on hydrocyanation of non-activated substrates is therefore highly desirable. In purely academic literature this has been investigated earlier. However, the catalyst loading is still high, and the reaction times are long, both indicating low activity leaving the challenge mostly unsolved. The catalytic activity can be increased only slightly, by adding a Lewis acid, which accelerates the reductive elimination and the HCN-addition to the nickel metal.[5] Overall, the activity remains not satisfactory, due to poor solubility of inorganic salts in organic solvents forcing oligomer formation. Therefore, application of a promotor, focused on better Lewis acid availability by de-oligomerization, appears viable.

Also, besides promotor application, the choice of a well-suited ligand is mandatory, since electronic and coordinative properties can form both catalytically active and inactive nickel complexes. Still, this catalytic activity can potentially be increased even further by optimizing the experimental procedure, that has been optimized for acetone cyanohydrin as the cyanide source and was kept for reasons of comparability even when pure HCN is applied.

Besides the needed activity increase in the hydrocyanation, a transfer to renewable resources is a step which should be taken, since 1,3-diene structures are widely represented in the nature like terpenes. For this purpose, especially monoterpenes are promising starting materials as they often feature 1,3-diene structures. Based on 1,3-dienes showing high activity in nickel-catalyzed hydrocyanations, it makes sense to use terpenes as a starting material for the production of nitriles through hydrocyanation. The renewable 1,3-diene β-myrcene is therefore almost ideal for this purpose. Surprisingly, no studies on β-myrcene hydrocyanation can be found in the scientific literature.

These challenges are the reasons why the following research gaps are to be addressed in this work in order to make this reaction applicable for a broader spectrum of substrates.

1. An enhancement in catalytic activity is a primary objective, which should be achieved by application of a more suited ligand. Additionally, promotors application for enhanced Nickel/Lewis acid-cooperativity is studied.
2. Within these studies, the experimental procedure is optimized to investigate and maximize the catalytic activity, as there is a significant knowledge gap regarding the true activity of nickel complexes in hydrocyanation in terms of TOF at low conversion.
3. To transfer the nickel-catalyzed hydrocyanation to β-myrcene as a renewable resource, detailed studies on product formation as well as catalytic activity are conducted.

If these gaps are filled, several obstacles towards a more widespread application of the nickel-catalyzed hydrocyanation are overcome, enabling process intensification and a more efficient nitrile production.

2 Theoretical Background

Within this chapter some of the most important historic as well as more recent developments are highlighted. Besides that, industrial applications are briefly discussed.

2.1 Laboratory scale nitrile synthesis

Nitriles are traditionally accessible through KOLBE synthesis, the nucleophilic substitution of halides with metal cyanides (Figure 2). In this reaction, a haloalkane is reacted with an alkali cyanide such as NaCN or KCN. As the cyanide anion is an ambivalent molecule, the nucleophilic attack can occur from both carbon and nitrogen. The attack of the carbon leads to the formation of the nitrile, whereas the attack of the nitrogen leads to the formation of the isonitrile as a by-product. The selectivity towards the desired product can be increased by using polar aprotic solvents such as dimethyl sulphoxide (DMSO). This favors an SN_2 reaction process, whereby the attack is preferably carried out by the more nucleophilic carbon.[2]

Figure 2: Laboratory scale nitrile synthesis.[2]

Unfortunately, this results in the production of stoichiometric quantities of metal salts as waste, which reduces the atom economy and leads to additional costs for the disposal of these salts. Furthermore, the haloalkane and the alkali cyanide must be produced in a preceding step. For this reason, KOLBE nitrile synthesis has so far been unattractive for the chemical industry.[2]

2.2 Industrially relevant nitrile synthesis

With a million tons produced annually, the DuPont adiponitrile (ADN **1**) technology is crucial to the industrial synthesis of adiponitrile.[6,7] This process involves three steps (Figure 3). In the first step, butadiene is converted via hydrocyanation to the linear 3-pentenenitrile (3PN **2**) and to the branched 2-methyl-3-butenenitrile (2M3BN **3**) as a byproduct. The 2M3BN **3** formed is then isomerized to 3PN **2**. In the third and final step, 3PN **2** is then converted to adipic acid dinitrile (AND **4**) by a second, Lewis acid-assisted hydrocyanation. ADN **4** is further used for the production of polymer nylon(6,6).[8]

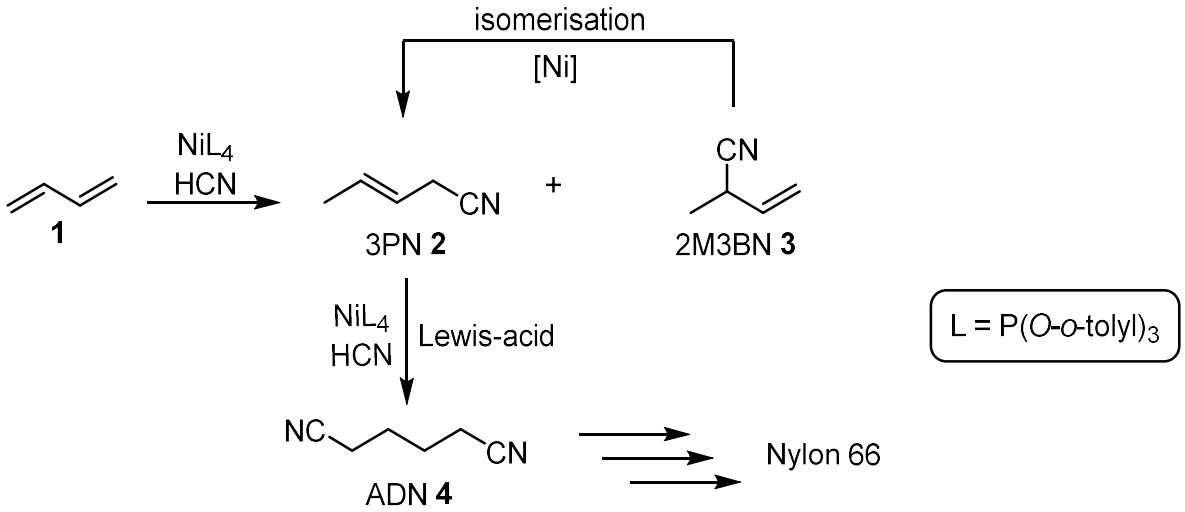

Figure 3: Reaction steps of the DuPont-ADN process.[8]

Usually P(O-*o*-tolyl)$_3$ is used as a ligand. The ligands influence on the catalyst are discussed in chapter 2.8.

2.3 Laboratory scale HCN synthesis

On a laboratory scale, HCN can be synthesized via an acid-base reaction of potassium cyanide or sodium cyanide with sulfuric acid.

$$2\ KCN + H_2SO_4 \rightarrow K_2SO_4 + 2\ HCN$$

The HCN can be obtained by condensation below its boiling point (25.7 °C).[9]

2.4 Toxicity of HCN and treatment of intoxications

Hydrogen cyanide is highly toxic and volatile. Exposure can be fatal within a few minutes.[10,11] Due to its volatility (boiling point 25.7 °C), inhalative exposure is a very significant threat.[12] HCN-concentrations in the surrounding air of 50-60 ppm are tolerable for humans for a short amount of time, without immediate or delayed effects. Life-threatening concentrations of 120-150 ppm can be fatal with an exposure time of 30 to 60 min, at 150 ppm death occurs after 30 min. With increasing concentrations of 200 ppm after 10 min death can occur. 300 ppm are instantly fatal.[13] Therefore, the Threshold limit value is 10 ppm. The oral absorption of cyanide salt solutions, for example, takes place more slowly and is inhibited, as cyanide is converted in the liver with thiosulphate to thiocyanate, which is less toxic and can be excreted.[11] Depending on the amount and route of exposure, external symptoms occur

after seconds to minutes. These include headaches, flushing, increased respiratory rate, palpitations, and dizziness. A lethal amount is followed by muscle cramps and respiratory arrest, which lead to death.[10,11] With a small amount, recovery can happen without specific treatments.[11] If the exposure or poisoning is recognized, specific treatment must be carried out. This should be done immediately as the poisoning progresses rapidly. Most of the antidotes used are usually toxic themselves and must therefore be administered in doses by an emergency doctor who has been called.

2.5 Applications of hydrogen cyanide in laboratory scale hydrocyanations and reaction procedure

Due to its high toxicity and low boiling point, hydrogen cyanide is difficult to handle. Therefore, large parts of the academic literature focuses on HCN-surrogates like TMSCN **5**/MeOH[14], acetone cyanohydrin (ACH **7**)[15–20], or zinc cyanide and water[21] to *in-situ* form hydrogen cyanide. More recent research focuses on transfer hydrocyanation, which utilizes the equilibrium, established by the nickel catalyst. The remaining low boiling alkene can be evaporated from the reaction mixture.[22–24]

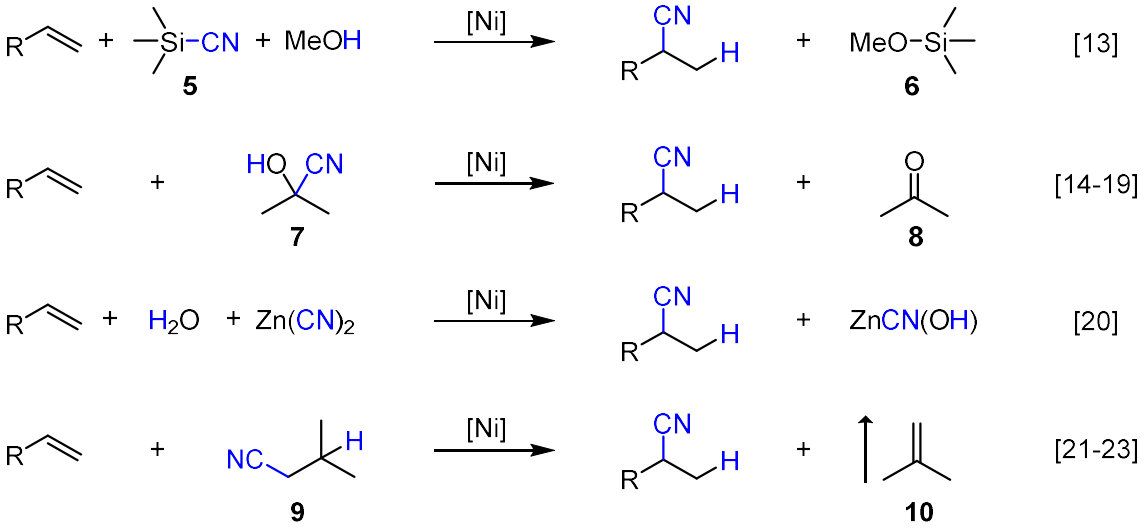

Figure 4: Cyanide sources used in hydrocyanation.[14–24]

Synthetic routes employing HCN surrogates are usually safer to be performed in the lab. Still, they are of little interest for larger scale industrial application. The formation of coupled products or byproducts severely diminishes the economic value of a process and is therefore highly undesirable. In contrast, pure hydrogen cyanide, produced via the ANDRUSSOW process or the BMA process, is readily used for large-scale hydrocyanation.[6] Unfortunately, the high toxicity of HCN requires increased safety standards, making this reasonably unattractive in

purely academic research—academic literature regarding this topic is limited. Nevertheless, addition reactions, like hydrocyanation, are most desired for large-scale processes. The absence of byproduct formation is a key desired advantage. Despite it's high toxicity, these advantages when applying pure HCN make further development in this field highly interesting.

In typical lab-scale hydrocyanation experiments first the catalyst is preformed, and all substrates are added after afterwards. Hydrogen cyanide, if used in pure form, is usually added via Eppendorf pipette, either neat or in solution.[8,25,26]

Typically Bis(1,5-cyclooctadiene)nickel(0) ($Ni(cod)_2$) is dissolved first, after which the ligand is added. [25–27] Vogt *et. al.* first dissolved the ligand. Which minimizes the potential of $Ni(cod)_2$ being deactivated over time.[14,28–31]

Hofmann *et al.* conducted studies revealing that the application of reduced catalyst concentrations, specifically 1 mol%, along with phosphonite ligands, can result in an impressive conversion rate exceeding 90% when exposed to pure hydrogen cyanide (HCN). In this study varying phosphonite ligands were applied, which yielded a maximum Turnover Number (TON) of 92 and a TOF of 61 h^{-1}. To the best of my knowledge, there is very limited data regarding the activity of nickel complexes in Hydrocyanation. These findings emphasize the need for further optimization in this particular field.[32]

In conclusion, early academic studies on hydrocyanation mainly used HCN surrogates like acetone cyanohydrin **7**, which requires elevated temperatures of 60 to 90 °C to liberate HCN. For reasons of comparability, these conditions were mostly kept in successive work, even when pure HCN was used as shown by studies by Bini. In these studies, at least 5 mol% of catalyst is required to achieve a maximum of 30% conversion of styrene **28** and 30% yield of 2-phenylpropionitril after 1 h at 90 °C.[5]

So far, there is limited research focused on optimizing the experimental methodology. To fill this gap, this work also focuses on the use of pure HCN and optimization of the reaction procedure to improve the activity of the Ni-based catalyst.

2.6 Enantioselective synthesis of fine chemical nitriles

In addition to this large-scale process in the production of AND (paragraph 2.2), it is possible to use hydrocyanation in the synthesis of fine chemicals such as pharmaceutical products or agrochemicals. These fine chemicals often require enantioselective synthesis. However, there is as yet no application in the synthesis of more complex products.[28] The lack of reliable synthesis procedures is a possible reason, but various successful enantioselective hydrocyanations have been reported in recent decades utilizing various enantiopure ligands.[14] Since there is only limited relevance of this application of hydrocyanation for this work, only some examples are shown.

First example is the hydrocyanation of 4-vinylphenol **11** (Figure 5, **A**). Using the asymmetric phosphine-phosphite ligand **15**, an enantiomeric excess of *ee* > 99% was achieved with a yield of 73%. Similarly good results were obtained with 3-vinylpyridine **78 13** with *ee* = 86% and a yield of 99% (Figure 5, **B**).[28]

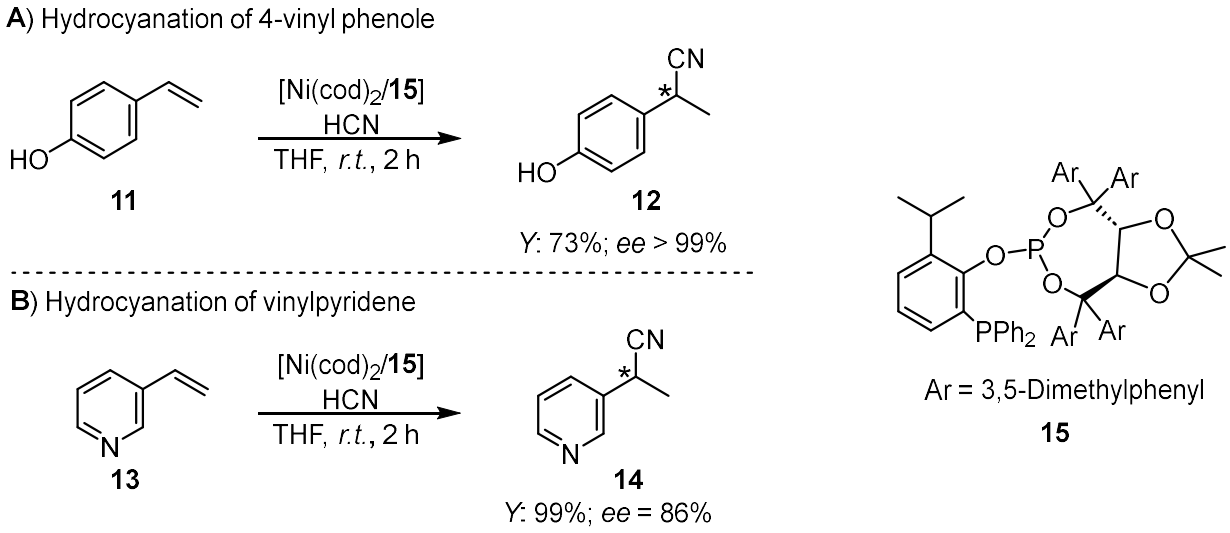

*Figure 5: Hydrocyanation of 4-vinylphenole and 3-vinylpyridine **78**. Reaction conditions: [Ni(cod)₂:L* = 1:1] 5 mol%, Addition of HCN (1.5 eq., 0.125 M in THF) within two hours.[28]*

These results are not only of academic interest but can also find technical application, which can be illustrated by the possible synthesis of the active pharmaceutical ingredient (S)-(+)-ibuprofen **18** (Figure 6). The yield in the hydrocyanation step is > 99% and the enantiomeric excess is 92%.[14]

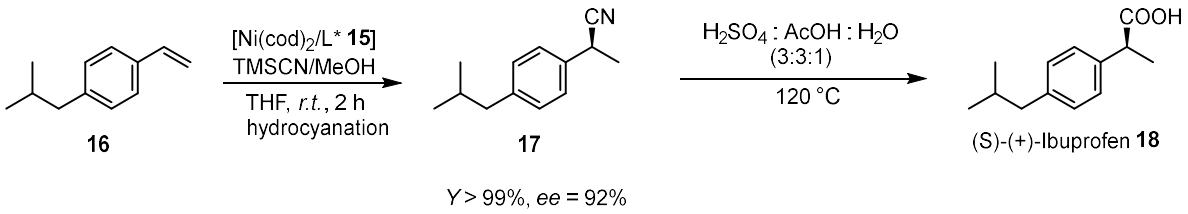

*Figure 6: Synthesis route of (S)-(+)-Ibuprofen **13** including hydrocyanation. Reaction conditions of the hydrocyanation step: [Ni(cod)$_2$:L* **15** = 1:1] 5 mol%, Addition of TMSCN **5** (1.5 eq., 0.125 M in THF over two hours.*[14]

This potential application on an industrial scale shows that already good results have been achieved, but there is still potential for improvement. Regarding the reaction shown above, this concerns the HCN source TMSCN **5**/MeOH, which is a less atom-economical reagent for HCN production. In addition, the catalyst loading of 5 mol% is comparatively high compared to other homogeneous catalytic industrial processes. If these challenges are overcome, this so far little-used reaction, can be applied more widely. For this purpose, a deeper understanding of the reaction and its process is necessary. Therefore, the mechanism, key steps and the influence of various components are discussed below.

2.7 Mechanism of the Nickel-catalyzed Hydrocyanation

Hydrocyanation is a homogeneously catalyzed reaction in which alkenes are converted into nitriles via a Ni^0/Ni^{II}-cycle. Hydrocyanation was first described in 1954 by ARTHUR *et al.* for non-functionalized alkenes. Nowadays, nickel complexes coordinated by phosphorus ligands are generally used as catalysts.[5, 15] The general mechanism of hydrocyanation for simple alkenes is shown below (Figure 7).

First, the catalytically active species **20** is formed by dissociation of a ligand from the precatalyst **19**. In the first step of the catalysis cycle, the oxidative addition of HCN to the catalytically active species II leads to the formation of the Ni(II) species **21**. The dissociation of a ligand then leads to the formation of the tetrahedral species **22**. To complex **22** an alkene substrate **23** can coordinate to the metal, thus forming complex **24**. The catalysis cycle can be closed by subsequent reductive elimination of complex **25a** or **25b** and association of a ligand. The catalyst can then enter a new cycle. During reductive elimination, the branched product **26a** (MARKOVNIKOV product) is formed starting from the species **25a** and the linear product **26b** (anti-MARKOVNIKOV product) is obtained starting from species **25b**.[2]

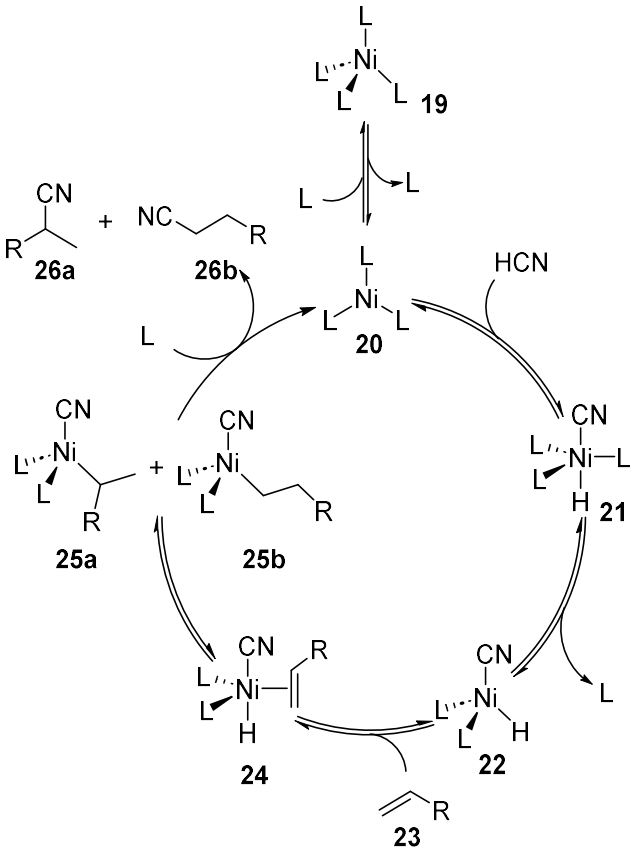

Figure 7: Catalytic cycle of a hydrocyanation of a monounsaturated alkene substrate.[2]

The rate-determining step in this catalytic cycle is the reductive elimination of the product nitrile.[2] This step can be accelerated using π-acceptor ligands like phosphites, which will be discussed in the following paragraphs.

2.8 Ligand effects on hydrocyanation

2.8.1 Monodentate ligands

To optimize hydrocyanation, these general aspects must be related to the decisive sub-steps of the catalytic mechanism. Looking at the electronic aspects, studies show that phosphite ligands, as better π-acceptor ligands, have higher activity compared to their phosphine derivatives.[1] This effect is due to the reduced electron density of the metal center, which favors dissociative and reductive elementary steps. Since the rate-determining step is the reductive elimination of the product, the overall reaction rate increases accordingly.[2,28]

Furthermore, π-acceptor ligands additionally reduce the deactivation of the catalytically active species. An increased electron density at the metal center due to strong σ donor ligands would

favor the Ni^{+II} oxidation state over the Ni^{0} oxidation state and thus promote the irreversible formation of the catalytically inactive $LNi(CN)_2$ species (Figure 9, **A**).[8]

Considering the steric properties, ligands with a larger space-filling show a higher activity in hydrocyanation. This can be illustrated by comparing P(O-*o*-tolyl)$_3$ **21** and P(O-*p*-tolyl)$_3$ **22** (Figure 8). The rate of ligand dissociation of P(O-*o*-tolyl)$_3$ **22** with a TOLMAN ligand cone angle of θ = 141° is increased by a factor of 10^8 in a Ni(P(O-*o*-tolyl)$_3$)$_4$ complex, compared to that of P(O-*p*-tolyl)$_3$ **21** (θ = 128°) in an analogous complex.[1] As a result, the catalytically active species is formed more quickly. In addition, the increased space requirement of bulky ligands generally leads to steric interactions. As a result, dissociative and reductive elementary steps are favored and thus the rate-determining step of the reaction is accelerated again.

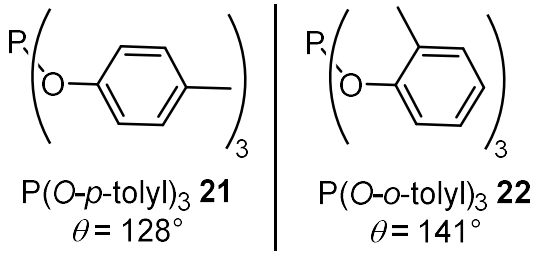

P(*O*-*p*-tolyl)$_3$ **21** θ = 128°

P(*O*-*o*-tolyl)$_3$ **22** θ = 141°

*Figure 8: Chemical structure and TOLMAN ligand cone angle of P(*O-p-*tolyl)$_3$ **21** and P(*O-o-*tolyl)$_3$ **22**.[1]*

A major disadvantage of monodentate ligands in hydrocyanation is their tendency to form catalytically inactive quadratic planar $L_2Ni(CN)_2$ species. This can be circumvented by the use of large bite angle bidentate ligands which will be discussed in the next paragraph.

2.8.2 Bidentate ligands

Catalytic activity can strongly be limited by catalyst deactivation. As described before, this is caused in particular by the irreversible formation of an $L_nNi(CN)_2$ species **24** (Figure 9, **A**). This reaction is favored by high concentrations of HCN and can be kept low in the application, for example by adding HCN in doses over time.[5,14,28]

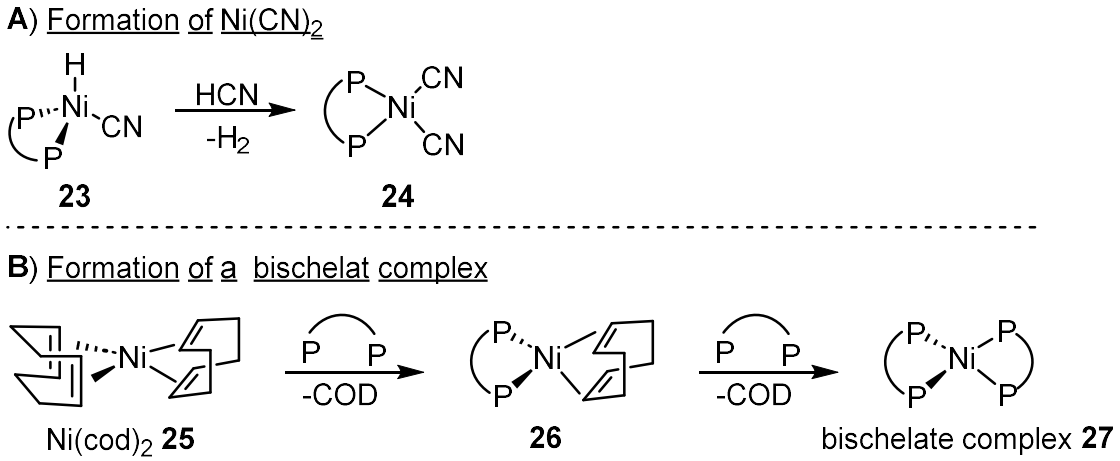

*Figure 9: Illustration of catalyst deactivation by **A**) The formation of a $Ni(CN)_2$ species **24** and **B**) The formation of a bischelate complex **27**.*[8,29]

Another way to inhibit deactivation is to use bidentate phosphorus ligands with large bite angles.[1] The complexes shown, which occur as intermediates in the catalysis cycle (Figure 7, species **21**, **22**, **24**, **25**), have a tetrahedral or trigonal bipyramidal structure. The ideal angle between the ligands is 109.4° in the tetragonal case and 120° for the equatorial positions in the trigonal bipyramidal case. In contrast, the catalytically inactive square planar structure of the $L_nNi(CN)_2$ **24** species has an optimal angle of 90°. Consequently, bidentate ligands with a bite angle of $ß_n$ > 100° stabilize the catalytically active species and the irreversible formation of the catalytically inactive $L_nNi(CN)_2$ **24** is inhibited.[25,30]

In addition, large bite angles also lead to less electron-rich metal centers, as the overlapping of the orbitals is hindered by the unfavorable geometry compared to smaller bite angle ligands. As a result, they inhibit the formation of the catalytically inactive species to a similar extent as electron-withdrawing ligands and even bidentate phosphane ligands such as bis-[(2-diphenylphosphino)-phenyl]-ether (DPEPhos **31**, $ß_n$ = 101 °) or (2,8-dimethyl-4,6-phenoxathiinediyl)bis(diphenylphosphine) (thixantphos **32**, $ß_n$ = 106 °) were able to achieve good results in hydrocyanation (Table 1, entry 3 and 4). In comparison, no catalytic activity was observed with monodentate triphenylphosphane (PPh_3) (entry 1) and when bidentate phosphane ligands with a small bite angle such as 1,2 bis(diphenylphosphine)ethane (DPPE **30**, $ß_n$ = 78 °) were used. The formation of nitriles was only detected in traces (entry 2).[31]

Table 1: Hydrocyanation of styrene applying various phosphorus ligands.[31]

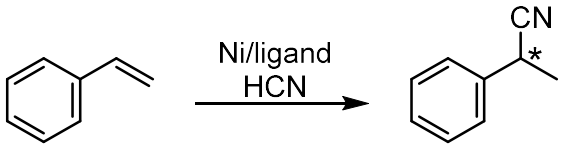

28 **29**

entry	ligand	β_n [°]	X [%]	Y [%]
1	PPh_3	-	-	-
2	Ph_2P PPh_2 DPPE **30**	78	< 1	ca. 40
3	O PPh_2 PPh_2 DPEPhos **31**	101	35 - 41	88 - 91
4	S O PPh_2 PPh_2 Thixantphos **32**	106	69 - 92	96 - 98

*Reaction conditions: Ni:ligand:styrene **28**:HCN = 1:1.2:28.5:17.5, toluene (2 mL), 60 °C, 18 h.*

Nevertheless, the high affinity of chelating π-acceptor ligands towards Ni^0 can lead to bischelate formation. Such bischelates are stable and catalytically inactive, making their formation prevention challenging (Figure 9, **B**).[33]

Most bidentate phosphane ligands form bischelate complexes in different ratios (Table 2). For the DPPE **30** ligand (entry 1), the formation of two five-membered rings in the bischelate complex is preferred over one five-membered ring in the mono-complex. This is even more pronounced for the six-membered rings of 1,3-bis(diphenylphosphine)propane **33** (DPPP, entry 2). Another factor is the flexibility of the ligand backbone. Particularly rigid ligands such as Xantphos **35** (entry 4) with a xanthene backbone favor the formation of Ni(phosphane)$_2$ **27** complexes, whereas more flexible ligands such as 2,2' bis(diphenylphosphino)biphenyl **34** (BiPheP, entry 3) or DPEPhos **31** (entry 5) show less or no formation of bischelates. One possible explanation is that more flexible ligands have a higher steric demand around the

metal center due to conformational adjustments, which energetically inhibits the association of a second ligand.[33]

Table 2: Ratio of the mono- and bis-chelate Ni complexes of various bidentate phosphine ligands.[33]

entry	ligand	ratio[a] monochelate : bischelate
1	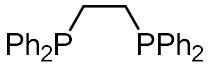 DPPE **30**	1:2
2	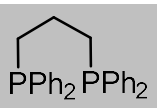 DPPP **33**	1:10
3	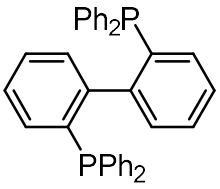 BiPheP **34**	3:1
4	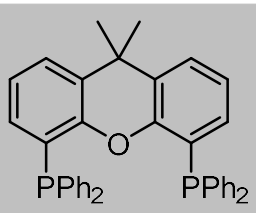 Xantphos **35**	1:8
5	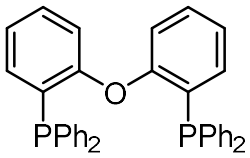 DPEPhos **31**	1:0

*a) Chelating phosphorus ligands and Ni(cod)$_2$ **25** were solved in in benzene-d^6 (0.75 mL) in a 1:1 ratio. After two hours the mixture was analyzed using ^{31}P-NMR.*

To summarize the ligand influences on hydrocyanation, a particularly catalytically active complex is formed by using phosphite ligands in comparison to phosphane ligands. This is due to their better π-acceptor property and is resulting in an accelerated reaction. In addition, bidentate ligands with bite angles of $ß_n > 100°$ are preferable to monodentate ligands, as these disfavor the irreversible formation of catalytically inactive LNi(CN)$_2$ **24** species.

Combining the mentioned characteristics large bite angles diphosphites or phosphine with strongly electron withdrawing substituents appear to be highly potent ligands for Ni-catalyzed

hydrocyanation. Typical examples are –CF_3-aryle groups, as shown by VOGT *et al.* when applying CF_3-Thixanthphos **36** in hydrocyanation of 1-octene **51** and Methyl 9-dec-1-enoate. Both selectivity and yield to the corresponding nitriles were improved.[27]

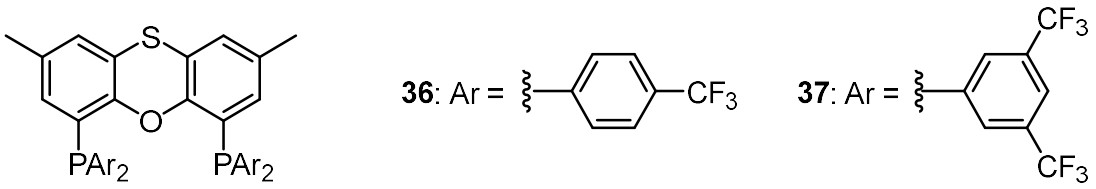

*Figure 10: Chemical structure of CF_3-Thixantphos ligands **26** and **37**.*

In styrene **28** hydrocyanation a similar ligand **37** was used, exceeding the yield achieved by the non-substituted Thixantphos **32**. (Table 2, entry 4).

Applying novel diphosphonite ligands **37** – **40** in the Ni-catalyzed hydrocyanation of styrene **28** with pure HCN, HOFMANN *et al.* were able to reduce the catalyst concentration to 1 mol%, still reaching a conversion of more than 90%.[32]

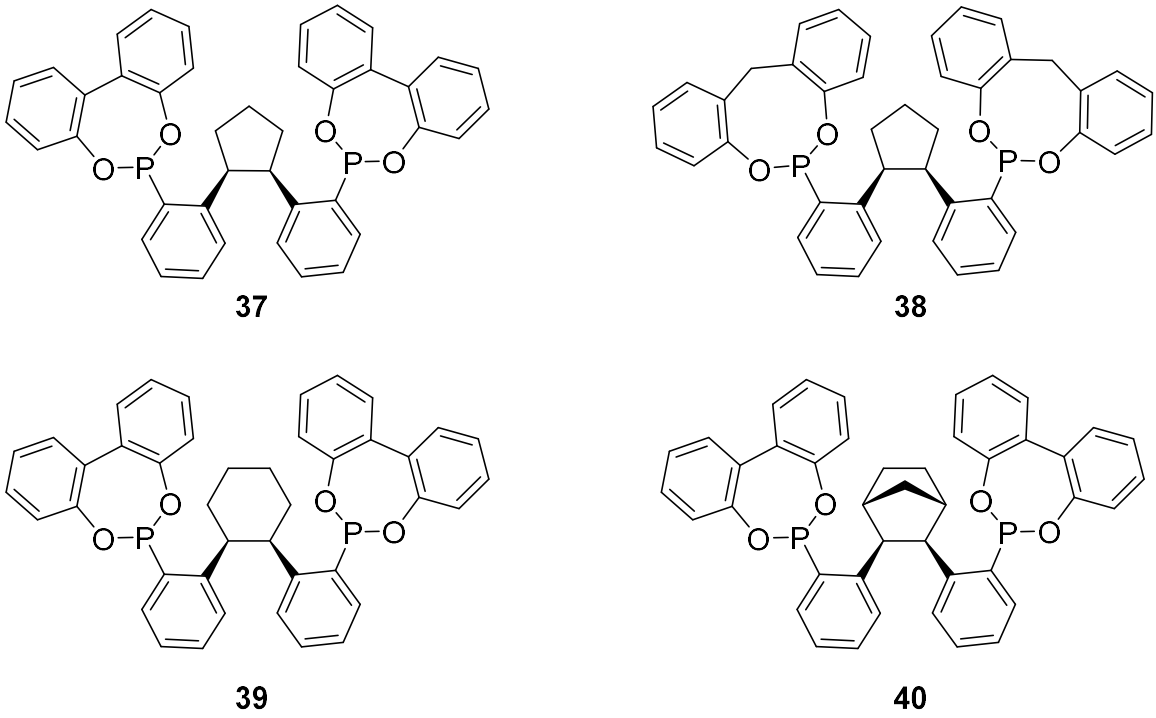

Figure 11: Ligands applied by HOFMANN et al.[32]

This translates to a maximum Turnover Number (TON) of 92. These findings emphasize the need for further optimization in this particular field.

The electron withdrawing character is even stronger in large bite angle phosphites. One of the first binol-based phosphites **41** has been applied by BAKER *et. al.* in butadiene hydrocyanation.[16]

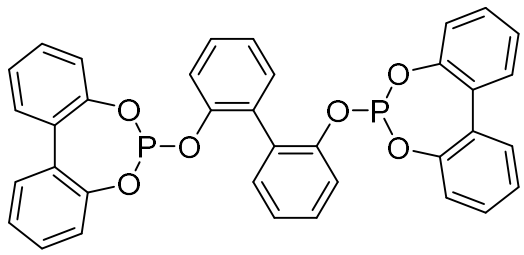

41

*Figure 12: Binol-based ligand **41** applied by BAKER et al.[16]*

One major downside here is the application of acetone cyanohydrin **7** as a cyano source making high temperatures of 180 °C and long reaction times necessary.

The more advanced Diphosphite ligand bippp **42** was published by VOGT *et.al.* requiring temperatures of only 90 °C.

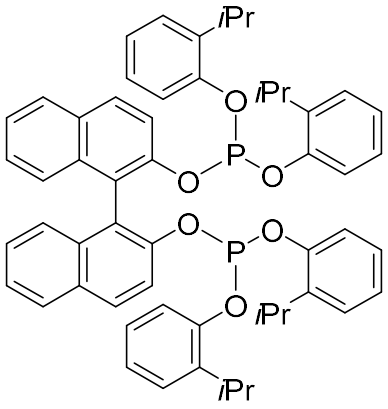

42

*Figure 13: Chemical structure of bippp **42** by Vogt et. al.[5]*

In contrast to other diphosphines used, application of bippp **42** resulted in quantitative styrene **28** conversion. Unfortunately, the reaction time remains long (19 h).[5]

Another promising Diphosphite ligand for hydrocyanation is BiPhePhos **43** (Figure 14), first described in patents by UNION CARBIDE.[34] It is extensively studied in rhodium catalyzed hydroformylation giving excellent yield, selectivity and *l:b*-ratios.[35–38]

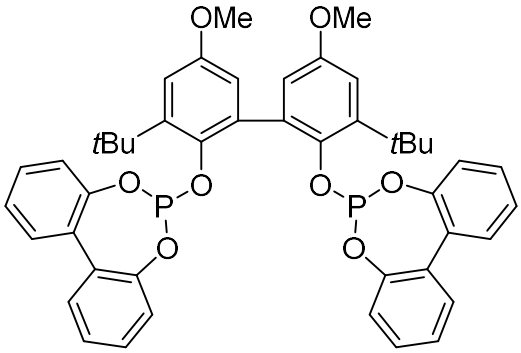

43

*Figure 14: Chemical structure of BiPhePhos **43**[34]*

Surprisingly, to the best of my knowledge, BiPhePhos **43** has rarely been studied in the field of Ni-catalyzed hydrocyanation, despite its commercial availability. Therefore, I decided to apply BiPhePhos **43**, in these studies, to further explore limitations of the hydrocyanation reaction, as it appears to be an ideal ligand for improving stability and activity of the hydrocyanation catalyst.

2.8.3 Hydrocyanation with Lewis acid cocatalyst

The influence of a Lewis acid cocatalyst is shown in the next section.

2.8.3.1 Vinylarene and Dienes

A Lewis acid cocatalyst has a strong influence on the catalytic cycle, which is discussed below in addition to the already discussed mechanism shown above (Figure 7).

To the catalyst, consisting of a metal center (nickel) and phosphorus ligands, the addition of a Lewis acid as a cocatalyst also plays a special role about the activity and selectivity of the reaction. Possible examples include $ZnCl_2$, BPh_3 and $AlCl_3$.[39,40]

These coordinate to the nitrogen atom of HCN and thus increase the acidity of the weak Brønsted acid (pk_a = 9), which leads to an acceleration of the formation of the hydridocyanide complex in the mechanism , species II) and increased stability.[39]

The additional influence on selectivity is particularly apparent in the conversion of vinyl arenes such as styrene **28** or conjugated dienes. As already described, these preferentially form the branched nitrile (MARKOVNIKOV product) in a hydrocyanation without the addition of a cocatalyst. With the addition of a suitable Lewis acid, a significant increase in yield towards the linear product (anti-MARKOVNIKOV product) can be observed.[5,8]

The underlying effect of this change in regioselectivity could be elucidated by DFT calculations for styrene **28** (Figure 15). The exclusive formation of the branched product **29b** compared to the linear product **29l** is due to the more favorable energetic position of the η^3-complex **46** compared to the σ-complex **45**, from which the branched product is irreversibly formed.[5,8]

With $AlCl_3$ as the Lewis acid used (Figure 15, right) and the resulting coordination to the HCN, all calculated states are lowered in energy. The substeps of the catalytic cycle remain unchanged and an π-complex (species **50**) or a σ-complex (species **49**) is formed again after the migratory insertion of styrene **28**. The π-complex **50** is energetically stabilized by the coordinated $AlCl_3$ to such an extent that the activation energy for product formation increases to such an extent that a quasi-stationary state is reached. This indirectly favors product formation via the σ-complex **49** and linear product **29l** (kinetic product) is formed.[5,8]

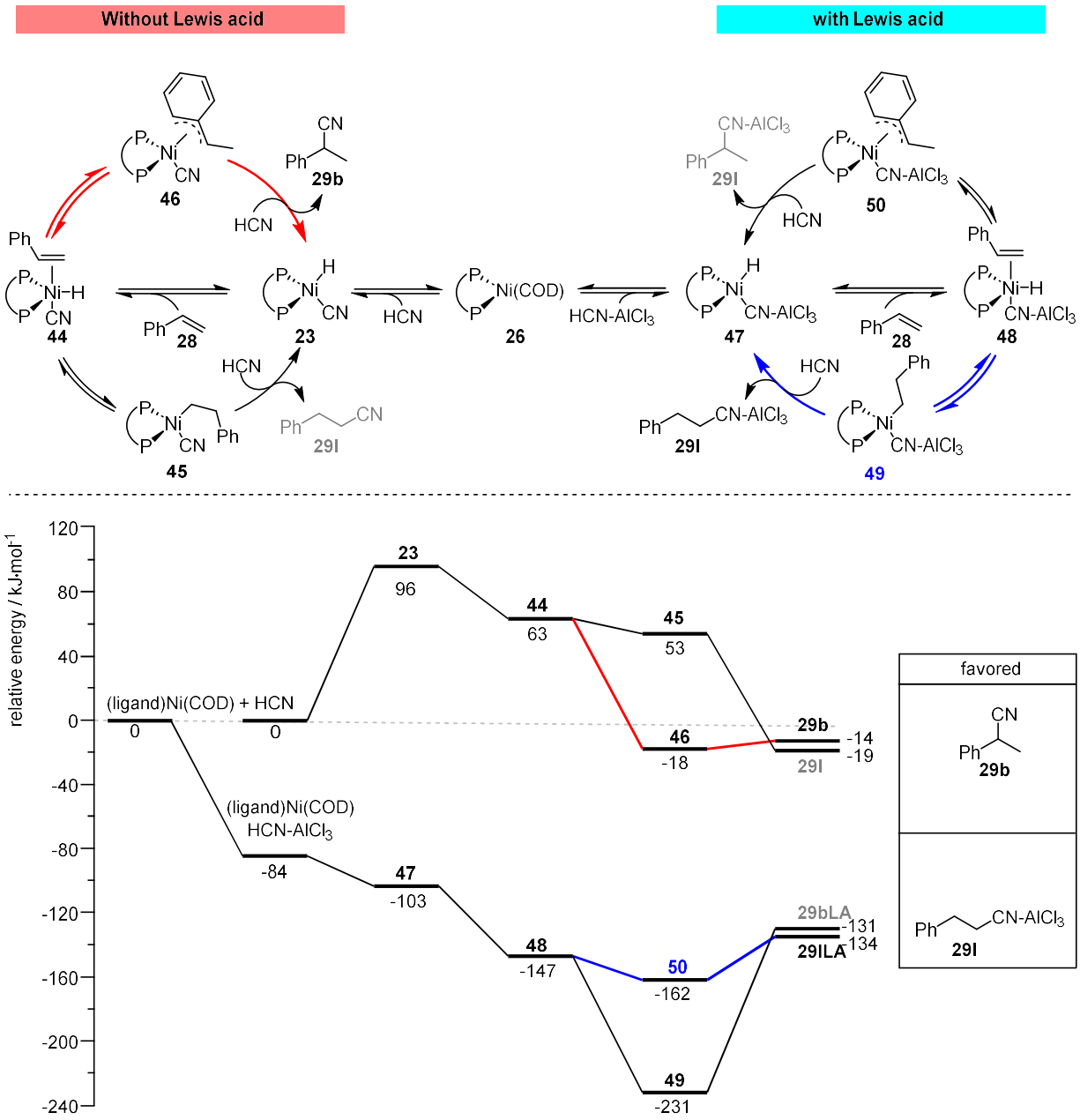

*Figure 15: Preferential formation of the branched product in styrene **28** hydrocyanation in the absence of $AlCl_3$ and preferential formation of the linear product in the presence of $AlCl_3$. Level of calculations: B3LYP, basis sets: Ni: 6-31+G(d),styrene **28**, HCN and $AlCl_3$: 6-311+G(d,p), phosphorus ligand (bippp **42**) P and O: 6-311+G(d,p), C and H atoms: Dunning/Huzinaga valence double-zeta Basis set.*[5,8]

This effect can be demonstrated by the experimental results in styrene **28** hydrocyanation with the phosphorus ligands DPEPhos **31** and Thixantphos **32** in the presence and absence of $AlCl_3$ (Table 3). Without cocatalyst, almost exclusively branched product **29b** was formed with both ligands (*l:b* = < 1:99), whereas a significant increase in linear product **29l** was observed in the presence of a Lewis acid. This is somewhat more pronounced with DPEPhos **31** (*l:b* = 23:77) compared to thixantphos **32** (*l:b* = 19:81).[5]

*Table 3: Styrene **28** hydrocyanation using DPEPhos **31** and thixantphos **32** in the presence and absence of $AlCl_3$.*[5]

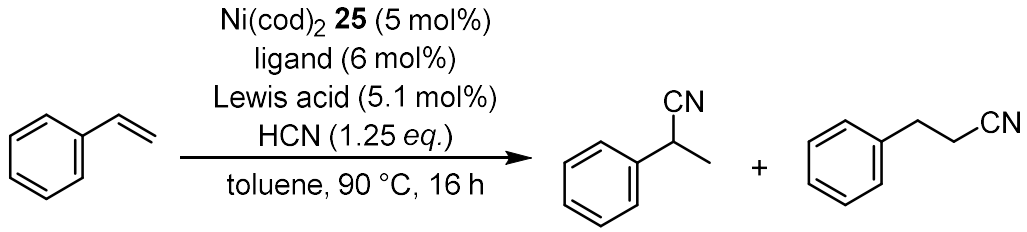

28 **29b** **29l**

entry	ligand	Lewis acid	*X* [%]	*S* [%]	*l*:*b*
1	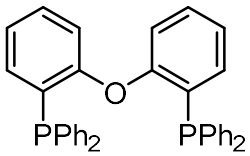 DPEPhos **31**	-	53	40	< 1:99
		$AlCl_3$	71	47	23:77
2	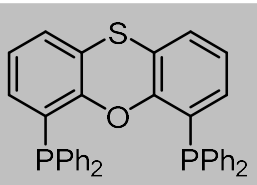 Thixantphos **32**	-	92	58	< 1:99
		$AlCl_3$	84	77	19:81

*Reaction conditions: 0.033 mmol [$Ni(cod)_2$ **25**], Ni:Lewis acid:ligand:styrene **28**:HCN = 1:1.05:1.2:20:25, toluene (1 mL), 90 °C, 16 h.*

Besides improved selectivity, the addition of a Lewis acid also increases the catalyst lifetime and turnover number (TON).[8] However, as shown by VOGT *et. al.*, using slow HCN addition technique via syringe pump, presence of a Lewis acid leads to reduced yield and selectivity (Table 4, entry 2).[5]

*Table 4: Styrene **28** hydrocyanation using slow HCN addition.[5]*

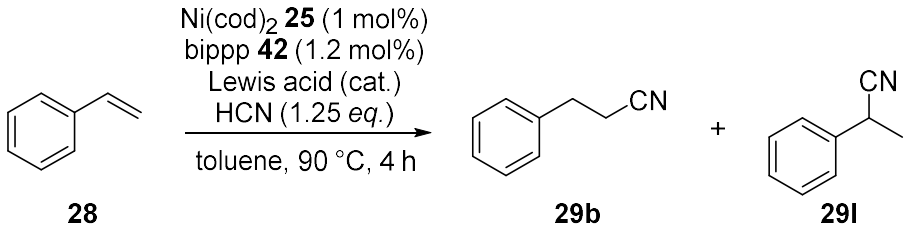

28 **29b** **29l**

entry	Lewis acid	Ni:Lewis acid	***X*** **[%]**	***Y***[a] **[%]**	***S*** **[%]**	***l*:*b***
1	-	-	99	99:0	> 99	7:93
2	$AlCl_3$	1:1.05	22	7	30	< 1:99
3	$AlCl_3$	1:20	> 99	2	2	< 1:99

*Reaction conditions: 0.00925 mmol [$Ni(cod)_2$ **25**], Ni:ligand:styrene **28**:HCN = 1:1.2:20:25, toluene (1 mL), 90 °C, 4 h. a): Yield to nitrile products.*

Increasing the Ni:Lewis acid ratio to 1:20 almost no nitrile product formation can be observed (Table 4, entry 3). The reasons for this are still unknown, as is the observation that a too high catalyst:cocatalyst ratio leads to a decreased selectivity towards the linear product.[5,40]

2.8.3.2 Monounsaturated hydrocarbons

Monounsaturated hydrocarbons also influence the regioselectivity and reaction rate,[4,8] but to the best of my knowledge, no theoretical investigation has yet been carried out as for styrene **28**.

In addition, a correlation between the steric influence of the hydrocarbon used and the *l:b*-ratio obtained by TAYLOR and SWIFT was found (Table 5).[4] Under constant reaction conditions, propene showed an *l:b*-ratio of 60:40 (entry 1), which could be increased to 95:5 (entry 2) for 1-hexene as a reactant with a longer hydrocarbon chain and to > 99:1 (entry 3) for isobutene due to branching in the chain.[4]

Table 5: Regioselectivity of hydrocyanation as a function of the monounsaturated hydrocarbon used.[4]

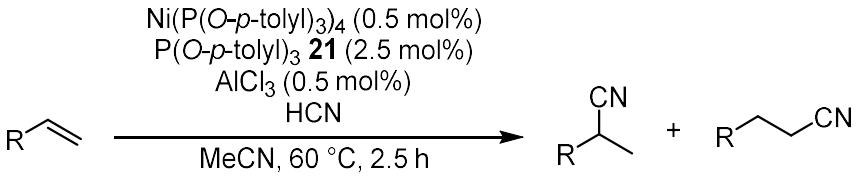

entry	unsaturated hydrocarbons	*l:b*
1	Propene	60:40
2	1-Hexene	95:5
3	Isobutene	> 99:1

*Reaction conditions: hydrocarbon (200 mmol), Ni(P(O-p-tolyl)$_3$)$_4$ (1 mmol), P(O-p-tolyl)$_3$ **21** (5 mmol), AlCl$_3$ (1 mmol), acetonitrile **79** (25 mL), 60 °C, 2.5 h. HCN was fed into the reaction mixture via an N_2 gas stream over time.*

The phosphorus ligands used also have a major influence on regioselectivity (Table 6).[27] In the hydrocyanation of 1-octene **51**, DPEPhos **31** only achieved an *l:b*-ratio of 29:71 (entry 1). A possible explanation for this poor result could be found in the flexible backbone of the ligand.

In addition to the direct hydrocyanation, the formed nickel-hydride species also cause an isomerization of the double bond along the hydrocarbon chain, which occurs much faster than the hydrocyanation.[4,8] The hydrocyanation of internal alkenes is particularly observed for ligands with a flexible backbone, since for these, conformal changes at the metal center are probably more favorable. Rigid ligands such as Thixantphos **32** (entry 2) with a xanthene backbone consequently achieve a much better *l:b*-ratio of 84:16.[27]

Both ligands show a good selectivity of 82% and 91%, respectively, but conversions of 44 and 46% are significantly reduced compared to their results for styrene **28** (Table 3).[5,27] Comparison of both reactants shows that vinylarenes are more reactive reactants, but the selectivity towards the linear product is higher with monounsaturated hydrocarbons.

*Table 6: Hydrocyanation of 1-octene **51** using different phosphorus ligands.*[27]

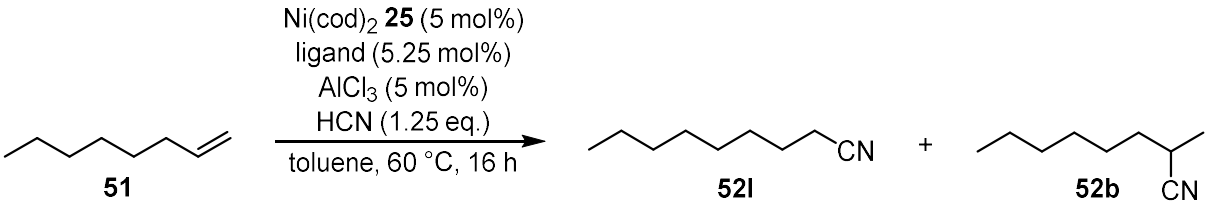

entry	ligand	*X* [%]	*S* [%]	*l:b*
1	DPEPhos **31**	44	82	29:71
2	Thixantphos **32**	46	91	84:16
3	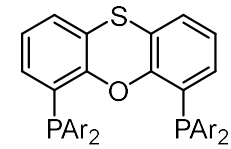 CF_3-Thixantphos **37**	53	96	n.d.
4[a]	P(*O*-*o*-tolyl)$_3$ **22**	62	82	82:18

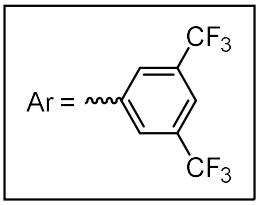

Reaction conditions: Ni:$AlCl_3$:ligand:substrate:HCN = 1:1:1.05:20:25, 60 °C, 16 h. a) ligand:Ni = 20:1.

Furthermore, a slightly increased 1-octene **51** conversion (46 to 53%) and nitrile selectivity (91 to 96%) was also achieved by modifying thixantphos to CF_3-thixantphos (Table 6, entry 3). This is due to the increased π-acceptor capabilities of the ligand due to the pronounced -I-effect of the CF_3 group. As already described in Chapter 2.8, this results in a more active catalyst complex, which yielded results comparable to the commercially used monodentate P(O-*o*-tolyl)$_3$ **22** ligand (Table 6, Entry 4). P(O-*o*-tolyl)$_3$ **22** had to be used in much greater excess to prevent catalyst deactivation.[27]

Another aspect also concerns the previously mentioned ability of the Ni catalyst to isomerize the double bond, which can not only have negative consequences for the *l:b*-ratio described above. The successful reaction of an octene **51** mixture with the phosphite ligand **53** was described, in which the internal double bonds are isomerized to the terminal position before hydrocyanation. A very good *l:b*-ratio of 94:6 was achieved with a nitrile yield of 92% (Figure 16).[19]

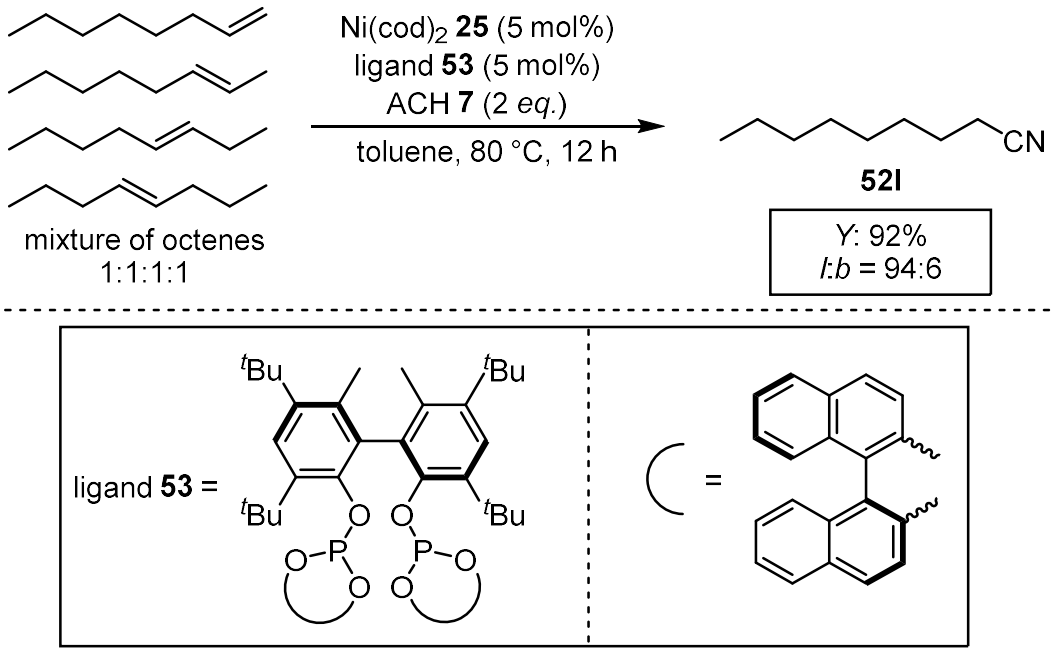

*Figure 16: Isomerizing hydrocyanation of an octene **51** mixture. Conditions: Octenes:ACH **7**:Ni(cod)$_2$ **25**:ligand **53** = 1:3:0.05:0.05, toluene (0.6 mL), 80 °C, 12 h.*[19]

2.8.4 Promotors in Lewis acid catalysis

In addition to the described application as a cocatalyst, Lewis acid catalysis itself is widely used in many organic transformations. For example, it is used in the MICHAEL addition,[41,42] in MANNICH type reactions,[43] or in DIELS-ALDER reactions.[7] The reaction step underlying all mechanisms is the coordination of the substrate to the Lewis acid. For example, nucleophilic attacks can be facilitated (MICHAEL Addition),[41,42] the energy of the lowest unoccupied molecular orbital (LUMO) can be reduced (DIELS-ALDER reaction)[7]or, as already described for the case of hydrocyanation, the coordination increases the acidity of the HCN.[39]

Furthermore, it is known that the reaction rate and also the yields can be increased by adding promoters/ligands.[41,43,44] In this regard, *N,N,N′,N′*-tetramethylethylenediamine **57** (TMEDA **57**) extensively used, and shows significantly increased yields in the MICHAEL addition of ethyl 3-oxobutanoate **54** and 3-buten-2-one **55**. This effect was particularly pronounced for M = Yb (entry 1).[41]

TMEDA **57** is also used in lithiation reactions with butyllithium reagents, for example.[45] In this case, larger, less reactive lithium aggregates are split into small, highly reactive species.[46–48]

*Table 7: Yield comparison of Lewis acid catalyzed MICHAEL addition of ethyl 3-oxobutanoate and 3-buten-2-one in the presence and absence of TMEDA **57**.*[41]

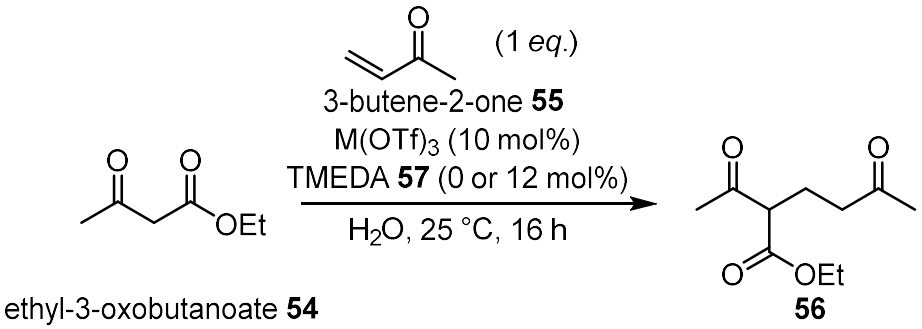

entry	M	*Y* (TMEDA 0 mol%)	*Y* (TMEDA 12 mol%)
1	Yb	12%	71%
2	Cu	10%	26%
3	Sc	12%	23%
4	La	26%	38%

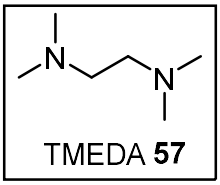

Since it is know that aluminum species form di-, tri-, tetramer, up to polymers adducts in solution,[49] it is surprising that, to the best of my knowledge, no studies regarding this approach has been conducted so far. An increase in both selectivity and catalyst activity would be likely, thus enabling usage of lower catalyst quantities and shorter reaction times.

Furthermore, with increased activity, new substrates for hydrocyanation appear interesting. In this work, the hydrocyanation conditions should be applied to renewable resources like *β*–myrcene **59**.

2.9 *β*-myrcene in homogeneous catalyzed reactions

Looking forward to more sustainable chemistry, renewable resources are of big importance. A chemically versatile compound is *β*-myrcene **59**, gained from pyrolysis of *β*-pinene **58** (Figure 17).[50]

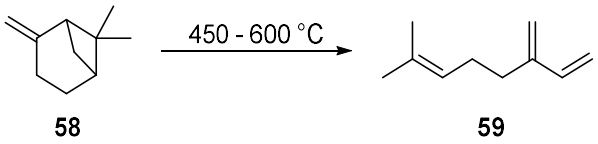

*Figure 17: Pyrolysis of β-pinene **58**.*[50]

β-Myrcene **59** can be further functionalized through various, homogeneous catalyzed reactions. These reactions can include, hydroformylation,[51] hydroalkoxylation,[52]

hydroamination,[53,54] hydroaminomethylation,[55] telomerisation,[53,56] metathesis,[57] carboxytelomerisation,[58] and methoxycarbonylation (Figure 18).[59]

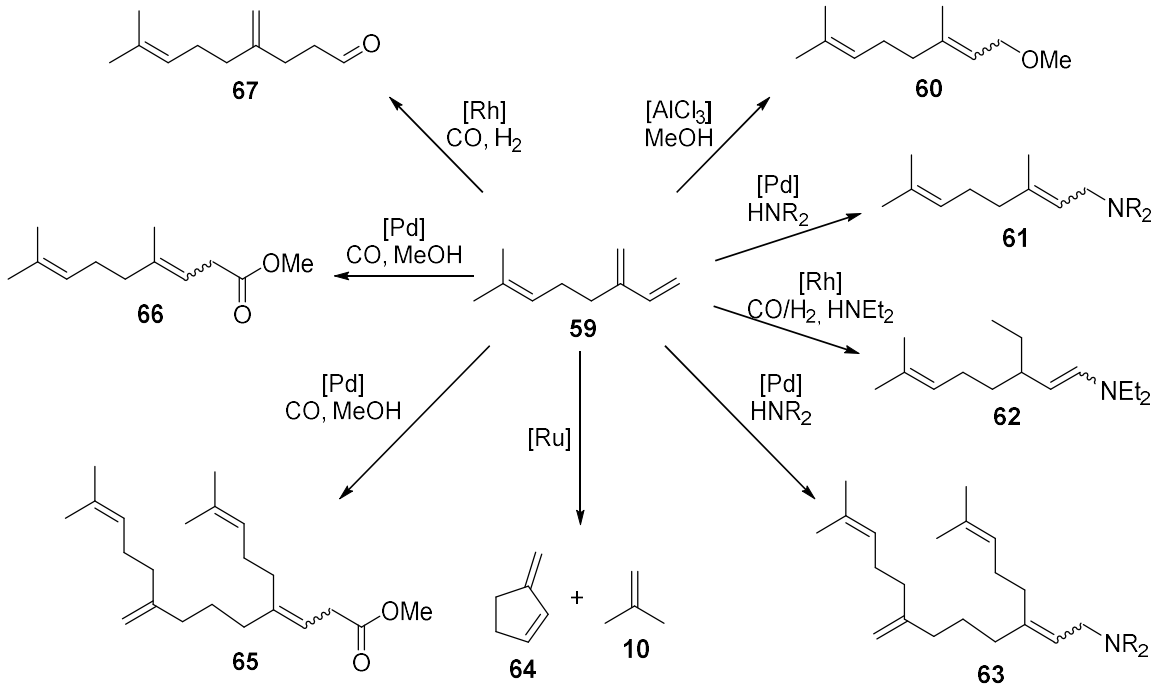

*Figure 18: Homogeneous catalyzed reactions of β-myrcene **59**.[51–59]*

To date, β-myrcene **59** has not been used in the synthesis of nitriles via hydrocyanation. Overall, β-myrcene **59** appears to be a suitable starting material for the synthesis of amins via hydrogenation of the corresponding linear nitrile. To fill this gap, the nickel-catalyzed hydrogenation of β-myrcene **59** is being investigated in this work.

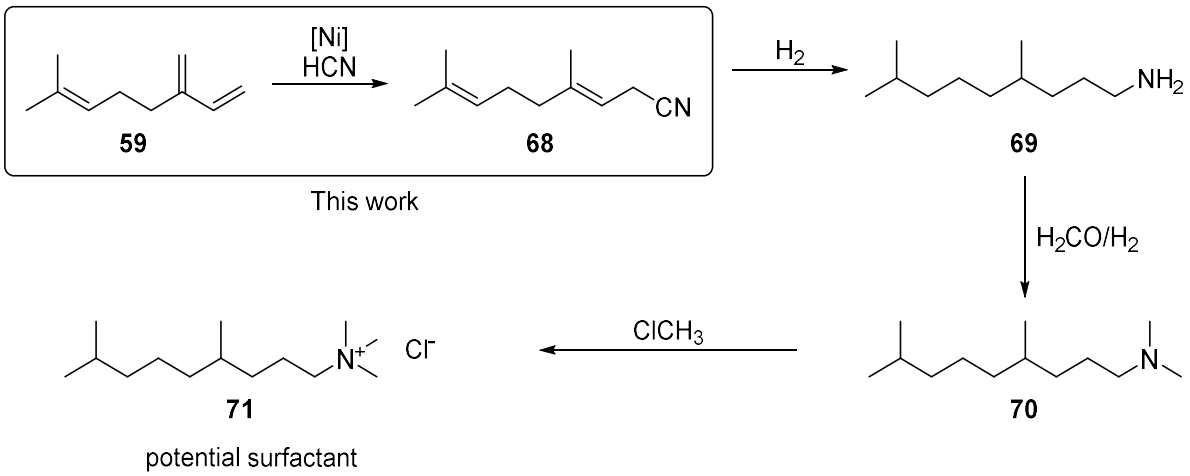

*Figure 19: C11-nitrile via hydrocyanation of β-myrcene **59** and follow-up functionalization to a quaternary amine as a surfactant.*

The amine can later be functionalized by methylation to a cationic quaternary amine, which might be interesting as a surfactant.[60]

To date, there is very limited literature discussing the hydrocyanation of substituted 1,3-dienes, which is presented below.

2.10 Hydrocyanation of other 1,3-dienes

Regarding the mechanistic investigations of the hydrocyanation of β-myrcene **59**, reference should be made to known hydrocyanations of 1,3-dienes.

1982, KEIM *et al.* published studies on the hydrocyanation of butadiene **1**, 1,3-pentadiene, and isoprene **73** using the nickel catalyst $Ni[P(OPh)_3]_4$. With an overall yield of 98%, butadiene **1** hydrocyanation predominantly yields the 1,4-adduct. In contrast, only 74% yield was obtained in 1,3-pentadiene **73** hydrocyanation. In this case, 2-methyl-3-pentenonitrile was formed exclusively, since the 1,4- and 1,2-adducts are of identical constitution.[61]

Furthermore, a yield of only 26% towards nitrile products was observed in the conversion of isoprene **73** to 3-methyl-3-pentenenenitrile **74** and 2,3-dimethyl-3-butenenitrile **75**. This indicates a steric hindrance of the methyl group, suggesting an allyl mechanism.[61]

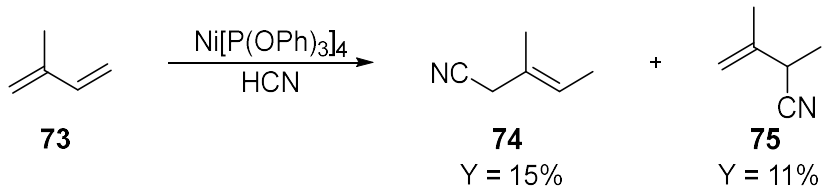

*Figure 20: Isoprene **73** hydrocyanation*[62]

Due to the strong structural similarity of isoprene and β-myrcene **59**, this hindrance is expected to be even stronger in β–myrcene **59**, making studies on activity even more significant.

3 Results and discussion

3.1 Chapter I: Influence of Promoters

In this chapter, the effects of promoters on the nickel/Lewis acid synergy are investigated regarding its impact on regioselectivity and catalytic activity.

3.1.1 General aspects and research gap

In typical organic synthesis focused literature, often times diphosphines are used because of their broad commercial availability and good chemical stability against various chemical functionalities. Unfortunately, these typically do not enable high activity hydrocyanation of more simple hydrocarbons like the activated styrene **28** and the non-activated 1-octene **51**, which are of interest in large scale industrial processes.

Since the rate determining step is the reductive elimination of the nitrile product (section 2.7), an electron withdrawing large bite angle ligand can accelerate the reductive elimination, thus accelerating the overall reaction rate. Furthermore, catalyst deactivation is disfavored by these characteristics as well (section 2.8). To achieve a high catalytic activity, application of a better suited ligand is promising. BiPhePhos **43**, as being a wide bite angle (123 °)[63] π-acceptor ligand, appears almost ideal for this purpose and its performance regarding substrate conversion, nitrile yield and catalytic activity is expected to exceed the well-known diphosphine ligands Xantphos **35** and DPEPhos **31**. Fortunately, BiPhePhos **43** is commercially available and is therefore applied within these studies.

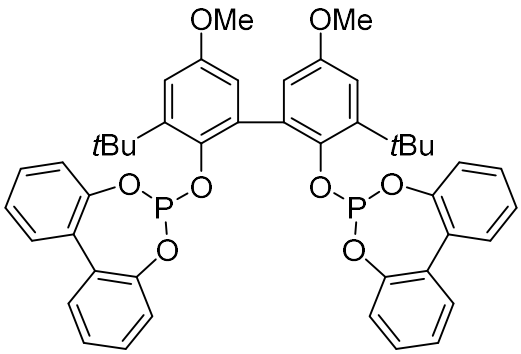

43

*Figure 21: Chemical structure of BiPhePhos **43**[34]*

Besides the use of an ideal ligand, the catalytic activity can be increased only slightly by Lewis acid addition, which accelerates the reductive elimination and the HCN-addition to the nickel metal[5]. Still, the activity remains not satisfactory. Due to poor solubility of inorganic salts in organic solvents, the Lewis acid forms oligomers, decreasing its chemical availability. As mentioned above (section 2.8.4), generally TMEDA **57** can be used in Lewis acid catalysis, which significantly increases the yields achieved.[7,42,43,64] Consequently, application of a promotor, focused on better Lewis acid availability by de-oligomerization in Lewis acid co-catalyzed hydrocyanations, appears feasible.

Furthermore, the Lewis acid favors the formation of the linear 1-phenylpropionitrile **29l** over the 2-phenylpropionitrile **29b**. An increased cooperativity between nickel and the Lewis acid is expected to result in increased *l:b*-ratios in styrene **28** hydrocyanation, which can be of particular interest in large scale processes. To date, the addition of TMEDA **57** or other cooperativity-enhancing components has not been reported in the field of hydrocyanation and is therefore investigated in the present work. If the catalytic activity can be increased by promotors, a huge step in process intensification in ADN-production is possible, as this method can be applied easily in the last Lewis acid assisted step of the process.

However, an in-depth analysis of the exact interaction between the Lewis acid and the promotors is not part of this work. As the focus of this work is increasing *l:b*-ratios and catalytic activity, candidates for promoters are to be tested and their influence on activity and selectivity evaluated.

3.1.2 Reaction setup and reaction system validation

At first, the experimental setup and operational procedure is discussed. For reasons of comparability, the experimental procedure is taken from literature, where it was developed for the nickel-catalyzed hydrocyanation using bidentate phosphine ligands. The reaction temperature is set to 90 °C and the reaction time to 19 h accordingly.[8,27] To ensure comparability of the results, the batch size is increased to 1 mmol of alkene substrate. Furthermore, by using a stock solution for setting up multiple reactions is advantageous, as the balancing error is reduced. Often times, a white suspension was formed in the otherwise colorless clear stock solution during catalyst preforming, the solvent amount had to be increased accordingly to ensure a complete catalyst dissolution. That way a precise catalyst concentration within the stock solution is ensured, which is mandatory for distributing the catalyst-solution to individual preparations. This assumption is supported by an NMR analysis of the white solid, that revealed that the catalytically active species BiPhePhosNi(cod) **26** precipitated (Figure 22).[65]

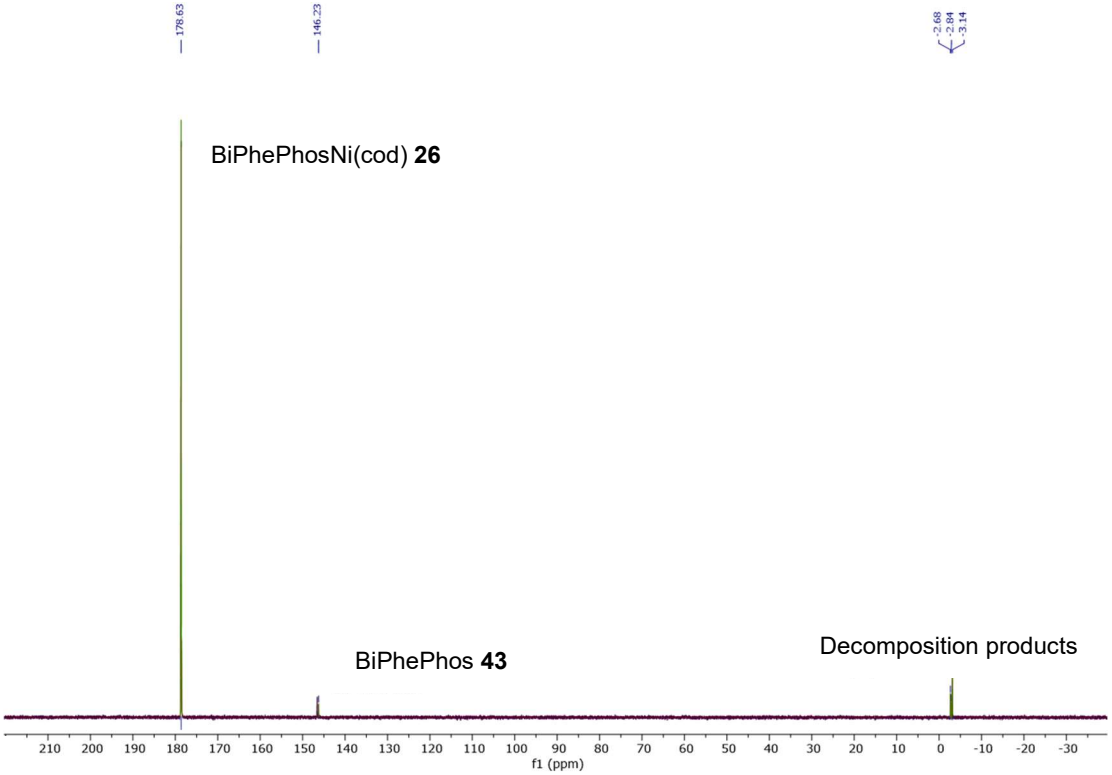

*Figure 22: $^{31}P\{^{1}H\}$-NMR (162 MHz, C_6D_6) of the white solid during catalyst preforming. (Decomposition products only formed after the sample had been in the NMR tube for two days). Reaction conditions: $Ni(cod)_2$ **25** (13.8 mg, 0.05 mmol, 1 eq.), BiPhePhos **43** (56.8 mg, 0.06 mmol, 1.2 eq.), toluene (2.5 mL), 1 h.*

Furthermore, HCN is added in its pure form at -50 °C in compliance with the safety measures (section 5.2). To start the reaction, the flask was placed in a pre-warmed oil bath heated to reaction temperature.

3.1.3 Nickel-BiPhePhos in styrene hydrocyanation

As Lewis acids have a strong effect on the *l:b*-ratio in styrene **28** hydrocyanation, the influence of promoters on the *l:b*-ratio should be stronger and thus easier to determine. Consequently, the initial focus is on styrene **28** as the model substrate. In order to increase the selectivity towards the linear product, in this section, studies on different Lewis acids and the influence of varying promotors are conducted. Later on, the influence of promotors Lewis acids and the use of promoters on the catalytic activity is investigated. Furthermore, as mentioned above, BiPhePhos **43** is applied in this studies, as it provides almost ideal characteristics for catalyzing the reaction effectively (section 3.1.1).

3.1.3.1 Styrene hydrocyanation without a Lewis acid

First, for validation of the experimental procedure, styrene **28** is hydrocyanated without Lewis acid using Xantphos **35**, and DPEPhos **31**. Based on the selected conditions, only the formation of the branched 2-phenylpropionitrile **29b** is expected. Furthermore, BiPhePhos **43** is first used in nickel-catalyzed hydrocyanation. Due to its large bite angle and strong electronic π-acceptance, using BiPhePhos **43** should result in increased conversion and yields (Table 8).

*Table 8: Styrene **28** hydrocyanation without Lewis acid using Xantphos **35**, DPEPhos **31**, and BiPhePhos **43**.*

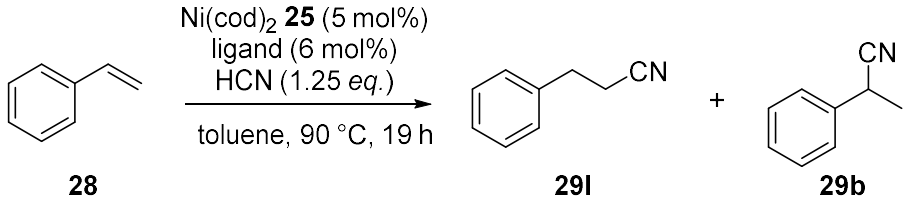

28 **29l** **29b**

entry	ligand	*X*[a)] [%]	*Y*[a), b)] [%]	*S*[c)] [%]	*l:b*[d)]
1[e)]	Xantphos **35**	71	71	> 99	< 1:99
2[f),5]	Xantphos **35**	74	63	85	< 1:99
3[e)]	DPEPhos **31**	54	26	49	< 6:93
4[f),5]	DPEPhos **31**	53	21	40	< 1:99
5[e)]	BiPhePhos **43**	> 99	> 99	> 99	< 1:99
6[f),5]	bippp **42**	> 99	86	86	9:91

*a): Based on GC analysis with n-decane as internal standard. b): Yield of nitrile products. c): Selectivity to nitrile products. d): ratio linear (**29l**) to branched (**29b**) nitrile product. e): Reaction conditions: Ni(cod)$_2$ **25** (13.8 mg, 0.05 mmol, 0.05 eq.) was dissolved in toluene (3 mL), and ligand (0.06 mmol, 0.06 eq.) was added. n-decane was added as an internal standard before the addition of styrene **28** (104 mg, 1 mmol, 1 eq.). The reaction mixture was cooled down (-50 °C), and HCN (50 µL, 1.25 mmol, 1.25 eq.) was added. The reaction mixture was then heated to 90 °C for 19 h. f): 0.033 mmol [Ni(cod)$_2$ **25**], Ni:ligand:styrene **28**:HCN = 1:1.2:20:25, 90 °C, 16 h, toluene (1 mL).*[5]

Using Xantphos **35** as a ligand (entry 1), literature results (entry 2) are exceeded, achieving an excellent selectivity of > 99% and yielding 71% of the nitrile product. As expected, the *l:b*-ratio is < 1:99 in absence of a Lewis acid. Applying DPEPhos **31** (entry 3), literature results (entry 4) were also exceeded, indicating a sound operational procedure enabling the first-ever application of BiPhePhos **43**. Interestingly, DPEPhos **31** shows a slight tendency towards forming the linear product **29l**. Nevertheless, the BiPhePhos **43** ligand (entry 5) outperforms the two phosphine ligands and achieves quantitative styrene **28** conversion to the nitrile products, indicating a very selective catalyst. The structural more rigid BiPhePhos **43** also outperforms the otherwise potent ligand bippp **42**, described by VOGT *et. al.* (entry 6).

After the successful hydrocyanation of styrene **28** in absence of a Lewis acid, the influence of various Lewis's acids and promotors are evaluated within the next section.

3.1.3.2 Styrene hydrocyanation in presence of Lewis acids

Within the following chapter, further ongoing investigations include a Lewis acid-cocatalyst to enable the formation of the linear 3-phenylpropionitrile **29l** (section 2.8.3.1). For that purpose, $AlCl_3$ is selected, as literature data is available for comparison even in combination with the two phosphine ligands DPEPhos **31** and Xantphos **35**.[5] First, no promotors are applied in the reaction mixture to obtain a benchmark result. Later in this subchapter, various promoters are added to determine the effects of promotors on the cooperativity between the nickel center and the Lewis acid.

3.1.3.2.1 Styrene hydrocyanation with $AlCl_3$ as the Lewis acid without promotors

First, the expected performance gains from using BiPhePhos **43** in presence of $AlCl_3$ are compared to the diphosphines Xantphos **35** and DPEPhos **31** in styrene **28** hydrocyanation (Table 9).

*Table 9: Styrene **28** hydrocyanation of styrene **28** with $AlCl_3$ as Lewis acid and using Xantphos **35**, DPEPhos **31**, and BiPhePhos **43** as ligands.*

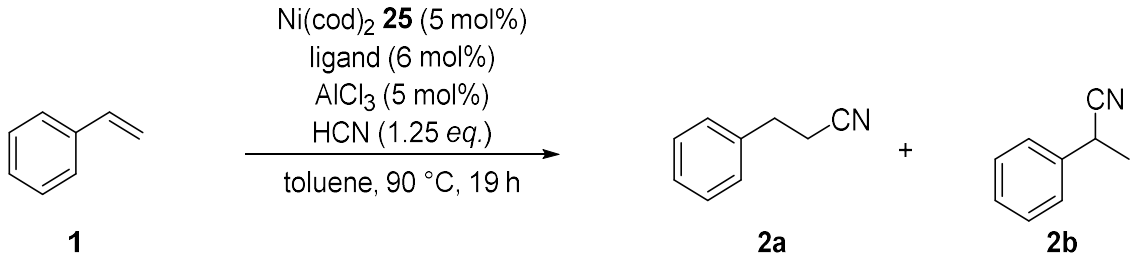

1 **2a** **2b**

entry	ligand	*X*[a)] [%]	*Y*[a), b)] [%]	*S*[c)] [%]	*l:b*[d)]
1[e)]	Xantphos **35**	40	40	> 99	9:91
2[f),5]	Xantphos **35**	97	62	64	6:94
3[e)]	DPEPhos **31**	39	39	> 99	46:54
4[f),5]	DPEPhos **31**	71	33	47	23:77
5[e)]	BiPhePhos **43**	> 99	98	98	66:34
6[f)5]	bippp **42**	> 99	51	51	74:26

*a): Based on GC analysis with n-decane as internal standard. b): Yield of nitrile products. c): Selectivity to nitrile products. d): ratio linear (**29l**) to branched (**29b**) nitrile product. e): Reaction conditions:*

*$Ni(cod)_2$ **25** (13.8 mg, 0.05 mmol, 0.05 eq.) was dissolved in toluene (3 mL). Ligand (0.06 mmol, 0.06 eq.) and $AlCl_3$ (6.7 mg, 0.05 mmol, 0.05 eq.) were added. n-decane was added as an internal standard before the addition of styrene **28** (104 mg, 1 mmol, 1 eq.). The reaction mixture was cooled down (-50 °C), and HCN (50 µL, 1.25 mmol, 1.25 eq.) was added. The reaction mixture was then heated to 90 °C for 19 h. f): 0.033 mmol [$Ni(cod)_2$ **25**], Ni:ligand:styrene **28**:HCN = 1:1.2:20:25, 90 °C, 16 h, toluene (1 mL).*[5]

Applying Xantphos **35** (Table 9, entry 1) resulted in a 40% conversion, which is significantly reduced compared to literature data (entry 2). However, since the reactions carried out within these studies shows excellent selectivity, the decrease in yield by 22% is not investigated further. The almost quantitative conversion and the reduced selectivity of 64% in the literature suggest styrene **28** polymerization. As anticipated, the *l:b*-ratio, is comparable.

A similar behavior can be observed with DPEPhos **31** (entry 3). The yield towards nitrile products was increased by 6% to 39% compared to literature (entry 4) while maintaining 39% conversion, resulting in excellent selectivity of > 99%. This indicates that styrene **28** polymerization does not occur within the here presented studies. In addition, the *l:b*-ratio is increased in favor of the linear product **29l** to 46:54. DPEPhos **31** already showed a more pronounced selectivity to the linear product without Lewis acid, which is further enhanced by adding a Lewis acid.

Best results are achievable when BiPhePhos **43** is applied (entry 5). The yield of nitrile product was again almost quantitative, and a suitable *l:b*-ratio of 66:34 was achieved. As expected, this is a significant increase compared to reactions in absence of a Lewis acid (*l:b* = < 1:99). When BiPhePhos **43** is used as a ligand, $AlCl_3$ as a Lewis acid enhances the selectivity towards the linear product **29l** significantly more than in combination with phosphines.

The *l:b*-ratio is somewhat lower than that of the bippp **42** ligand used in the literature (74:26), which can be attributed to the increased rigidity giving less space for conformational changes in transition states. When using bippp **42** on the other hand, the total yield of nitriles is significantly reduced to 51% indicating early catalyst deactivation followed by temperature-induced styrene **28** polymerization.

In order to find an ideal combination of BiPhePhos **43** and Lewis acid, further Lewis acids should be applied in the styrene **28** hydrocyanation under the set conditions.

3.1.3.2.2 $ZnCl_2$, $La(OTf)_3$, and BPh_3 in styrene hydrocyanation

In literature, $ZnCl_2$ and BPh_3 are frequently used as alternatives to $AlCl_3$ in hydrocyanation. As shown in the literature, these generally exhibit lesser selectivity towards the linear product **29l**.[5] However, their influence on the BiPhePhos **43** system remains unknown and is therefore

investigated in these studies. Furthermore, the use of $La(OTf)_3$ is a Lewis acid not been reported in literature on hydrocyanation. Therefore, the results will be of great interest, especially since positive effects of TMEDA **57** application, a possible promoter, have already been observed for $La(OTf)_3$ in Lewis acid catalysis.[41]

*Table 10: Styrene **28** hydrocyanation using BiPhePhos **43** with different Lewis-acids and solvents.*

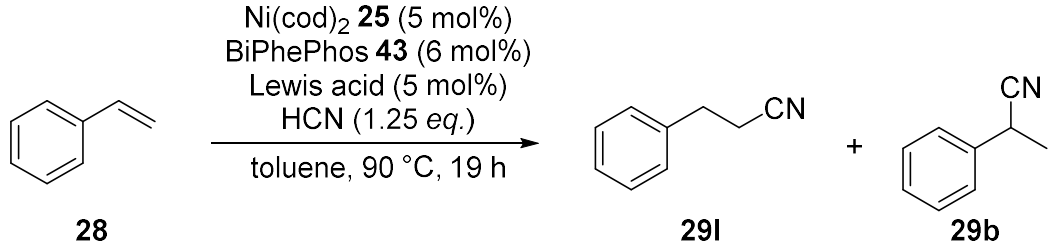

28 **29l** **29b**

entry	Lewis acid	***X*** [a] [%]	***Y*** [a), b)] [%]	***S*** [c)] [%]	***l:b*** [d)]
1	$ZnCl_2$	> 99	> 99	> 99	5:95
2[e)]	$ZnCl_2$	> 99	85	85	15:85
3[e)]	$AlCl_3$	40	31	78	52:48
4	$La(OTf)_3$	> 99	96	96	1:99
5	BPh_3	> 99	91	91	10:90

*Reaction conditions: $Ni(cod)_2$ **25** (13.8 mg, 0.05 mmol, 0.05 eq.) was dissolved in toluene (3 mL). BiPhePhos **43** (47.4 mg, 0.06 mmol, 0.06 eq.) and Lewis acid (0.05 mmol, 0.05 eq.) were added. n-decane was added as an internal standard before the addition of styrene **28** (104 mg, 1 mmol, 1 eq.). The reaction mixture was cooled down (-50 °C), and HCN (50 µL, 1.25 mmol, 1.25 eq.) was added. The reaction mixture was then heated to 90 °C for 19 h. a): Based on GC analysis with n-decane as internal standard. b): Yield of nitrile products. c): Selectivity to nitrile products. d): ratio linear (**29l**) to branched (**29b**) nitrile product. e): THF as solvent.*

In the reactions, $ZnCl_2$ showed a quantitative yield of nitrile products (Table 10, entry 1). The *l:b*-ratio of only 5:95 is significantly worse than the 66:34 previously achieved with $AlCl_3$, indicating that the $ZnCl_2$ did not participate in the reaction mechanism. This might be due to poor $ZnCl_2$ solubility which was still noticeable after prolonged stirring.

Therefore, a change of solvent from toluene to THF was carried out. That way, when using $ZnCl_2$, a slightly reduced yield to 85% (entry 2) can be observed. On the contrary, the *l:b*-ratio could be slightly increased to 15:85. Therefore the molecular availability was increased by better $ZnCl_2$ solubility.

The solvent change for $AlCl_3$ was also carried out as a comparative value (entry 3). Surprisingly, the opposite behavior was observed here as a very strong white suspension was formed. Conversion and yield dropped significantly to 40% and 31% respectively, compared to the results in toluene (Table 9, entry 5). The *l:b*-ratio of 52:48 is also significantly reduced and therefore THF was excluded as a solvent and toluene was retained for the following reactions.

$La(OTf)_3$ (entry 4) showed the same behavior as $ZnCl_2$ in toluene, due to the low solubility in toluene. An attempt to dissolve $La(OTf)_3$ in THF failed and was therefore not used in further investigations.

BPh_3 as the last Lewis acid did not exhibit this solubility problem but only achieved an *l:b*-ratio of 10:90 and a yield of 91% making further use of BPh_3 not reasonable.

All Lewis acids used thus showed high conversions with good to excellent selectivities to nitrile products. However, obtaining the linear product **29l** in an excess ratio of about 2:1 is only possible with $AlCl_3$ as the Lewis acid. For $ZnCl_2$ and $La(OTf)_3$ the key shortcoming is the lower solubility in toluene. $AlCl_3$ was therefore selected as the Lewis acid for investigating the influence of possible promoters, to push the selectivity the linear product even further.

As the benchmark results are presented in this section, the influence of promotors can be investigated.

3.1.3.3 Influence of promotors on selectivity

Due to the low solubility of $AlCl_3$ in toluene, $AlCl_3$-oligomer formation can be suspected. That way, the chemical availability is reduced, resulting in more branched product **29b** being formed. To increase the chemical availability, theses oligomer chains need to be deaggregated, by a promotor. These are aimed to act as a ligand specifically for the Lewis acid resulting in $AlCl_3$-oligomer deaggregation. This concept has already been used in Lewis acid catalysis (2.8.4).[45] In case of the nickel-catalyzed hydrocyanation, using a promotor is expected to result in higher *l:b*-ratios with is investigated next. Thus, as TMEDA **57** enabled better Lewis acid availability, it appears to be a promising candidate as a promoter in hydrocyanation. A 1:1 ratio $AlCl_3$:TEMDA **57** is chosen within the following reaction.

*Table 11: Styrene **28** hydrocyanation using $AlCl_3$ as Lewis acid and TMEDA **57** as promoter.*

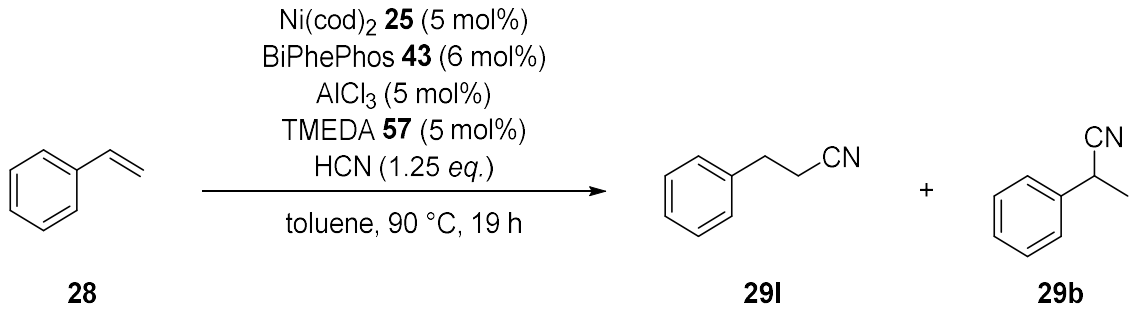

28 **29l** **29b**

entry	HCN Source	*X*[a)] [%]	*Y*[a), b)] [%]	*S*[c)] [%]	*l:b*[d)]
1[e)]	HCN	6	< 1	12	> 1:99[e]

*a): Based on GC analysis with n-decane as internal standard. b): Yield of nitrile products. c): Selectivity to nitrile products. d): ratio linear (**29l**) to branched (**29b**) nitrile product. e): Reaction conditions: $Ni(cod)_2$ **25** (13.8 mg, 0.05 mmol, 0.05 eq.) was dissolved in toluene (3 mL). BiPhePhos **43** (47.4 mg, 0.06 mmol, 0.06 eq.), $AlCl_3$ (6.7 mg, 0.05 mmol, 0.05 eq.), and TMEDA **57** (5.8 mg, 0.05 mmol, 0.05 eq.) were added. n-decane was added as an internal standard before the addition of styrene **28** (104 mg, 1 mmol, 1 eq.). The reaction mixture was cooled down (-50 °C), and HCN (50 µL, 1.25 mmol, 1.25 eq.) was added. The reaction mixture was then heated to 90 °C for 19 h.*

Unfortunately, only traces of nitrile product can be observed. (Table 11). It can be suspected that TMEDA **57** not only coordinates to the Lewis acid but also distorts the reaction mechanism. Therefore, TMEDA **57** is applied in various concentrations to the styrene **28** hydrocyanation in the absence of $AlCl_3$ (Table 12).

*Table 12: Styrene **28** hydrocyanation without Lewis acid with different TMEDA **57** concentrations*

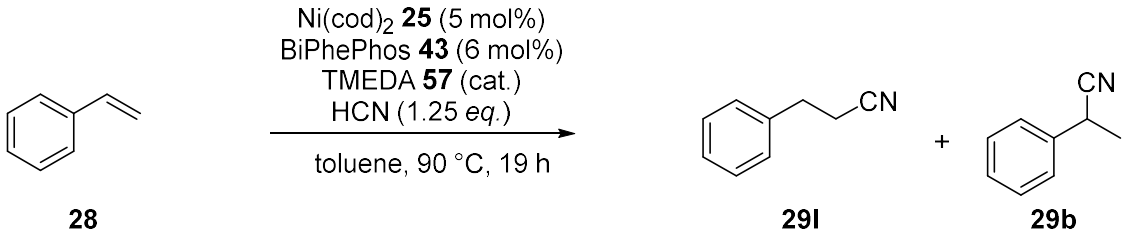

28 **29l** **29b**

entry	*eq.* (TMEDA 57) [mol%]	*X*[a] [%]	*Y*[a), b)] [%]	*S*[c)] [%]	*l:b*[d)]
1	12.5	7	5	69	< 1:99
2	5	5	4	83	< 1:99
3	2.5	46	45	98	< 1:99

*a): Based on GC analysis with n-decane as internal standard. b): Yield of nitrile products. c): Selectivity to nitrile products. d): ratio linear (**29l**) to branched (**29b**) nitrile product. e): Reaction conditions: Ni(cod)$_2$ **25** (13.8 mg, 0.05 mmol, 0.05 eq.) was dissolved in toluene (3 mL). BiPhePhos **43** (47.4 mg, 0.06 mmol, 0.06 eq.), AlCl$_3$ (6.7 mg, 0.05 mmol, 0.05 eq.), and TMEDA **57** were added. n-decane was added as an internal standard before the addition of styrene **28** (104 mg, 1 mmol, 1 eq.). The reaction mixture was cooled down (-50 °C), and HCN (50 µL, 1.25 mmol, 1.25 eq.) was added. The reaction mixture was then heated to 90 °C for 19 h.*

Applying a 1:1-ratio or higher of TMEDA **57** to Ni (entry 1 and 2) conversion only reaches < 10%, almost completely deactivating the catalyst. Lower ratios, of 1:2 TMEADA to Ni, still allow 46% conversion and 45% yield (entry 3). Based on the observed inhibitory effect on the catalytic mechanism, TMEDA **57** can be excluded as a promoter in nickel-catalyzed hydrocyanations. Other possible promoters are considered in the following.

Because of the high sensitivity of phosphites such as BiPhePhos **43** to acid-catalyzed hydrolysis, it is necessary to exclude proton containing hydroxyl functionality from these investigations. The selection of possible promoters was in conclusion limited to Lewis basic nitrogen containing substances (Figure 23).

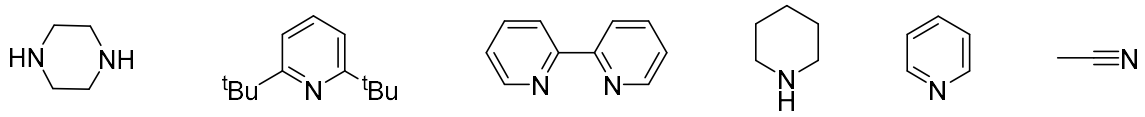

piperazine **74** 2,6-di(tert-butyl)-pyridine **75** 2,2'-bipyridine **76** piperidine **77** pyridine **78** acetonitrile **78**

pK_B = 8.7 pK_B = 9.1 pK_B = 9.6 pK_B = 6.2 pK_B = 8.8

Figure 23: Potential promotors in hydrocyanation.[2,66,67]

Additionally, only weak bases were selected, as a connection between excessive coordination ability (basicity) and a negative influence on hydrocyanation was considered (coordination to the nickel center).

*Table 13: Styrene **28** hydrocyanation using different promotors.*

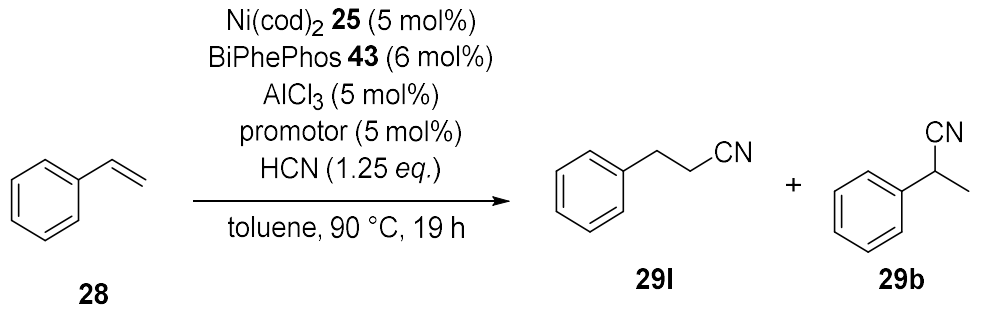

entry	promotor	$X^{a)}$ [%]	$Y^{a), b)}$ [%]	$S^{c)}$ [%]	*l:b*[d)]
1	none	> 99	98	98	66:34
2	piperazine **74**	> 99	> 99	> 99	4:96
3	2,6-di(*tert.*-butyl)-pyridine **75**	> 99	99	99	20:80
4	2,2'-bipyridine **76**	> 99	93	93	21:79
5	piperidine **77**	> 99	90	90	45:55
6	pyridine **78**	> 99	> 99	> 99	78:22
7	acetonitrile **79**	> 99	97	97	78:22

*Reaction conditions: $Ni(cod)_2$ **25** (13.8 mg, 0.05 mmol, 0.05 eq.) was dissolved in toluene (3 mL). BiPhePhos **43** (47.4 mg, 0.06 mmol, 0.06 eq.), $AlCl_3$ (6.7 mg, 0.05 mmol, 0.05 eq.), and the promoter (0.05 mmol, 0.05 mol%) were added. n-decane was added as an internal standard before the addition of styrene **28** (104 mg, 1 mmol, 1 eq.). The reaction mixture was cooled down (-50 °C), and HCN (50 µL, 1.25 mmol, 1.25 eq.) was added. The reaction mixture was then heated to 90 °C for 19 h. a): Based on GC analysis with n-decane as internal standard. b): Yield of nitrile products. c): Selectivity to nitrile products. d): ratio linear (**29l**) to branched (**29b**) nitrile product.*

It was found that, unlike TEMEDA **57**, none of the used promoters resulted in decreased conversion or yield. (Table 13). Selectivity towards the nitrile product was excellent throughout all promotors, making the *l:b*-ratio particularly worth looking at. Differences there can be explained by different interactions between the promotor and the $AlCl_3$.

With piperazine **74** (entry 2), the *l:b*-ratio dropped drastically to 4:96, which practically corresponds to the level without the addition of Lewis acid. Formation of a suspension can be observed after piperazine **74** addition, similar to TMEDA **57**. A potential explanation is that the Lewis acid-base pair formed has poor solubility in toluene, precipitated, and was therefore no longer available for the catalytic mechanism, resulting in the formation of the branched product **29b**. Using 2,6-di(*tert.*-butyl)-pyridine **75** (entry 3) and 2,2'-bipyridine **76** (entry 4) achieved reduced *l:b*-ratios of 20:80. This is probably due to increased steric hindrance caused by the bulky *tert.*-butyl groups with 2,6-di(*tert.*-butyl)-pyridine **75** and by the strong complex formation and coordination shielding caused by the two nitrogen donoratoms in 2,2'-bipyridine **76** respectively. With piperidine **77** (entry 5), there was a slight decrease in yield and selectivity to 90% while maintaining complete conversion. However, an *l:b*-ratio of 45:55 compared to 66:34 in the absence of $AlCl_3$ indicates a medium-strong coordination of the promoter towards $AlCl_3$. It appears that the effect is less strong compared to piperidine **77** due to the presence of only one donor atom.

L:b-ratios achieved by using both pyridine **78** (entry 6) and acetonitrile **79** (entry 7) are particularly noteworthy, as they increased the *l:b*-ratio to 78:22, compared to 66:34 in the absence of a promotor (entry 7). Pyridine **78** and acetonitrile **79** both have a low steric requirement due to their flat or rod shape respectively. The reactions carried out in these studies show that even catalytic amounts are sufficient to achieve a positive effect (entry 4). These results clearly show that the cooperation between the nickel catalyst and the Lewis acid cocatalyst can be enhanced by a promotor application. Further studies, outside the scope of this thesis, could concentrate on exploring the interaction between the promoter and $AlCl_3$ through modern spectroscopy like NMR.

As the Lewis acid enables higher reaction rates (section 2.8.3), the enhanced nickel/Lewis acid cooperativity, can impact the catalytic activity. Therefore, in the following (section 3.1.3.5), reaction profiles are monitored to determine the reaction rate. Besides that, the impact of pyridine **78** and acetonitrile **79** on other Lewis acids is being examined to explore limitations in the selection of Lewis acids.

3.1.3.4 $ZnCl_2$ und $La(OTf)_3$ with promotors in styrene hydrocyanation

As observed in previous reactions, $ZnCl_2$ and $La(OTf)_3$ show limited solubility in toluene (section 3.1.3.2.2), which might be improved by adding a promotor. Therefore, pyridine **78** and acetonitrile **79** were added to the reaction mixture (Table 14).

*Table 14: Styrene **28** hydrocyanation using $ZnCl_2$ and $La(OTf)_3$ with promoters.*

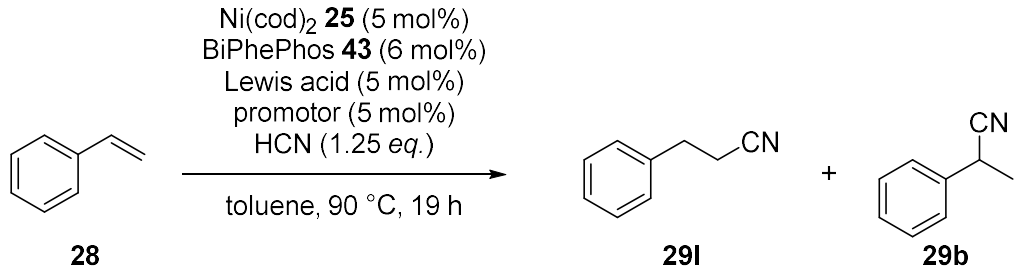

28 **29l** **29b**

entry	Lewis-acid	promotor	***X*** [a] [%]	***Y*** [a), b)] [%]	***S*** [c)] [%]	***l:b*** [d)]
1	$ZnCl_2$	acetonitrile **79**	> 99	> 99	> 99	6:94
2	$ZnCl_2$	pyridine **78**	> 99	99	99	5:95
3	$ZnCl_2$	none	> 99	> 99	> 99	5:95
4	$La(OTf)_3$	acetonitrile **79**	> 99	> 99	> 99	5:95
5	$La(OTf)_3$	pyridine **78**	> 99	> 99	> 99	5:95
6	$La(OTf)_3$	none	> 99	96	96	1:99

*Reaction conditions: $Ni(cod)_2$ **25** (13.8 mg, 0.05 mmol, 0.05 eq.) was dissolved in toluene (3 mL). BiPhePhos **43** (47.4 mg, 0.06 mmol, 0.06 eq.), Lewis-acid (0.05 mmol, 0.05 eq.), and the promoter (0.05 mmol, 0.05 mol%) were added. n-decane was added as an internal standard before the addition of styrene **28** (104 mg, 1 mmol, 1 eq.). The reaction mixture was cooled down (-50 °C), and HCN (50 µL, 1.25 mmol, 1.25 eq.) was added. The reaction mixture was then heated to 90 °C for 19 h. a): Based on GC analysis with n-decane as internal standard. b): Yield of nitrile products. c): Selectivity to nitrile products. d): ratio linear (**29l**) to branched (**29b**) nitrile product.*

As styrene **28** conversion and nitrile yields are quantitative, *l:b*-ratios remained at a low level of a maximum of 5:95 indicating no effect of the Lewis acid on the catalytic cycle. Visually, no improvement in solubility can be observed with the addition of the promoters.

This demonstrates that the cooperativity between the nickel-BiPhePhos **43** catalyst system and $AlCl_3$ is best and can be further enhanced by the addition of pyridine **78** and acetonitrile **79** as promoters.

Next, the influence of various promotors on the catalytic activity in styrene **28** hydrocyanation is investigated.

3.1.3.5 Influence of promotors on activity

Besides the selectivity influencing properties of the Lewis acid, the Lewis acid can also enhance the catalytic activity. Consequently, with enhanced availability of the Lewis acid by addition of a promotor, an increased reaction rate is expected.

For activity investigations, the reaction protocol remained unchanged, but the reaction mixture was scaled-up by a factor of 6 to a reaction volume of 18 mL sufficient for taking samples. Besides that, the lid of the reaction vessel was replaced by an unused septum for taking samples during the reaction time. Generally, it is assumed that applying BiPhePhos **43** results in a significantly faster reaction compared to phosphine ligands. Reaction profiles were recorded using 5, 2.5, and 1 mol% catalyst. First, no promotors are added to the reaction mixture to obtain a reference result.

Both reactions containing 5 mol% and 2.5 mol% showed > 85% selectivity towards both nitrile products and reached complete conversion within the first 15 minutes resulting in an identical reaction profile (Figure 24).

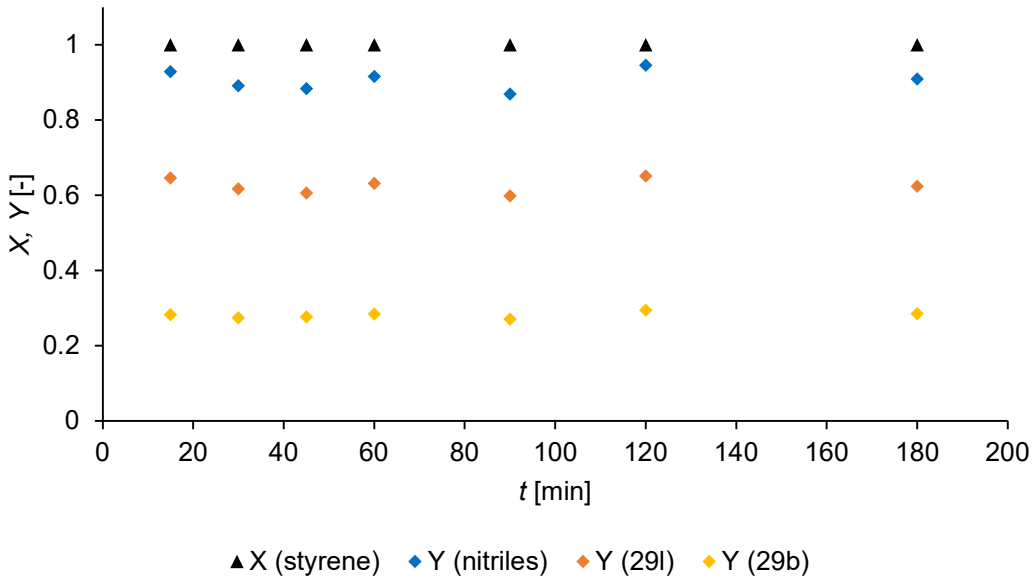

*Figure 24: Reaction profile of a 90 °C styrene **28** hydrocyanation using 2.5 mol% catalyst without promotor. Reaction conditions: $Ni(cod)_2$ **25** (41.3 mg, 0.15 mmol, 0.025 eq.) was dissolved in toluene (18 mL). BiPhePhos **43** (141.6 mg, 0.18 mmol, 0.03 eq.), and $AlCl_3$ (20.0 mg, 0.15 mmol, 0.025 eq.) were added. n-decane was added as an internal standard before the addition of styrene **28** (625.2 mg, 6 mmol, 1 eq.). The reaction mixture was cooled down (-50 °C), and HCN (300 µL, 7.5 mmol, 1.25 eq.) was added. The reaction mixture was then heated to 90 °C. X and Y are based on GC analysis with n-decane as the internal standard.*

When 1 mol% of catalyst is used, a the reaction stoped after 15 min again and a maximum nitrile yield of 52% is achieved. Despite the lowered nitrile yield, the slower reaction rate, as well as incomplete conversion makes it ideal for further investigations. Therefore, a reaction profile of the first 15 minutes of the reaction is recorded (Figure 25). Since the reaction vessel is being cooled down to -50 °C for HCN addition and is heated heating to 90 °C reaction temperature, a temperature profile can be expected which is monitored.

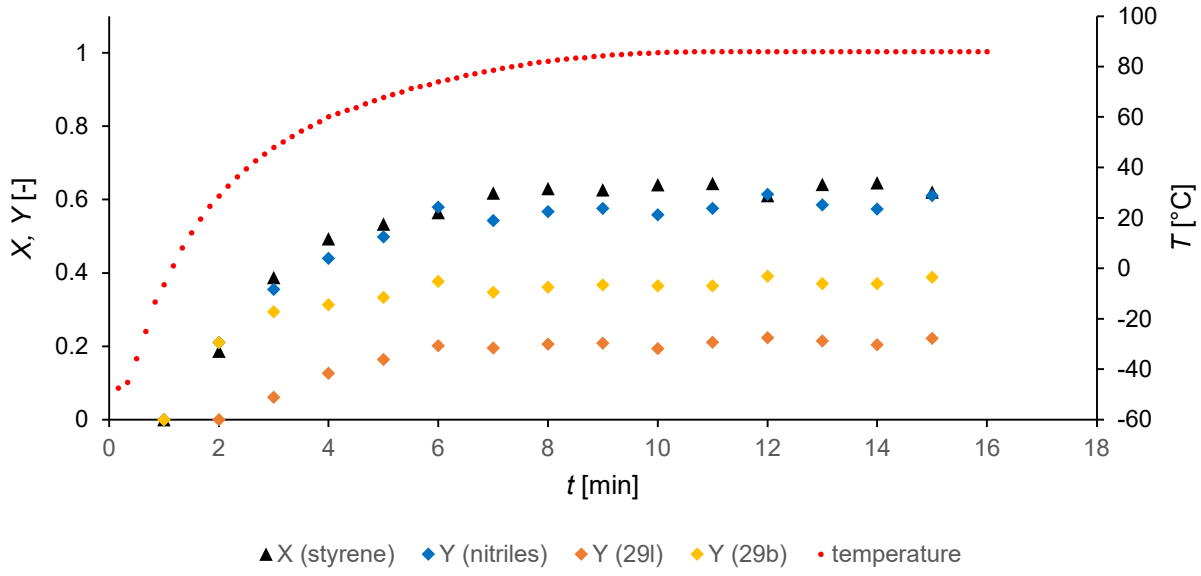

*Figure 25: Reaction profile of a 90 °C styrene **28** hydrocyanation using 1 mol% catalyst without promotor. Reaction conditions: $Ni(cod)_2$ **25** (16.5 mg, 0.06 mmol, 0.01 eq.) was dissolved in toluene (18 mL). BiPhePhos **43** (56.6 mg, 0.072 mmol, 0.012 eq.), and $AlCl_3$ (8.0 mg, 0.06 mmol, 0.01 eq.) were added. n-decane was added as an internal standard before the addition of styrene **28** (625.2 mg, 6 mmol, 1 eq.). The reaction mixture was cooled down (-50 °C), and HCN (300 µL, 7.5 mmol, 1.25 eq.) was added. The reaction mixture was then heated to 90 °C. X and Y are based on GC analysis with n-decane as the internal standard.*

The internal temperature increases rapidly, reaching room temperature within 1.67 minutes, which appears to initiate the hydrocyanation reaction. A reaction temperature exceeding 80 °C is achieved after 7.5 minutes. At this point, the hydrocyanation reaction, exhibits no additional changes in conversion or yield, suggesting catalyst deactivation.

Interestingly, when looking at the formation of the nitrile products, initially only branched product **29b** is formed. An almost exclusive formation of linear product **29l** is detected after three minutes. In particular, the formation of only branched product **29b** at the reaction start drastically reduces the *l:b*-ratio. A possible explanation for the delayed onset of the selectivity-reversing effect of the Lewis is the temperature profile. This finding can be explained by the low solubility of $AlCl_3$ in the solvent. When the reaction solution is cooled down to -50 °C, a suspension is formed which only completely dissolves again after warming for the first few

minutes. According to these findings, the precipitated species is most likely $AlCl_3$ and therefore not available to the reaction to the required extent initially. This also explains differences in *l:b*-ratios between the larger scale reactions used in reaction profile monitoring and the previously smaller reaction scales, as the smaller reaction volumes heat up significantly faster (section 7.1).

The limited yield of only 58% results in a poor TON to 57, but corresponds to previous investigations presented here.

Moreover, in this thesis it is shown, that BiPhePhos **43** is a potent ligand enabling high-activity hydrocyanation—a TOF_{20} of 624 h^{-1} is achieved. Since promotors are able to enhance the nickel/Lewis acid cooperation, a promotor effect on the catalytic activity seems feasible. Therefore, reaction profiles of styrene **28** hydrocyanation are monitored with acetonitrile **79** and pyridine **78** present in the reaction mixture (Table 15).

*Table 15: Promotors influence on the catalytic activity of nickel/BiPhePhos **43** in styrene **28** hydrocyanation.*

entry	promotor	$X^{a)}$ [%]	$Y^{a), b)}$ [%]	$S^{c)}$ [%]	*TON*	TOF_{20} [h^{-1}]	$l:b^{d)}$
1	-	63	56	91	57	624[e)]	36:64
2	acetonitrile **79**	67	61	90	61	804[f)]	29:71
3	pyridine **78**	43	33	77	34	366[g)]	11:89

*Reaction conditions: $Ni(cod)_2$ **25** (16.5 mg, 0.06 mmol, 0.01 eq.) was dissolved in toluene (18 mL). BiPhePhos **43** (56.6 mg, 0.072 mmol, 0.012 eq.) $AlCl_3$ (8.0 mg, 0.06 mmol, 0.01 eq.) and the promotor (if applicable, 0.06 mmol, 0.01 eq.) were added. n-decane was added as an internal standard before the addition of styrene **28** (625.2 mg, 6 mmol, 1 eq.). The reaction mixture was cooled down (-50 °C), and HCN (300 µL, 7.5 mmol, 1.25 eq.) was added. The reaction mixture was then heated to 90 °C. a): Based on GC analysis with n-decane as internal standard. b): Yield of nitrile products. c): Selectivity to nitrile products. d): ratio linear to branched nitrile product. e): Fit curve: $X=0.5t^3-7.0222t^2+39.235t-32.88$, $R^2=0.9997$. f): Fit curve: $X=0.9413t^3-12.351t^2+58.804t-43.474$, $R^2=0.9888$. g): Fit curve: $X=0.6622t^3-6.9262t^2+26.557t-16.08$, $R^2 = 1$.*

Indeed, it was found, that the presence of promotors affects the catalytic activity substantially. Appling acetonitrile **79**, the TOF_{20} increased to 804 h^{-1}, whereas pyridine **78** caused a decrease in the catalytic activity to 366 h^{-1}. The reduced activity in the presence of pyridine **78** can be explained by steric hindrance around the Al-center caused by the pyridine **78** ring compared to acetonitrile **79**. On the other hand, acetonitrile **79** appears to cause better chemical availability of the $AlCl_3$ by deaggregation.

Sufficient selectivities to nitrile products above 90% are achievable without any promotor or when acetonitrile **79** is applied. A reduced selectivity of 77% can be observed when pyridine **78** is used, which also reduces the catalytic activity and therefore allows styrene **28** polymerization to occur as a side reaction. With pyridine **78**, yield is also limited to 33%, suggesting catalyst deactivation at higher temperatures, further emphasizing the temperature influence on the *l:b*-ratio. Therefore, to circumvent these potentially catalyst deactivating higher temperatures, follow-up investigations include lower reaction temperatures.

3.1.3.6 Styrene hydrocyanation at lower reaction temperatures

In prior studies examining the reaction profile, it was discovered, that the reaction reached a steady state upon reaching 80 °C. One plausible explanation for this phenomenon is deactivation of the BiPhePhos/nickel catalyst at elevated temperatures. In the studies presented above, it was demonstrated, that when applying a 5 mol% catalyst the reaction was already completed before reaching 90 °C.

Consequently, at lower temperatures and with reduced catalyst loadings, higher conversions and yields are expected. Therefore, reduced catalyst loadings are used in styrene **28** hydrocyanations at both room temperature and 90 °C (Table 16).

*Table 16: Styrene **28** hydrocyanation at different catalyst loadings and temperatures.*

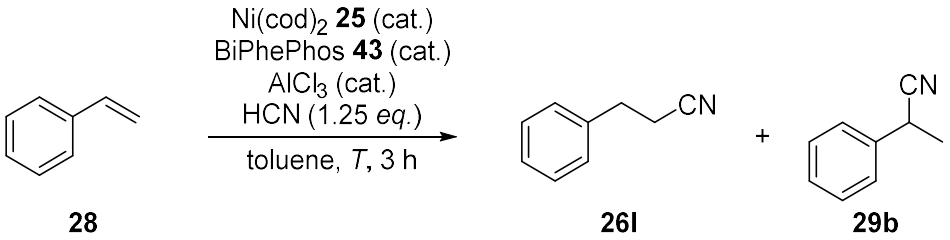

28 **26l** **29b**

entry	*eq.* Ni(cod)$_2$ [mol%]	*T* [°C]	*X*[a)] [%]	*Y*[a), b)] [%]	*S*[c)] [%]
1	5	90	> 99	98	98
2	5	22	> 99	98	98
3	2.5	90	> 99	86	86
4	2.5	22	> 99	91	91
5	1	90	41	32	84
6	1	22	59	55	94

*Reaction conditions: Ni(cod)$_2$ **25** was dissolved in toluene (3 mL). BiPhePhos **43**, AlCl$_3$, and the promoter were added. n-decane was added as an internal standard before the addition of styrene **28** (104 mg, 1 mmol, 1 eq.). The reaction mixture was cooled down (-50 °C), and HCN (50 µL, 1.25 mmol, 1.25 eq.) was added. The reaction mixture was then warmed to the reaction temperature for 19 h. a): Based on GC analysis with n-decane as internal standard. b): Yield of nitrile products. c): Selectivity to nitrile products. d): ratio linear (**29l**) to branched (**29b**) nitrile product.*

The reaction system shows very good styrene **28** conversion and nitrile yields at room temperature, matching the 90 °C results (entries 1 and 2). When using 2.5 mol% catalyst, a quantitative conversion with good selectivities to the product nitriles was again achieved at both temperatures (entries 3 and 4). The selectivity to nitrile products is slightly higher at room temperature indicating less styrene **28** polymerization. As already hypothesized, with 1 mol% catalyst (entries 5 and 6), a higher conversion, yield and selectivity to the nitrile product is observed at room temperature compared to 90 °C. This proves that catalyst deactivation proceeds much slower at lower temperatures consequently giving more time for the hydrocyanation to occur.

In conclusion, the use of the BiPhePhos **43**/nickel catalyst, as well as AlCl$_3$ in combination with promotors show advantages in styrene **28** hydrocyanation regarding nitrile yield, selectivity and catalytic activity. This achieved optimizations should be transferred to other,

non-activated substrates like 1-octeme **51** as these simple alkenes are unable to form a η^3-complex thus showing lower activity in the nickel-catalyzed hydrocyanation (section 2.8.3). Hence, for the following investigations in this chapter, 1-octene **51** is used as a substrate.

3.1.4 Nickel-BiPhePhos in 1-octene hydrocyanation

After the BiPhePhos **43** reaction system had been successfully tested in the hydrocyanation of styrene **28**, studies presented in this paragraph, aim to transfer the achieved optimizations to the non-activated substrate 1-octene **51**.

First, 1-octene **51** is hydrocyanated in the absence and presence of the Lewis acid $AlCl_3$.

3.1.4.1 1-Octen hydrocyanation without $AlCl_3$

Unfortunately, when no Lewis acid is applied no significant 1-octene **51** conversion and only traces of nitrile product are observed at ambient temperature. Even when the temperature is raised to 90 °C and the reaction time is extended to 19 h, no product formation can be detected

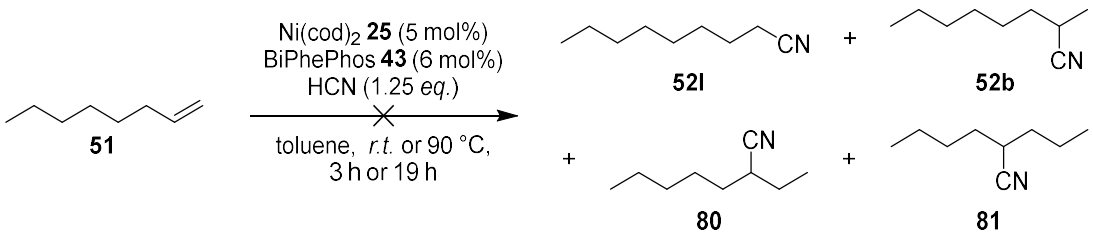

*Figure 26: 1-octene **51** hydrocyanation in the absence of a Lewis acid.*

Further investigations use $AlCl_3$, as this Lewis acid cocatalyst. An increase in catalytic activity can be expected.

3.1.4.2 1-Octene hydrocyanation with $AlCl_3$ as the Lewis

As shown above, the 1-octene **51** hydrocyanation severely lacks overall reactivity. Therefore, $AlCl_3$ is added as a co-catalyst to improve 1-octene **51** conversion and nitrile yield. Besides BiPhePhos **43**, the two diphosphine ligands Xantphos **35** and DPEPhos **31** are applied to investigate the impact of different ligand classes. Due to the strong π-acceptor capabilities of BiPhePhos **43** compared to Xantphos **35** and DPEPhos **31**, using BiPhePhos an increase in conversion and yield is expected. (Table 17).

*Table 17: 1-Octene **51** hydrocyanation using different ligands.*

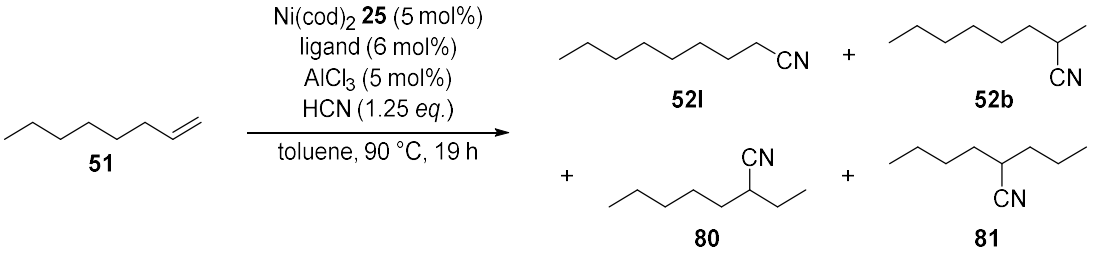

entry	ligand	$X^{a)}$ [%]	$Y^{a), b)}$ [%]	$S^{c)}$ [%]	*l:b*[d)]
1	Xantphos **35**	6	traces	-	-
2	DPEPhos **31**	36	17	47	79:21
3	BiPhePhos **43**	> 99	87	87	77:23

*Reaction conditions: $Ni(cod)_2$ **25** (13.8 mg, 0.05 mmol, 0.05 eq.) was dissolved in toluene (3 mL). Ligand (0.06 mmol, 0.06 eq.) and $AlCl_3$ (6.7 mg, 0.05 mmol, 0.05 eq.) were added. n-decane was added as an internal standard before the addition of 1-octene **51** (112.2 mg, 1 mmol, 1 eq.). The reaction mixture was cooled down (-50 °C), and HCN (50 µL, 1.25 mmol, 1.25 eq.) was added. The reaction mixture* was then heated to 90 °C for *19* h. *a): Based on GC analysis with n-decane as internal standard, b): Yield of nitrile products c): Selectivity to nitrile products d): ratio linear (**52l**) to branched (**52b**, **80**, **81**) nitrile product.*

Applying Xantphos **35**, only traces of nitrile product can be observed (entry 1), which demonstrates the low catalytic activity of the Ni-catalyst towards non-activated alkenes. In the presence of DPEPhos **31** (entry 2), conversion can be enhanced to 36%. Unfortunately, yield and selectivity are strongly reduced and therefore not satisfactory.

As expected, BiPhePhos **43** showed significantly improved conversion and yield (entry 3), surpassing the results achieved with both phosphine ligands. The *l:b*-ratio of 77:23 is also acceptable, but falls short of the high expectations resulting from the structural similarity to ligand **53** as described previously (section 2.8.3.2). This discrepancy is likely due to the increased structural rigidity of ligand **53** backbone resulting from the presence of two *tert*.-butyl groups.

Given that BiPhePhos **43** forms a highly effective catalyst complex, BiPhePhos **43** is kept as the ligand of choice. Additionally, since $AlCl_3$ proved advantageous in 1-octene **51** hydrocyanation, the cooperation between nickel and $AlCl_3$ should be enhances by using a promoter.

3.1.4.3 Promotors in 1-octene hydrocyanation

As promotors can enhance the nickel/Lewis acid cooperation, an enhanced nickel / Lewis acid cooperation is suspected to result in a higher *l:b*-ratio and higher reaction rates. That way, less time is available for catalyst deactivation resulting in an increased nitrile yield.

To evaluate the promotors influence on the 1-octene **51** hydrocyanation, pyridine **78** and acetonitrile **79** are added to the reaction mixture, as they have already shown their positive potential in combination with $AlCl_3$ in the styrene **28** hydrocyanation. In addition, to emphasize the general significance of this work regardless of the substrate, piperidine **77** and 2,6-di(*tert.*-butyl)-pyridine **78** will be investigated as well (Table 18).

*Table 18: 1-Octene **51** hydrocyanation using different promotors.*

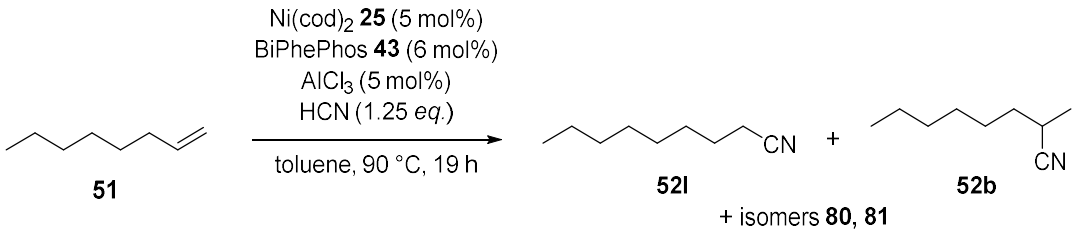

entry	promotor	*X*[a] [%]	*Y*[a), b)] [%]	*S*[c)] [%]	*l:b*[d)]
1	none	> 99	87	87	77:23
2	2,6-di(*tert.*-butyl)-pyridine **75**	56	48	86	69:31
3	piperidine **77**	25	14	57	68:32
4	pyridine **78**	56	47	85	73:27
5	acetonitrile **79**	55	48	87	72:28

*Reaction conditions: $Ni(cod)_2$ **25** (13.8 mg, 0.05 mmol, 0.05 eq.) was dissolved in toluene (3 mL). BiPhePhos **43** (47.4 mg, 0.06 mmol, 0.06 eq.), $AlCl_3$ (6.7 mg, 0.05 mmol, 0.05 eq.), and the promoter (0.05 mmol, 0.05 mol%) were added. n-decane was added as an internal standard before the addition of 1-octene **51** (112,2 mg, 1 mmol, 1 eq.). The reaction mixture was cooled down (-50 °C), and HCN (50 µL, 1.25 mmol, 1.25 eq.) was added. The reaction mixture was then heated to 90 °C for 19 h. a): Based on GC analysis with n-decane as internal standard. b): Yield of nitrile products. c): Selectivity to nitrile products. d): ratio linear to branched nitrile product.*

All promotors show strongly reduced styrene **28** conversions ranging from 55 to 56% (2,6-di(*tert.*-butyl)-pyridine **75**, pyridine **78**, and acetonitrilie **79** (entries 2,4 and 5) and 25%

(piperidine **77**; entry 3) respectively. Furthermore *l:b*-ratios decreased marginally to approximately 70:30. This renders further investigations on promoters in 1-octene **51** hydrocyanation unfeasible.

These results are indeed surprising, as the promoters initially only influenced the *l:b*-ratio in styrene **28** hydrocyanation without influencing the substrate conversion. This might be derived from the overall higher activity of styrene **28** and could therefore remain unrecognized during previous investigations exclusively focused on styrene **28**. Therefore, the catalytic activity in 1-octene **51** hydrocyanation is investigated next.

3.1.4.4 Catalytic activity of Nickel/BiPhePhos in 1-octene hydrocyanation

In 1-octene **51** hydrocyanation, the addition of a promoter was already found to have an inhibitory effect on conversion and yield. Thus, the catalytic activity of this less reactive substrate is of particular interest and therefore investigated in this paragraph.

As lower catalyst loadings are favored for precise reaction progress tracking, lowering the catalyst loading needs investigation first. The catalyst amount is reduced from 5 mol% to 2.5 mol% and 1 mol% respectively. As temperatures of 90 °C already proved its catalyst-deactivating potential in styrene **28** hydrocyanation. It is expected that this deactivation occurs in 1-octene **51** hydrocyanation as well. Consequently, further investigations focus on a reduction in reaction temperature to better balance catalyst deactivation and hydrocyanation activity (Table 19).

*Table 19: 1-Octene **51** hydrocyanation at different temperatures and catalyst loadings.*

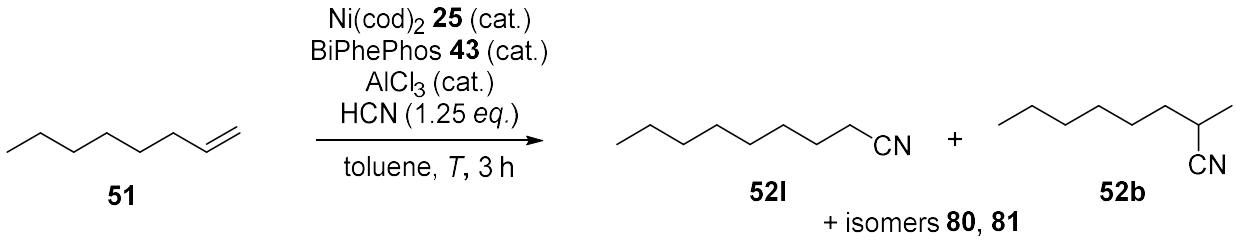

entry	*eq.* Ni(cod)$_2$ [mol%]	*T* [°C]	*X*[a)] [%]	*Y*[a), b)] [%]	*S*[c)] [%]	*l:b*[d)]
1	5	90	99	91	92	78:22
2	5	22	98	85	87	81:19
3	2.5	90	19	8	42	59:41
4	2.5	22	56	43	77	80:20
5	1	90	-	-	-	-
6[c]	1	22	-	-	-	-

*Reaction conditions: Ni(cod)$_2$ **25** was dissolved in toluene (3 mL). BiPhePhos **43**, and AlCl$_3$ were added. n-decane was added as an internal standard before the addition of 1-octene **51** (112 mg, 1 mmol, 1 eq.). The reaction mixture was cooled down (-50 °C), and HCN (50 µL, 1.25 mmol, 1.25 eq.) was added. The reaction mixture was then warmed to reaction temperature for 19 h. a): Based on GC analysis with n-decane as internal standard. b): Yield of nitrile products. c): Selectivity to nitrile products. d): ratio linear to branched nitrile product.*

When using a catalyst loading of 5 mol%, lowering the reaction temperature from 90 °C (entry 1) to 22 °C (entry 2) results in no major changes regarding conversion, yield, selectivity, and *l:b*-ratio. This strongly demonstrates the catalytic potential of BiPhePhos **43** at ambient temperatures—even when non-activated olefins are applied. At ambient temperature, when reducing the catalyst loading to 2.5 mol% (entry 4) a conversion of 56% was achieved, increasing 1-octene **51** conversion by a factor of three compared to 90 °C (entry 3). Furthermore it can be found, that ambient temperatures increase the *l:b*-ratio. This can be explained by a stronger kinetic control of the reaction, with apparently favors the linear product. It can be concluded, that following the results obtained with styrene **28**, conversion, yield, and selectivity benefit from lower temperatures as well which helps prevent catalyst deactivation.

When using a catalyst quantity of 1 mol%, no nitrile product formation can be detected either at 90 °C (entry 5) or at room temperature (entry 6). In this case, catalyst deactivation is

therefore faster than the time required to start the product formation, which can be explained by impurities within one of the major components of the reaction mixture—this was already suspected during investigations using styrene **28** (section 3.1.3). This impurity can be contained within, toluene, HCN, or 1-octene **51**. For further evaluation, these relevant reaction compounds were doubled in each case (Table 20, entries 2 to 4) to meet the *component*:Ni-ratio of the 2.5 mol% preparations.

*Table 20: 1-Octene **51** hydrocyanation varying the composition of the reaction mixture.*

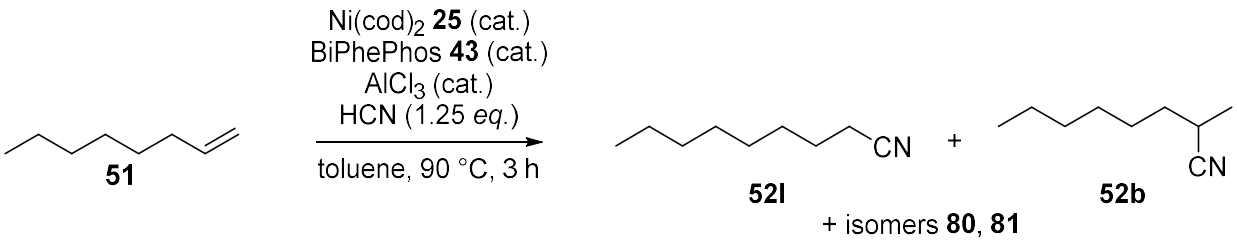

entry	*compound doubled*	*eq.* Ni(cod)$_2$ [mol%]	*X*[a)] [%]	*Y*[a), b)] [%]	*S*[c)] [%]	*l:b*[d)]
1[a)]	-	5	99	91	92	78:22
2[b)]	-	2.5	19	8	42	59:41
3[d)]	toluene	5	83	70	84	75:25
4[e)]	HCN	5	98	85	87	66:34
5[f)]	1-octene **51**	2.5	53	40	76	70:30

*Reaction conditions: Ni(cod)$_2$ **25** was dissolved in toluene (3 mL). BiPhePhos **43**, and AlCl$_3$ were added. n-decane was added as an internal standard before the addition of 1-octene **51** (112 mg, 1 mmol, 1 eq.). The reaction mixture was cooled down (-50 °C), and HCN (50 µL, 1.25 mmol, 1.25 eq.) was added. The reaction mixture was then heated to 90 °C for 19 h. a): Based on GC analysis with n-decane as internal standard. b): Yield of nitrile products. c): Selectivity to nitrile products. d): ratio linear to branched nitrile product.*

Doubling the toluene amount, conversion decreased slightly to 83%. This is likely due to the higher dilution, resulting in a lower reaction rate giving the catalyst more time for deactivation. However, conversion and yield didn't drop significantly, making toluene an unlikely source of the impurities. Excessive HCN concentration can be a decisive factor a catalyst deactivation in nickel-catalyzed hydrocyanations (section 2.8.2). Subsequently, the amount of HCN was doubled to 2.5 equivalents, doubling the HCN:Ni ratio (entry 4). Surprisingly, however, the reaction carried out still showed a high conversion of 98% and a yield of 85%. In conclusion,

excessive HCN concentration can be excluded as a deactivation source. Lastly, 1-octene **51** is doubled (entry 5), consequently, resulting in a substoichiometric HCN amount. As expected, conversion drops to 53%, which can be attributed to HCN deficiency.

In conclusion, the hypothesis of impurities within one of the components could not be confirmed. Therefore, impurities due to shortcomings in the operational procedure such as oxygen contamination are likely and investigated within chapter II.

For reasons of comparability, the operational procedure is kept, and the catalytic activity is investigated. Therefore, a reaction profile at 90 °C is monitored using 5 mol% of catalyst ensuring quantitative conversion.

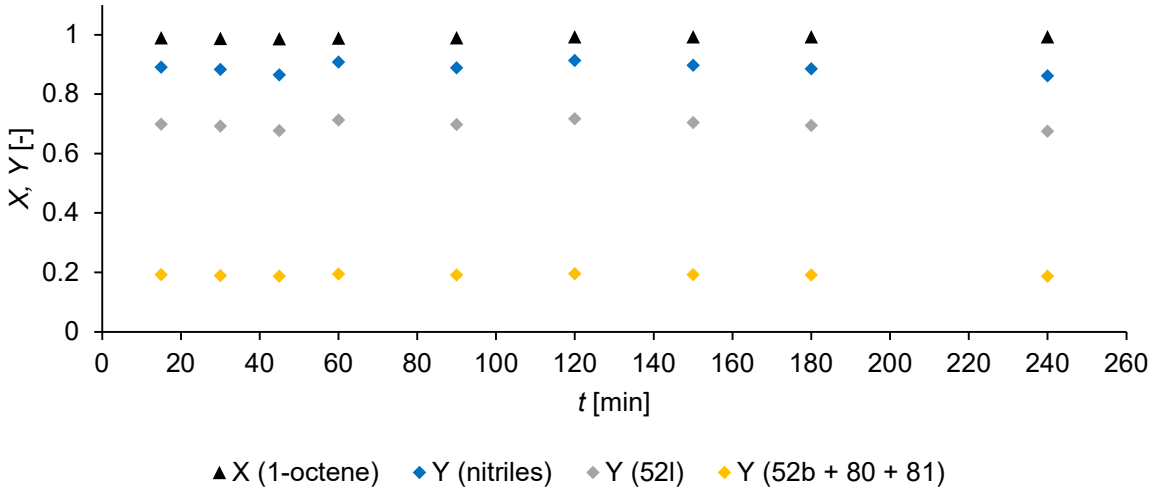

*Figure 27: Reaction profile for 1-octene **51** hydrocyanation. Reaction conditions: $Ni(cod)_2$ **25** (82.5 mg, 0.3 mmol, 0.05 eq.) was dissolved in toluene (18 mL). BiPhePhos **43** (283.2 mg, 0.36 mmol, 0.06 eq.), and $AlCl_3$ (40.0 mg, 0.3 mmol, 0.05 eq.) were added. n-decane was added as an internal standard before the addition of 1-octene **51** (673.4 mg, 6 mmol, 1 eq.). The reaction mixture was cooled down (-50 °C), and HCN (300 µL, 7.5 mmol, 1.25 eq.) was added. The reaction mixture was then heated to 90 °C. X and Y are based on GC analysis with n-decane as the internal standard.*

The reaction reaches a steady state within the first 15 minutes, which highlights the high activity of the catalyst. The *l:b*-ratio is 78:22 and identical with previous studies. As 1-octene **51** hydrocyanation does not process in absence of the $AlCl_3$, solubility issues of the Lewis acid do not influence the *l:b*-ratio, resulting in the expected *l:b*-ratio of 78:22. Due to the rapid reaction progress, the time interval of the samples is reduced to ensure precise reaction tracking (Figure 28).

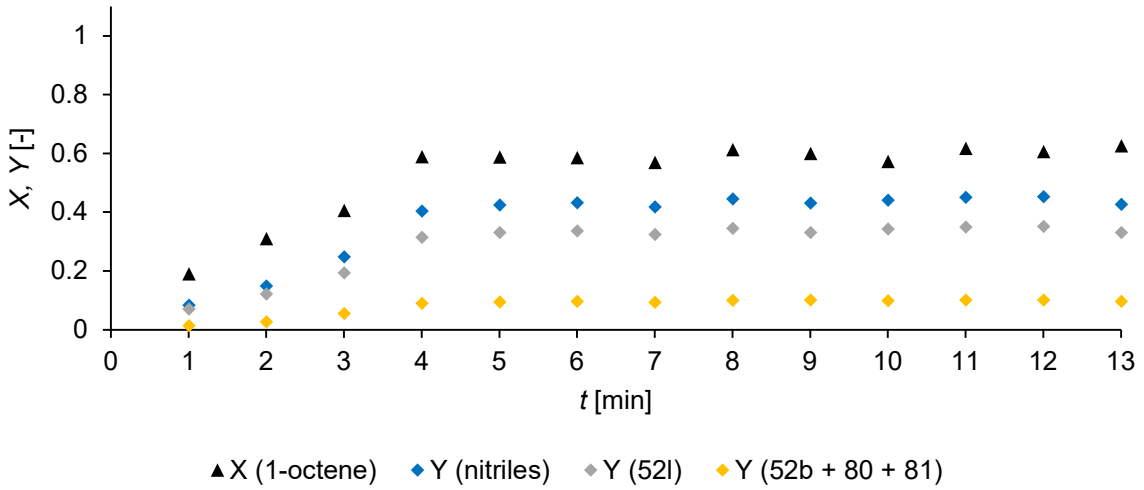

*Figure 28: Reaction profile for 1-octene **51** hydrocyanation. Reaction conditions: $Ni(cod)_2$ **25** (82.5 mg, 0.3 mmol, 0.05 eq.) was dissolved in toluene (18 mL). BiPhePhos **43** (283.2 mg, 0.036 mmol, 0.06 eq.), and $AlCl_3$ (40.0 mg, 0.3 mmol, 0.05 eq.) were added. n-decane was added as an internal standard before the addition of 1-octene **51** (673.4 mg, 6 mmol, 1 eq.). The reaction mixture was cooled down (-50 °C), and HCN (300 µL, 7.5 mmol, 1.25 eq.) was added. The reaction mixture was then heated to 90 °C for 19 h. X and Y are based on GC analysis with n-decane as the internal standard.*

Surprisingly, 1-octene **51** conversion stops after 4 minutes. A potential reason is oxygen contamination while taking samples. Fortunately, 20% conversion was already surpassed allowing TOF_{20} determination to 95 h^{-1}. 1-Octene **51** hydrocyanation therefore proceeds about 6.5 times slower compared to styrene **28**. The TON was determined to be 21 from previously monitored reaction profiles (Figure 27), which is about one-third of that previously achieved for styrene **28** and can be attributed to the higher amount of catalyst required.

Due to time constraints, the reaction profile could not be repeated at ambient temperature or with a reduced catalyst loading.

3.1.5 Chapter I: Conclusions and outlook

In this chapter, BiPhePhos **43** was applied in styrene **28** and 1-octene **51** hydrocyanation as this electron withdrawing ligand features a wide bite angle. It is suspected that these characteristics accelerate the reductive elimination as the rate determining step (section 2.7). The investigations presented in this chapter focused on nitrile yield, *l:b*-ratio and catalytic activity. Due to BiPhePhos **43** application in styrene **28** hydrocyanation, conversion, and yield are quantitative and therefore significantly increased compared to the well-established diphosphine ligands Xantphos **35** (*X* = 71%, *Y* = 71%) and DPEPhos **31** (*X* = 54, *Y* = 21%). This shows the great potential of the BiPhePhos **43** ligand in nickel-catalyzed hydrocyanations and next further conditions can be investigated.

When adding $AlCl_3$ to the reaction mixture, to invert the *l:b*-ratio towards the formation of the linear product (section 2.8.3.1), BiPhePhos **43** (*X* > 99%, *Y* = 98%) surpasses the results obtained with alternative ligands (**35**: *X* = 40%, *Y* = 40%; **31**: *X* = 39%, *Y* = 39%) significantly Also, the *l:b*-ratio is increased to 66:34 compared to 46:45 (**31**) and 9:91 (**35**). Besides the ligand choice, an *l:b*-ratio influencing effect this strong is limited to $AlCl_3$ only and almost nonexistent with BPh_3 (10:90) or $ZnCl_2$ (5:95). In conclusion, in this thesis it was shown that the choice of the Lewis acid has a major impact on the *l:b*-ratio.

Since a high catalytic activity is crucial for industrial application of the hydrocyanation, the catalytic activity is investigated in presence of $AlCl_3$. In this case, BiPhePhos **43** enables a catalytic activity of 624 h^{-1}—the first ever reported TOF_{20} for this reaction. Due to the poor solubility of the $AlCl_3$ in the organic solvent, this is suspected to form oligomers reducing its chemical availability. Therefore, a promotor can be added, which aims to deaggregate these oligomers increasing the cooperation between the nickel catalyst and the $AlCl_3$ cocatalyst. That way, in this thesis, a promotor was added to the reaction mixture for the first time in the nickel-catalyzed hydrocyanation and thus, the catalytic activity was increased. Among all tested promoters, a catalytic amount of acetonitrile **79** as the promotor proved most effective in increasing the catalytic activity to 804 h^{-1} and the *l:b*-ratio to 78:22. Future investigations, not conducted in this thesis, should focus on, spectroscopic methods to evaluate the exact mechanism behind the Lewis acid/promotor interaction.

Generally, the reactions studied here, showed a higher reaction rate as expected. As the reaction mixture is cooled down to -50 °C for the HCN addition and then warmed to reaction temperature, the temperature profile derived from this operational procedure was found to be of key importance. It was found that the hydrocyanation reaction already comes to a end before reaching the 90 °C reaction temperature. Reaction profiles measured with lowered catalyst loadings show, that the catalyst is deactivated at temperatures above 75 °C. Hence,

at lower catalyst loadings (1 mol%), choosing ambient temperature maintains the catalyst's activity and results in higher styrene **28** conversion and nitrile yield. Looking forward, carrying out hydrocyanations at isothermal conditions using pure HCN while complying with all safety measures remains challenging and will be investigated in the next chapter.

Furthermore, non-activated alkenes like 1-octene **51** cannot form a η^3-complex (section 2.8.3.1), resulting in low activity in hydrocyanation. It was found, that hydrocyanation of 1-octene **51** without $AlCl_3$ is not possible, even when using 5 mol% nickel-catalyst. To tackle the overall lack of activity, the activity increasing potential of the BiPhePhos/$AlCl_3$-combination was then utilized in 1-octene **51** hydrocyanation, where BiPhePhos **43** yields 87% C9-nitrile outperforming DPEPhos **31** (Y = 17%) and Xantphos **35** (Y < 1%). Within subsequent investigations on activity a TOF_{20} of 95 h^{-1} was observed for 1-octene **51** indicating that 1-octene **51** hydrocyanation is about 6.5 times slower than styrene **28** hydrocyanation. Despite its low reactivity in the nickel-catalyzed hydrocyanation, it was found that 1-octene **51** hydrocyanation still progresses at ambient temperatures resulting in higher conversions and yields when lower catalyst loadings are used. This effect is even more pronounced in 1-octene **51** hydrocyanation compared to styrene **28** and can, due to the lower reaction rate, be attributed to catalyst deactivation via $BiPhePhos_2Ni$ bischelate formation at elevated temperatures

In order to increase the catalytic activity by enhanced nickel/Lewis acid cooperation in this particular interesting reaction, a promotor was applied in the 1-octene **51** hydrocyanation, transferring the conditions optimized for styrene **28** to the non-activated 1-octene **51**. Unfortunately, in 1-octene **51** hydrocyanation, promotors can't increase the cooperation of the nickel catalyst and the Lewis acid $AlCl_3$, as they have a strong inhibitory effect on conversion and yield.

Looking forward, detailed investigations on the catalyst's stability is of great importance, as a comprehensively active catalyst is mandatory for achieving high activities. In the present studies, the catalyst was found to be deactivated at higher temperatures. To prevent catalyst deactivation and to maintain the high catalytic activity, optimizing the experimental procedure is a worthwhile aim for future work in this exciting and forward-looking field. For this purpose, instead of adding HCN in one portion at low temperatures, gradually adding HCN at reaction temperature over time can prevent catalyst deactivation. This approach would eliminate the temperature profile associated with the current method,

Consequently, the optimization of the operational procedure is investigated in the next chapter.

3.2 Chapter II: Nickel-Based Hydrocyanation Catalysts: Investigating Stability, Enhancing Procedures, Obtaining High Activity

3.2.1 Research gap and general aspects

Early academic studies on hydrocyanation mainly used HCN surrogates like acetone cyanohydrin **7**, which require elevated temperatures of 60 to 90 °C to liberate HCN. For reasons of comparability, these conditions were mostly kept in successive work, even when pure HCN was used. Unfortunately, formation of catalytically inactive L_2Ni-bischelates occurs especially at elevated temperatures[65], reducing the catalytic potential. While bischelate formation is reversible for diphosphines, the Ni-bischelates formed with chelating π-acceptor ligands, like diphosphites, tend to be quite stable.[25] Consequently, the irreversible BiPhePhos$_2$Ni-bischelate **27** formation may lead to complete catalyst deactivation over time, thus significantly reducing the overall catalytic activity (Figure 29).

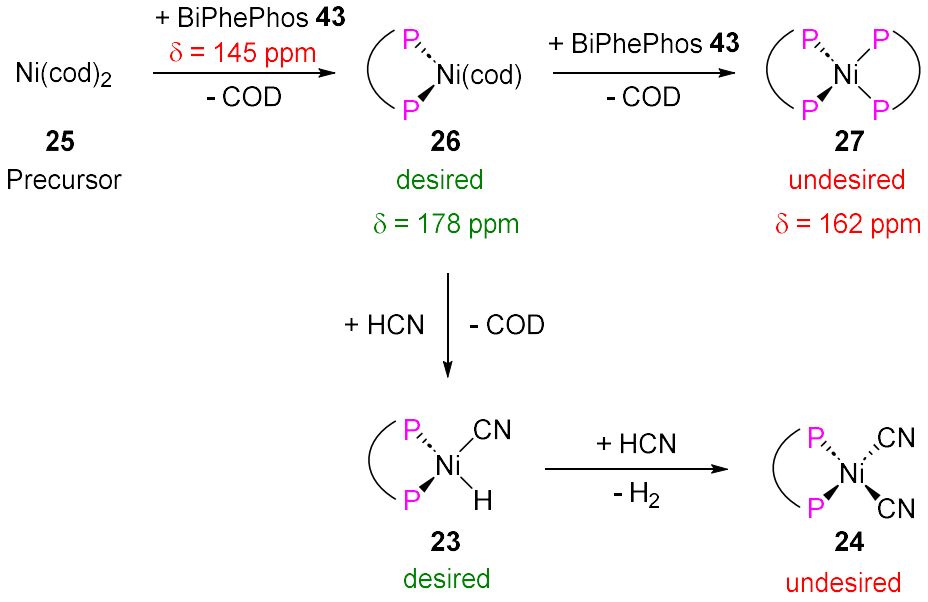

Figure 29: Catalyst preforming and deactivation by bischelate formation and corresponding ^{31}P-NMR shifts.[65]

Lower temperatures are therefore worth investigating, as there is limited research focused on optimizing the experimental methodology to prevent this bischelate formation.

Besides that, the use of surrogates as the cyanide source significantly reduces the atom-economy and that way cut the hydrocyanations main advantage over traditional synthetic routs and is not suitable for large scale processes. Therefore, in this work, pure hydrogen cyanide is used. In literature, hydrogen cyanide, if used in pure form, is usually added via Eppendorf pipette, either neat or in solution.[8,25,26] To date, there are no studies investigating the impact

of the HCN addition technique on the catalytic performance, which will be conducted in the present thesis.

Unfortunately, the preformed catalyst BiPhePhosNi(cod) **26** can potentially be deactivated by BiPhePhosNi(CN)$_2$ **24** formation as well. The stability of BiPhePhosNi(cod) **26** against various HCN concentrations is not known in literature to this day and therefore investigated in this chapter.

Moreover, there is very limited knowledge regarding the true activity of nickel complexes in hydrocyanation in terms of TOF at low conversion. Applying different diphosphonite ligands in the Ni-catalyzed hydrocyanation of styrene **28** with pure HCN, HOFMANN *et al*. were able to reduce the catalyst concentration to 1 mol%, still reaching a conversion of more than 90%.[32] This translates to a maximum Turnover Number (TON) of 92. Which regard to large scale processes, this is still not satisfactory and emphasizes the need for further optimization in this particular field. This chapter therefore focuses on ideal conditions for achieving a high catalytic activity, which has not been done so far.

To fill these gaps, this work focuses on the use of pure HCN and optimization of the reaction procedure to improve stability and to maintain the maximum catalysts activity throughout the reaction.

In addition, further studies on the influence of the Lewis acid $AlCl_3$ on the catalysts stability are needed, as it remains unclear why increased Ni:$AlCl_3$ ratios of 1:20 severely lower nitrile yields (section 2.8.3).[5] Hence, further ongoing studies focusing on the catalyst's stability in terms of the nickel to Lewis acid ratio are carried out in this chapter.

3.2.2 Optimization of the operational procedure of lab-scale hydrocyanations

Since nickel(0)-catalysts are highly sensitive—especially towards oxygen, it is often handled inside a glovebox in literature focused on $Ni(cod)_2$ **25**.[68–70] literature regarding hydrocyanation often misses this information, leaving its use unknown. In these studies, to exclude oxygen contamination during catalyst preforming, and to ensure excellent $Ni(cod)_2$-purity (section 5.9.1) the preforming is exclusively carried out in an inert glovebox atmosphere. By that, reproducible and consistent results can be obtained.

Furthermore, contaminations within the reaction mixture are a likely cause for catalyst deactivation. This is manifested visually by the transition from a colorless (no deactivation) to a yellow-green (partially deactivated) to an orange-brown solution (fully deactivated), which shows no catalytic activity (Figure 30) and can be proven by ^{31}P-NMR (Figure 31).

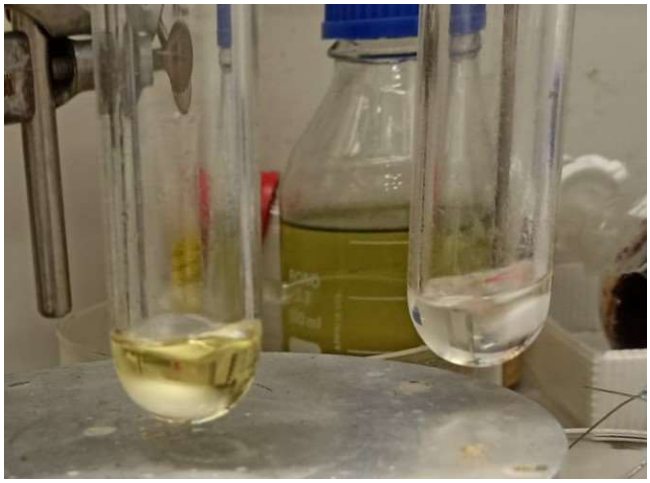

Figure 30: Catalyst preforming solutions partially deactivated (left) and non-deactivated (right).

It can be observed that the colorless solution contains active BiPhePhosNi(cod) **26** only. The yellow-green, partially deactivated solution already predominantly contains free BiPhePhos **43** ligand. After full deactivation to an orange-brown solution, only the free ligand can be detected and bischelate formation does not occur.

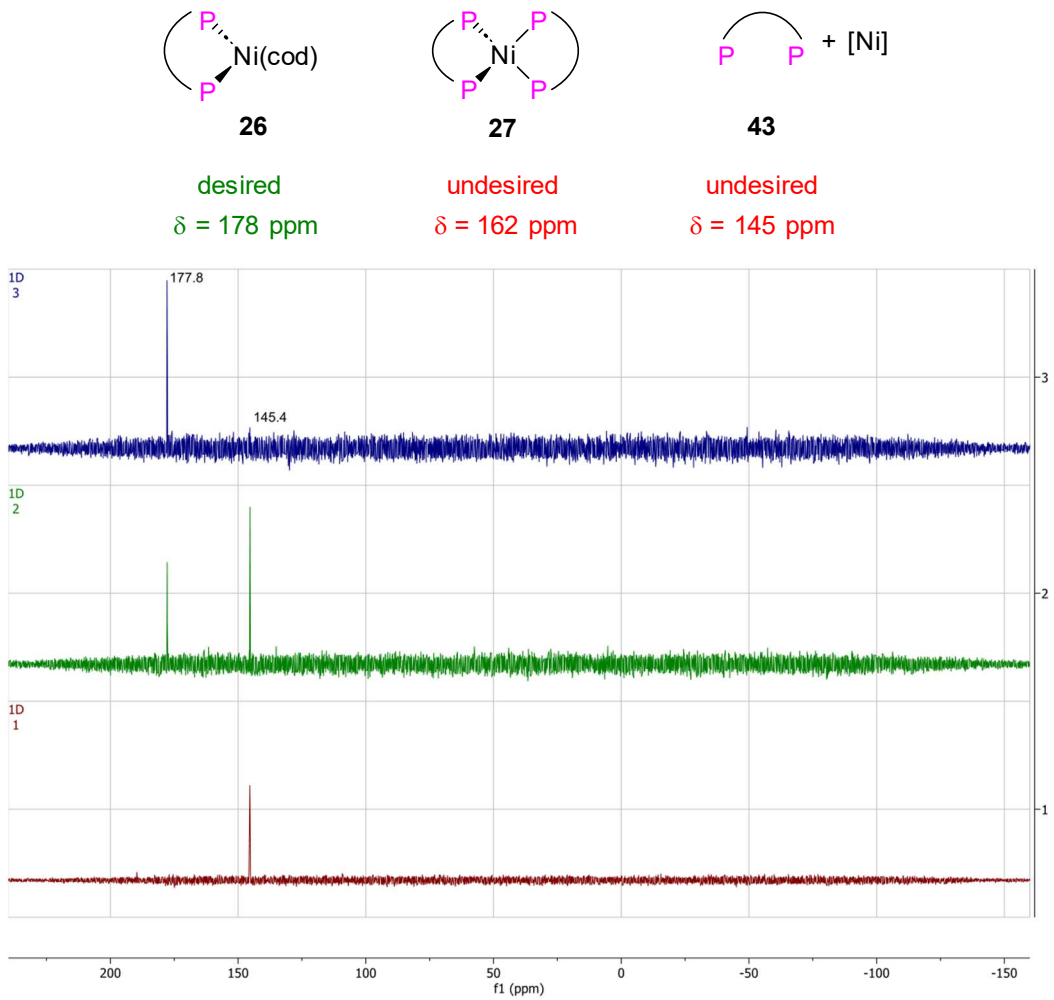

Figure 31: ^{31}P-NMR of the performing solution showing no deactivation (top), partial deactivation (middle), and full deactivation (bottom).

If major parts of the present catalyst are already deactivated before the reaction start, a drastic decrease in catalytic activity is the result. It is suspected that these oxygen contaminations are potentially derived from insufficient component purification as well as the reaction procedure itself, such as opening the flask, even in argon counterflow. Therefore, by optimizing the reaction protocol, such contaminations are to be excluded in a structured manner to maintain the high catalytic activity.

First, to exclude contamination by the GC-standard *n*-decane and opening of the reaction flask in argon countercurrent, the operational procedures were systematically varied while maintaining identical stoichiometry (Table 21). Initially, after preforming of the catalyst and substrate addition, *n*-decane was added as an internal standard in the reaction mixture for analysis by gas chromatography (GC) (entry 1). Hydrogen cyanide was added neat by Eppendorf pipette at −50 °C, resulting in a mere 5% conversion of styrene **28**, and no product formation was observed. Adding the GC standard *n*-decane after the reaction to mitigate the potential for e.g. oxygen contamination (entry 2), a modest enhancement in performance was

achieved, with 19% conversion and 14% yield. Introducing hydrogen cyanide as a solution in toluene at 22 °C markedly elevated both conversion and yield to 96% (Table 21, entry 3). This clearly shows that lowering the temperature to −50 °C while adding pure HCN via Eppendorf pipette hurts the effectiveness of the catalyst systems tested. Utilizing a rubber septum notably streamlines the operational procedure, minimizing the risk of contamination, resulting in quantitative conversion and yield (Table 21, entry 4).

*Table 21: Different operational procedure for styrene **28** hydrocyanation.*

entry	*n*-decane addition	*T* @ HCN addition [°C]	*S*eptum usage	*X*[a)] [%]	*Y*[a), b)] [%]	*S*[c)] [%]
1	before reaction[d)]	-50	No	5	0	0
2	after reaction[e)]	-50	No	19	14	75
3	after reaction[f)]	*r.t.*	No	96	96	> 99
4	after reaction[f)]	*r.t.*	Yes	> 99	> 99	> 99

*a): Based on GC analysis with n-decane as an internal standard. b): Yield of the branched product. c): Selectivity to product nitriles. d): Reaction conditions: BiPhePhos **43** (4.7 mg, 0.006 mmol) was dissolved in toluene (3 mL), and $Ni(cod)_2$ **25** (1.4 mg, 0.005 mmol, 0.005 eq.) was added. n-decane was added as an internal standard before the addition of styrene **28** (104 mg, 1 mmol, 1 eq.). The reaction mixture was cooled down (−50 °C), and HCN (50 µL, 1.25 mmol, 1.25 eq.) was added. The reaction mixture was then warmed to 22 °C for 3 h. e): BiPhePhos **43** (4.7 mg, 0.006 mmol) was dissolved in toluene (3 mL), and $Ni(cod)_2$ **25** (1.4 mg, 0.005 mmol, 0.5 mol%) was added. Styrene **28** (104 mg, 1 mmol, 1 eq.) was then added. The reaction mixture was cooled down (−50 °C), and HCN (50 µL, 1.25 mmol, 1.25 eq.) was added. The reaction mixture was warmed to 22 °C. After the reaction time of 3 h at 22 °C, n-decane was added as an internal standard after the reaction. f): BiPhePhos **43** (4.7 mg, 0.006 mmol) was dissolved in toluene (2 mL) and $Ni(cod)_2$ **25** (1.4 mg, 0.005 mmol, 0.5 mol%) was added. Styrene **28** (104 mg, 1 mmol, 1 eq.) was then added. HCN (50 µL, 1.25 mmol, 1.25 eq.) was dissolved in cold toluene (1 mL) in a separate flask and injected into the reaction vessel. After the reaction time of 3 h at 22 °C, n-decane was added as an internal standard.*

To date, no literature can be found that demonstrates the significant influence of the HCN addition technique and its temperature dependency. With these optimizations, the operational

procedure has been established. Further investigations are carried out on the catalyst's stability.

3.2.3 Stability of Nickel catalysts in absence of a Lewis acid

3.2.3.1 Stability of BiPhePhosNi(cod) **26**

Based on the literature, the catalyst preforming was carried out by dissolving the precursor $Ni(cod)_2$ **25** and BiPhePhos **43** in toluene. As the importance of the catalyst preforming was already demonstrated (section 3.2.2), the stability of the nickel catalyst is first investigated in absence of hydrogen cyanide. The mixture is analyzed at 22 °C using ^{31}P-NMR. The aim is to form the catalytically active species BiPhePhosNi(cod) **26** and investigate its long-term stability. Via ^{31}P-NMR, the catalyst BiPhePhosNi(cod) **26** can be detected (δ = 177.8 ppm) as well as the free BiPhePhos **43** ligand (δ = 145.4 ppm).[65]

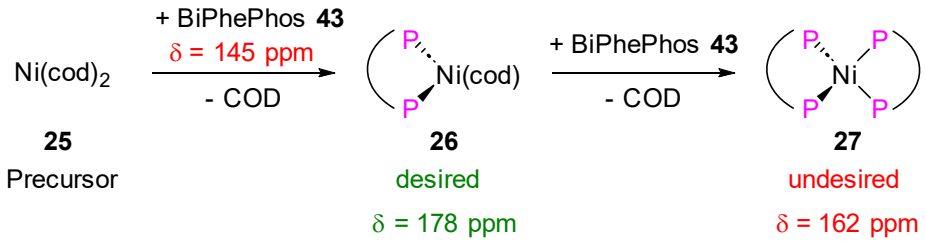

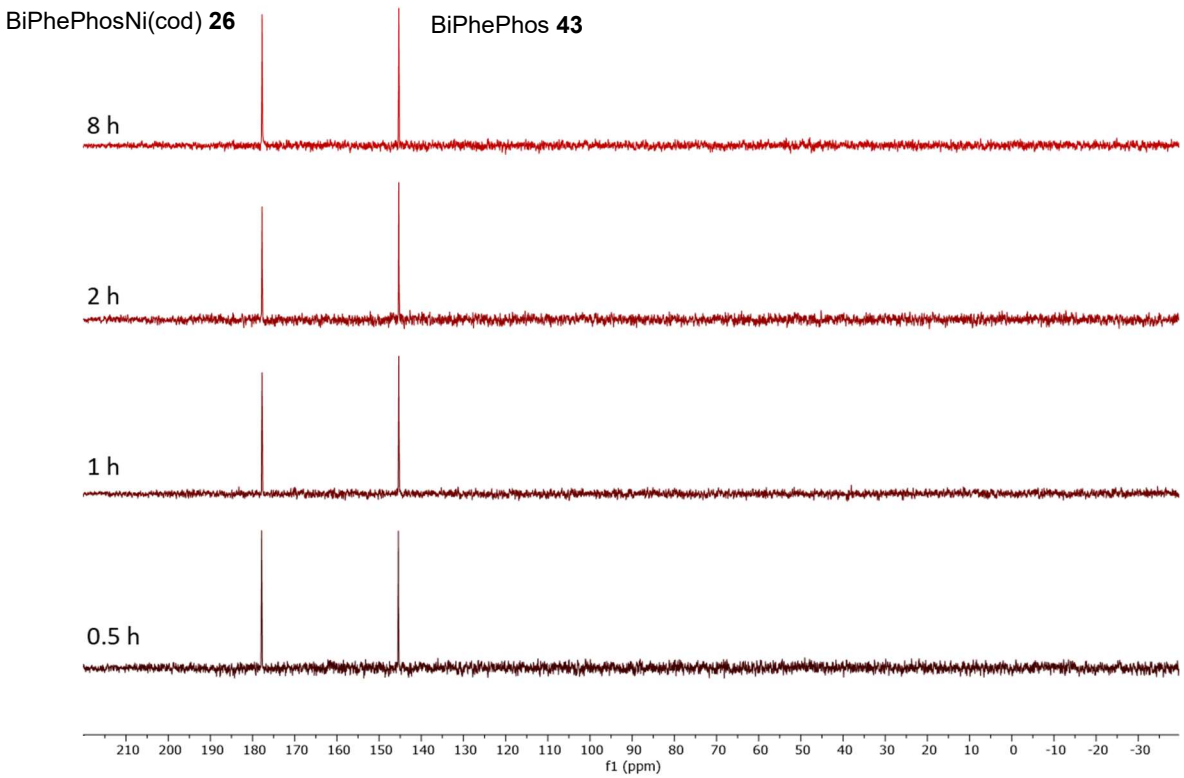

*Figure 32: $^{31}P\{^1H\}$-NMR (162 MHz, toluene) of the preforming solution. Reaction conditions: BiPhePhos **43** (56.8 mg, 6 mmol, 1.2 eq.) is dissolved in toluene (3 mL). $Ni(cod)_2$ **25** (13.8 mg, 5 mmol, 1 eq.) is added. At the indicated time points, approximately 0.6 mL of the solution was withdrawn from the mixture and analyzed by NMR.*

It was found that the ratio of the peak areas remained constant at around 1:1 over the entire observation period of 8 h (Figure 32). Suppose that BiPhePhos **43** is present in 40% excess in relation to the precatalyst, the catalyst is only formed at equilibrium to about 80% in relation to the $Ni(cod)_2$ **25** used.

Since nickel-catalyzed hydrocyanations are carried out at 90 °C, the following preforming studies are carried out at 90 °C (Figure 33).

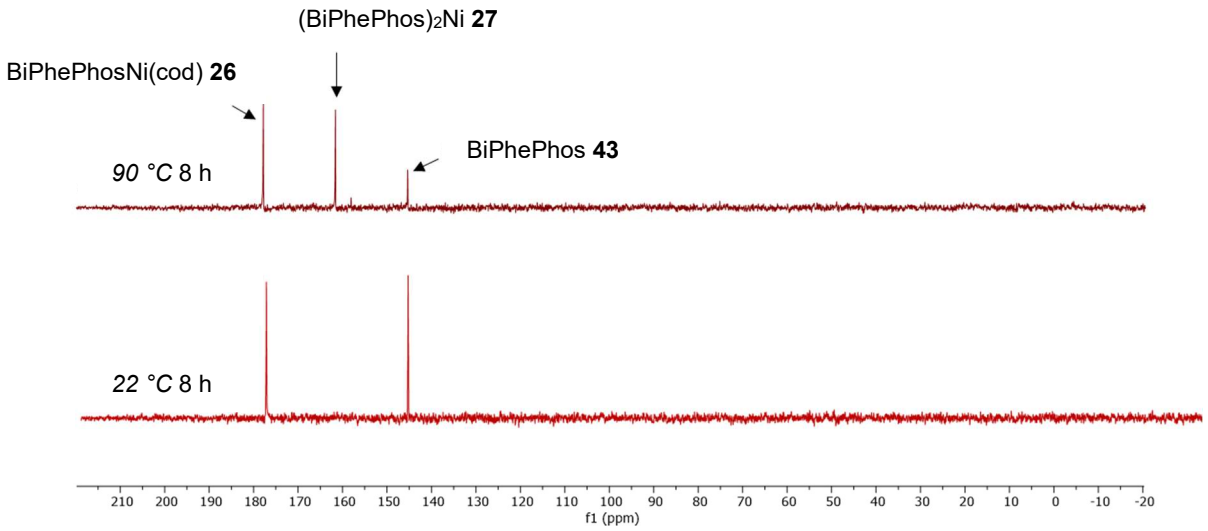

*Figure 33: $^{31}P\{^{1}H\}$-NMR (162 MHz, toluene) of the preforming solution at 90 °C (top) and 22 °C (bottom). Reaction conditions: BiPhePhos **43** (56.8 mg, 6 mmol, 1.2 eq.) is dissolved in toluene (3 mL). $Ni(cod)_2$ **25** (13.8 mg, 5 mmol, 1 eq.) is added. Top: 90 °C for 4 h. Bottom: 25 °C for 8 h.*

Here, in addition to the formation of the catalyst (about 80% after 2 h), an NMR signal of the catalytically inactive bischelate complex $(BiPhePhos)_2Ni$ **27** was also detected at δ = 161.6 ppm, which is according to literature.[65] This shows that 90 °C the catalyst is deactivated via bischelate formation over time, thus, negatively affecting the catalytic activity and productivity.

Besides bischelate formation, catalyst deactivation can proceed in the form of Ni(II)cyanide-species formed by an excess of HCN. To further investigate the catalyst tolerance against large HCN concentrations, different HCN amounts are added to the active species BiPhePhosNi(cod) **26** which is expected to immediately form BiPhePhosNi(H)CN **23**.

For determination of the ^{31}P-NMR-shift of the catalytic active cyanide containing catalyst an attempt was made to synthesize BiPhePhosNi(H)CN **23** in a targeted manner. For this purpose, five equivalents of HCN are added to the corresponding solution of BiPhePhosNi(cod) **26**. Using one equivalent HCN is insufficient, as four equivalents can be consumed by hydrocyanation of COD. The reaction mixture was analyzed by ^{31}P-NMR.

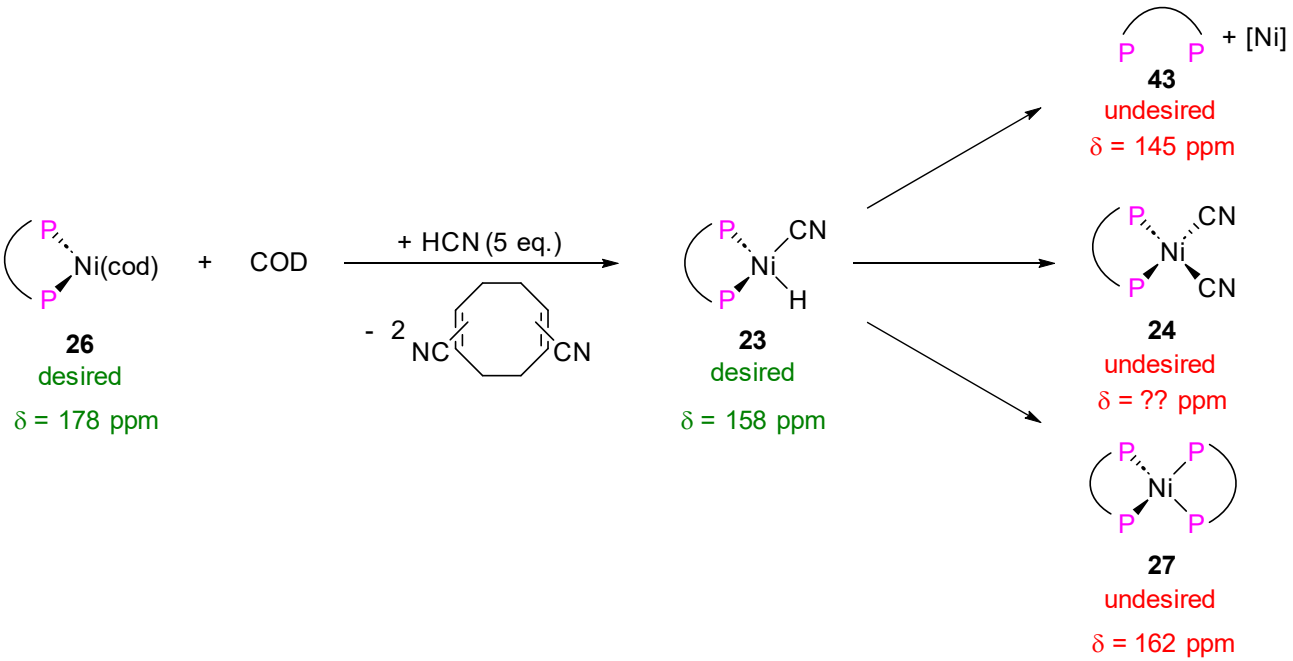

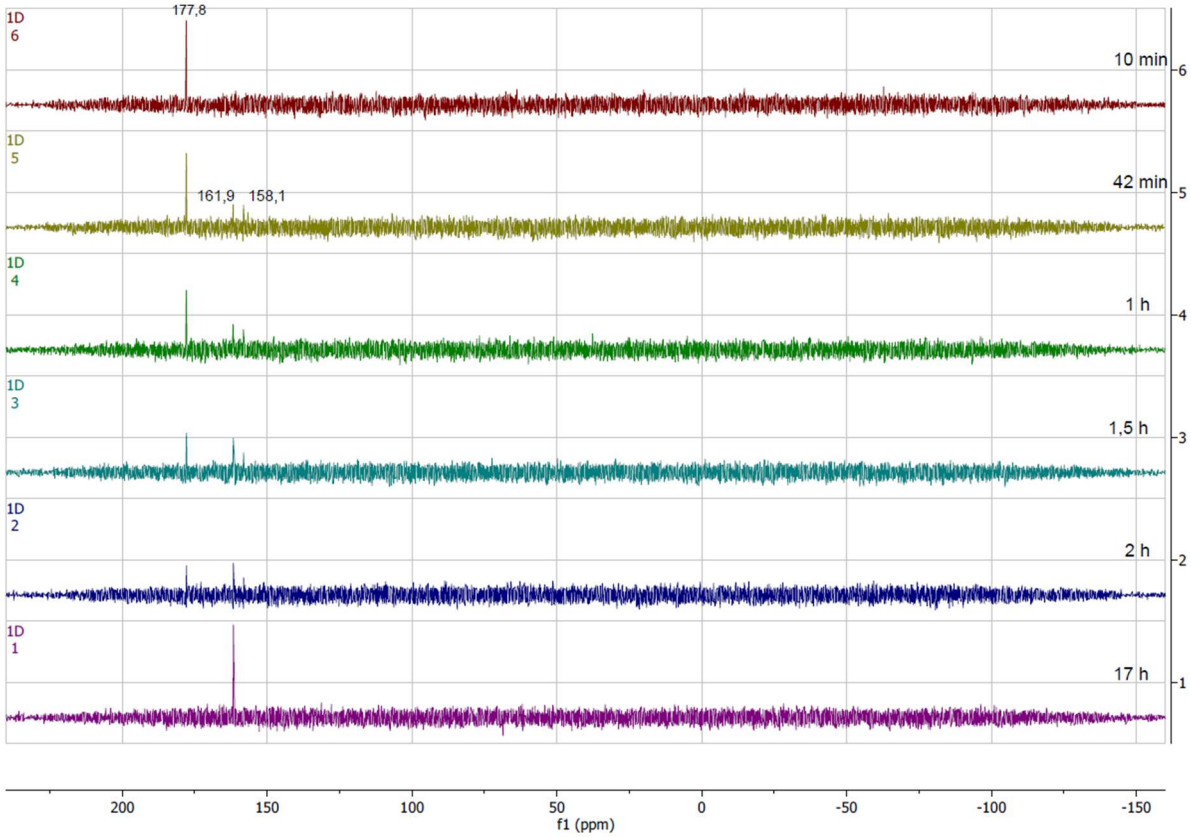

*Figure 34: $^{31}P\{^{1}H\}$-NMR (162 MHz, toluene) of the reaction of BiPhePhosNi(cod) **26** with HCN, Ni:HCN = 1:5 at room temperature. Reaction conditions: BiPhePhos **43** (31.7 mg, 4 mmol, 1.2 eq.) was dissolved in toluene (2 mL) and $Ni(cod)_2$ **25** (9.2 mg, 3.3 mmol, 1 eq.) was added. HCN (6.69 µL, 16.7 mmol, 5 eq.) was then added to the mixture.*

No change can be observed 10 minutes after addition. After around 40 minutes, two new signals at 161.9 and 158.1 ppm are detected. After 17 h only the 161.9 ppm signal of the

catalytically inactive bisschelate species $(BiPhePhos)_2Ni$ **27** is remaining, indicating complete catalyst's deactivation. This indicates the formation of $(BiPhePhos)_2Ni$ **27** in presence of HCN, as this is not the case in absence of HCN. One likely explanation is that the existing COD equivalents were hydrocyanated, and thus cannot stabilize an intermediate BiPhePhosNi-species that is formed after HCN dissociation from BiPhePhosNi(H)CN **23**. This makes bischelate formation easily possible. On a positive note, the second signal at 158.1 can be assigned to the catalytically active complex BiPhePhosNi(H)CN **23**. The catalytically active species BiPhePhosNi(H)CN **23** is still present 2 h after the HCN addition. This proves the existing catalytic potential of the present reaction mixture. However, the low Ni:HCN ratio of 1:5 should be pointed out again, corresponding to a catalyst loading of 25 mol% (at 1.25 *eq.* HCN in relation to the substrate, not present here).

Therefore, the used HCN amount is further increased to 1:25 corresponding to a theoretical catalyst loading of 5 mol%, which is well established in the literature. An increased HCN excess is expected to increase the amount of BiPhePhosNi(H)CN **23** formed as HCN loss to the gas phase is insignificant (Figure 35).

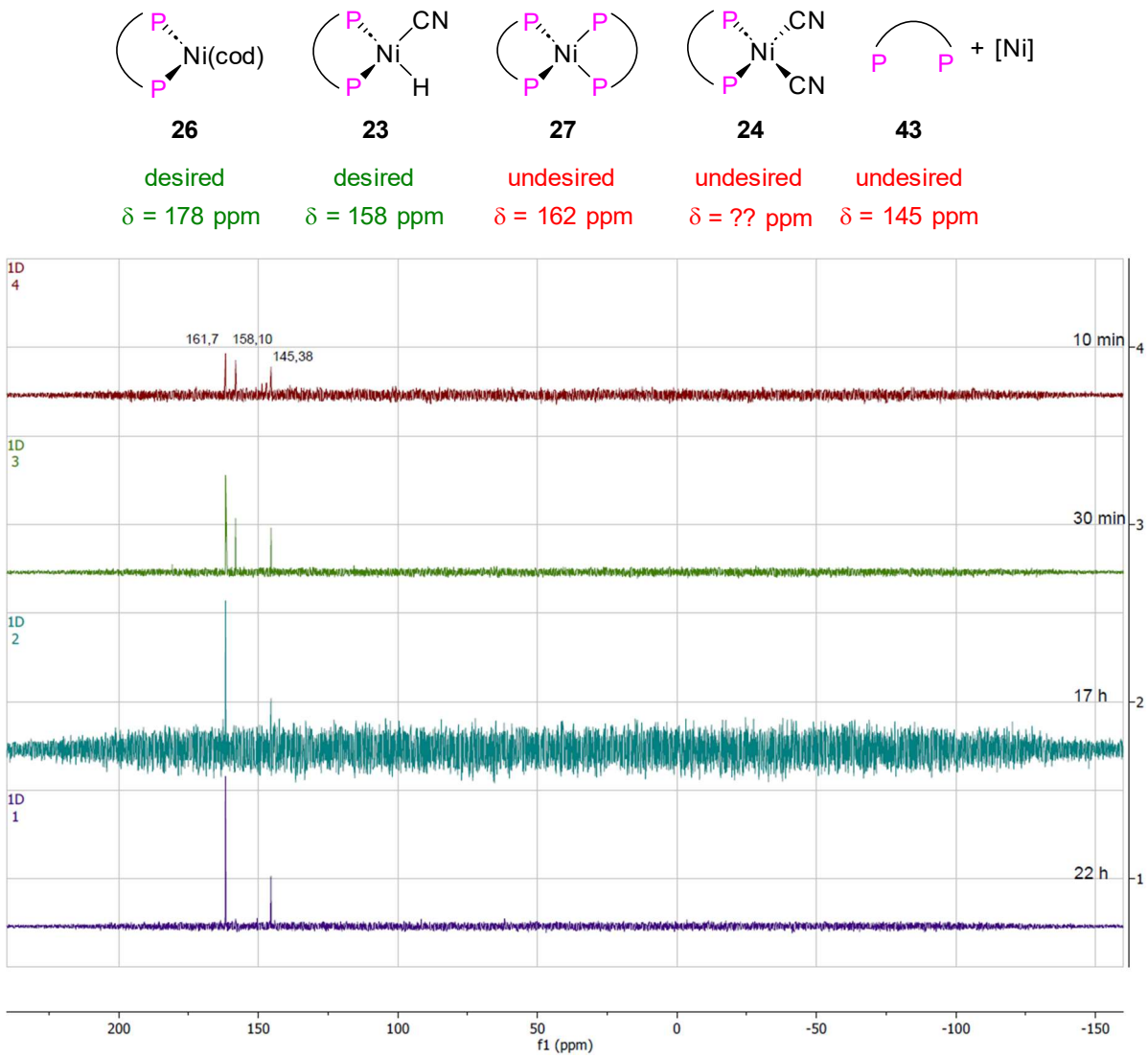

*Figure 35: $^{31}P\{^{1}H\}$-NMR (162 MHz, toluene) of the reaction of BiPhePhosNi(cod) **26** with HCN, Ni:HCN = 1:25 at room temperature. Reaction conditions: BiPhePhos **43** (22.2 mg, 0.028 mmol, 1.2 eq.) was dissolved in toluene (1.4 mL) and $Ni(cod)_2$ **25** (6.5 mg, 0.024 mmol, 1 eq.) was added. HCN (23.4 µL, 0.588 mmol, 25 eq.) was then added to the mixture.*

Signals are also found here at 161.7 and 158.1 ppm. The active species BiPhePhosNi(cod) **26** is no longer detectable here.

A new signal can be observed at 145.4 ppm, which can be assigned to the free ligand. Conversely, this indicates that parts of the ligand are dissociated from the nickel center. The remaining nickel is possibly present in the form of $Ni(CN)_2$. Apart from ligand dissociation, the 20% ligand excess is also detected.

However, it is known from literature and from previous work in this particular field that a catalyst loading of 5 mol% is more than sufficient for effective styrene **28** hydrocyanation, making complete catalyst deactivation unlikely. Several things are conceivable here. On the one hand, the remaining amount of catalytically active BiPhePhosNi(H)CN **23** ($\delta(^{31}P)$ = 158.1 ppm) may

be sufficient to achieve quantitative conversion. On the other hand, each NMR measurement represents an average value over the measurement time period (15 minutes) in which further deactivation occurs. Unfortunately, shorter measurement intervals result in a lower resolution of the recorded spectra. This could only be compensated by reducing the concentration of all components. Unfortunately, this would further reduce the similarity of the NMR-reaction conditions, which are similar to the original reaction mixture, and therefore reduce the informative value.

Anyhow, for the purpose of process intensification, a lower catalyst loading is desirable. Therefore, within the next investigation, a catalyst loading of 1 and 0.5 mol% is investigated, by increasing the HCN concentration further. Based on the previous studies, an even faster deactivation is expected (Figure 36).

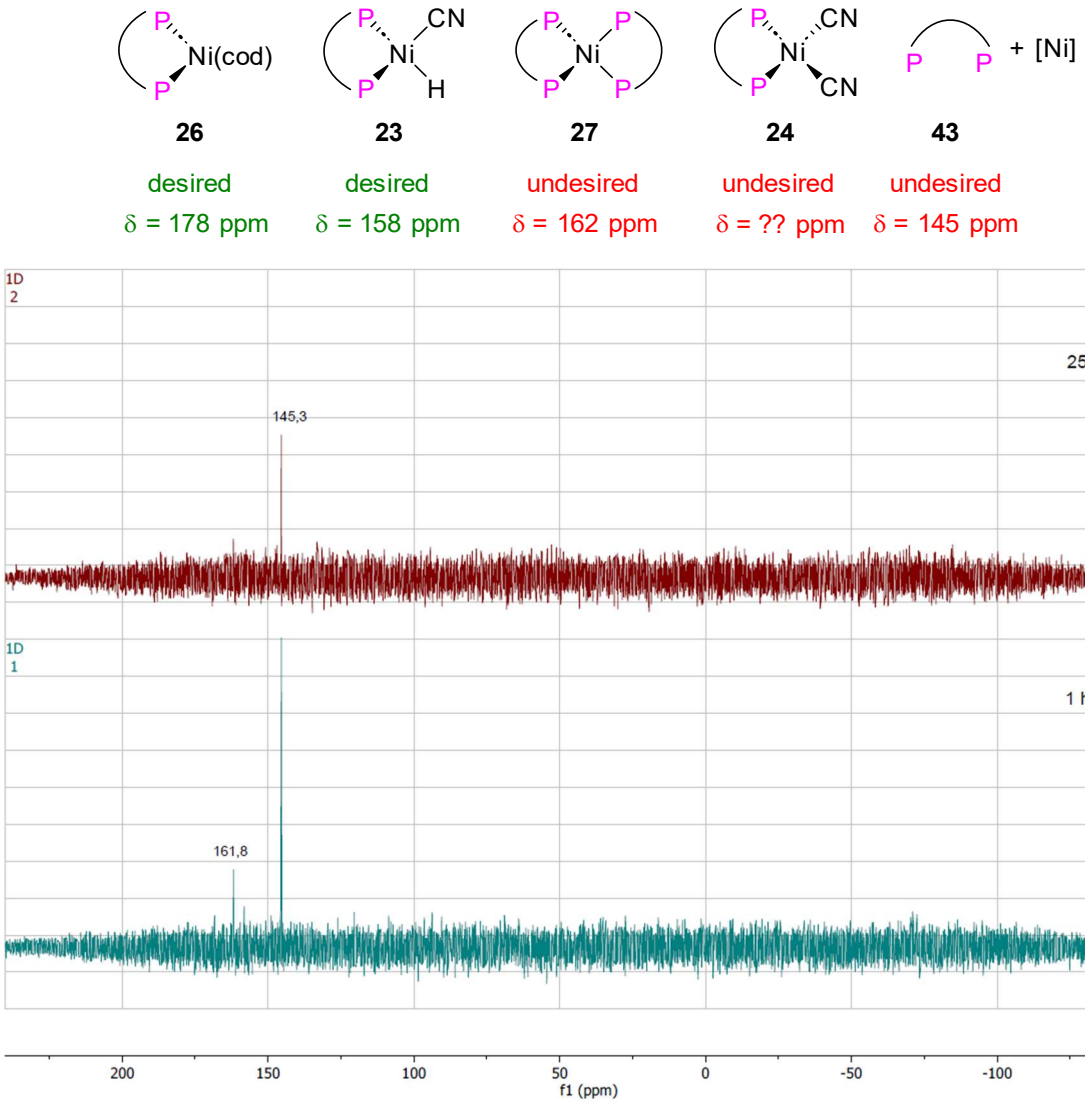

*Figure 36: $^{31}P\{^{1}H\}$-NMR spectrum (162 MHz, toluene) of the reaction of BiPhePhosNi(cod) **26** with HCN, Ni:HCN = 1:125: at room temperature. Reaction conditions: BiPhePhos **43** (9.5 mg, 0.012 mmol,*

1.2 eq.) was dissolved in toluene (0.6 mL) and Ni(cod)$_2$ ***25*** *(2.8 mg, 0.01 mmol, 1 eq.) was added. HCN (50 µL, 1.25 mmol, 125 eq.) was then added to the mixture.*

After 25 minutes, the first sample shows hardly any significant amounts of catalytically active species. Large quantities of the free ligand can be observed. After another 35 minutes, no significant changes occurred.

When using 250 equivalents of HCN, a white-green precipitate forms immediately upon addition, which indicates the formation of BiPhePhosNi(CN)$_2$ or Ni(CN)$_2$. That way, due to the precipitate collecting at the bottom of the NMR tube, reducing ligand concentration in the solution, lower NMR signal intensities are observed.

It should also be noted that throughout the NMR studies, increased substance concentrations were used to obtain high-resolution NMR spectra. The different concentrations are compared in the following Table 22, as this might not be representative of a reaction mixture and, therefore, reduced the informative value of the investigations.

Table 22: Different concentrations between reaction solution and NMR solution using the example of theoretical 1 mol% = Ni: HCN = 1:125.

	During NMR-*S*tudies	**Within reaction**
Ni:HCN	**1:125**	**1:125**
***c* (Ni) [mmol/L]**	**16.72**	**3.33**
***c* (BiPhePhos) [mol/L]**	**20.06**	**4.00**
***c* (HCN) [mol/L]**	**2.09**	**0.42**

A systematic risk within this approach is the presence of paramagnetic nickel species significantly suppressing signal detection. To circumvent these limitations of NMR-based investigations, the activity after HCN addition is investigated by adding styrene **28**, which is then converted to 2-phenylpropionitrile accordingly if catalytic active species are still present.

3.2.3.2 Analysis through styrene hydrocyanation

For the reasons mentioned above, a different procedure is chosen next. In this procedure, the catalyst BiPhePhosNi(cod) **26** was first mixed with HCN after preforming. After 30 minutes, styrene **28** was added and the reaction time of 3 hours starts. That way, the catalytic active is

detected indirectly by this method (Table 23). Due to the absence of a Lewis acid, only the formation of the branched product is expected.

*Table 23: Delayed styrene **28** addition for investigation of the remaining catalytic activity.*

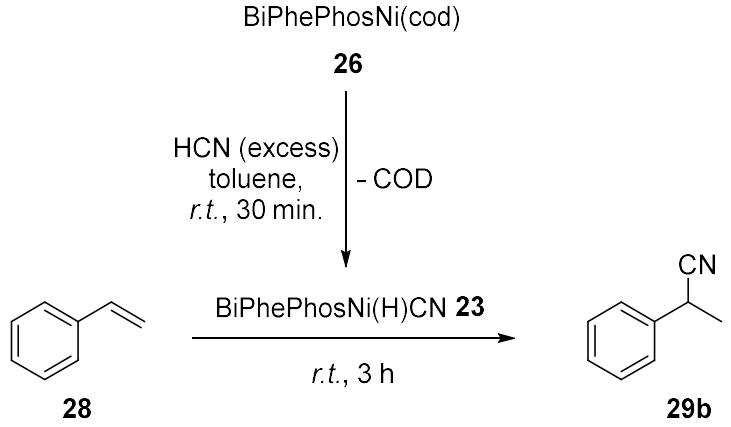

entry	*eq.* $Ni(cod)_2$ [mol%]	Ni:HCN ratio	*X*[a)] [%]	*Y*[a), b)] [%]	*S*[c)] [%]
1	5	25	81	81	> 99
2	1	125	98	99	> 99
3[d)]	1	125	99	99	> 99
4	0.5	250	65	65	> 99
5[d)]	0.5	250	> 99	99	> 99
6	0.1	1250	7	0	0

*Reaction conditions: BiPhePhos **43** was dissolved in toluene (2 mL) and $Ni(cod)_2$ **25** was added. HCN (50 µL, 1.25 mmol, 1.25 eq.) is then dissolved in cold toluene (1 mL) in a separate flask and injected into the reaction vessel. After 30 minutes, styrene **28** (104 mg, 1 mmol, 1 eq.) is added. After the reaction time of 3 h, n-decane was added as internal standard. a): Based on GC analysis with n-decane as internal standard, linear:branched product. b): Yield of the branched product. c): Selectivity to product nitriles. d): No delayed styrene **28** addition.*

First, the selectivities for the branched product are consistently excellent. No other products can be observed. With a Ni:HCN ratio of 1:125 under normal conditions (entry 3), the same results can be achieved as with the subsequent addition of styrene **28** (entry 2), proving that the catalyst stays active at least over a 30-minute period. Major catalyst deactivation occurs if

250 *eq.* HCN are applied to the nickel catalyst within the first 30 minutes resulting in yield and conversion beeing reduced to 65% (entry 4). In comparison, quantitative conversion and yield are achievable when going through the optimized reaction protocol (entry 5). This highlights the shortcomings of the above NMR studies, which have shown immediate catalyst deactivation when 125 or even 250 *eq.* of HCN are applied. These shortcomings are likely to consist of an NMR spectrum showing an average value over 15 minutes. Furthermore, a significant shortcoming is the potential contamination with oxygen when transferring the reaction solution to the NMR tube despite extreme care. The results obtained from this delayed styrene **28** addition can be regarded as more reliable.

If 1250 *eq.* of HCN are applied, no nitrile product formation can be observed, due to immediate catalyst deactivation (entry 6).

3.2.4 Stability of BiPhePhosNi(H)CN in presence of a Lewis acid

A strong impact of the Lewis acid on selectivity is already described in literature—using $AlCl_3$, the linear nitrile product is favored over the branched product in styrene **28** hydrocyanation.[5] However, it's impact on the catalysts stability remains largely unknown. During previous investigations, it was noticed that adding a Lewis acid led to deactivation of the catalyst (section 3.1.3.2). Therefore, further investigations are now being carried out regarding the catalyst stability in presence of a Lewis acid. The aim is to determine the maximum ratio of $Ni(cod)_2$ **25** to $AlCl_3$ at which the nickel remains catalytically active. The exact reason for the drop in conversion and yield when the Ni:$AlCl_3$-ration exceeds 1:5 ratio remains unknown. To fill this gap, the Ni:$AlCl_3$-ratio is investigated.

3.2.4.1 Lewis acid without solving in THF

According to the conditions mentioned in chapter I, no THF was added first. A Ni:Al ratio of 1:1 is selected, as it is well established.

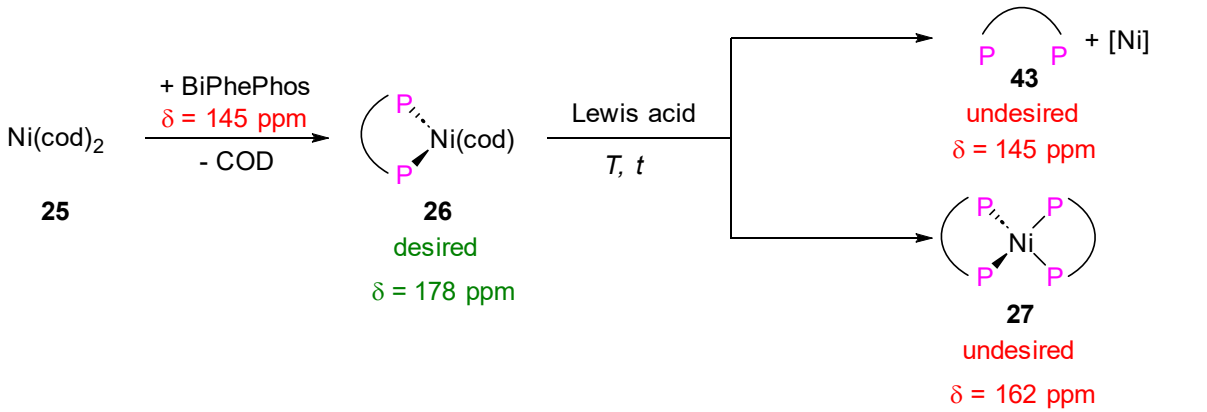

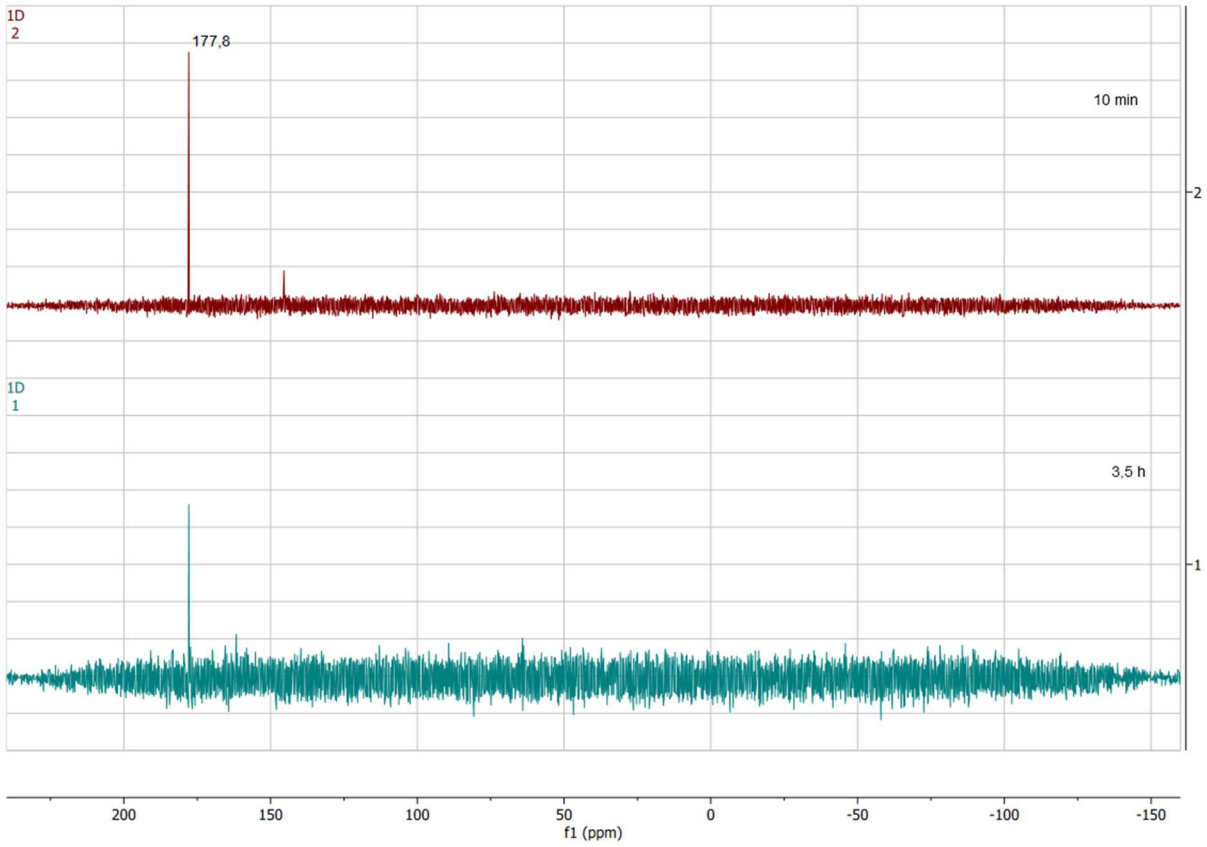

*Figure 37: $^{31}P\{^{1}H\}$-NMR spectra (162 MHz, toluene) of the reaction of BiPhePhosNi(cod) **26** with $AlCl_3$, Ni:Al = 1:1 at room temperature. Reaction conditions: BiPhePhos **43** (26.3 mg, 0.03 mmol, 1.2 eq.) was dissolved in toluene (0.75 mL) and $Ni(cod)_2$ **25** (7.7 mg, 0.028 mmol, 1 eq.) was added. $AlCl_3$ (3.7 mg, 0.028 mmol, 1 eq.) was then added to the mixture.*

After 10 minutes, a signal can be observed at 177.8 ppm, that can be assigned to the catalytically active species BiPhePhosNi(cod) **26**. This signal is still detectable after 3.5 h but with reduced intensity, as a precipitate can be observed over time. This precipitate collects at the lower end of the NMR tube and cannot be measured there. This drastically decreases the concentration of the catalyst in solution resulting in reduced NMR signal intensities and increased signal-to-noise ratio. A moderate stability was observed, and the ratio was further increased to 1:5 (Figure 38).

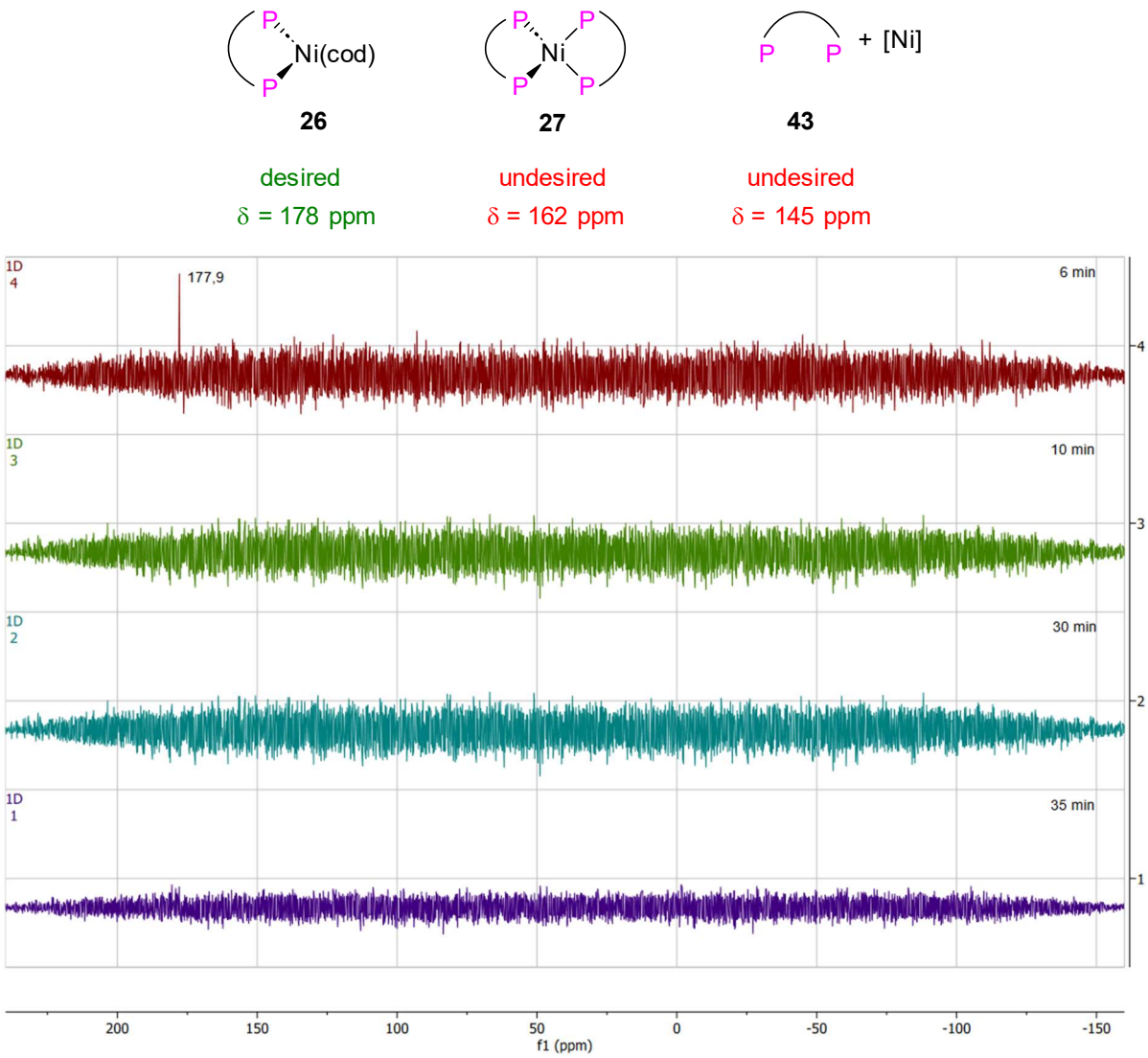

*Figure 38: $^{31}P\{^{1}H\}$-NMR spectra (162 MHz, Toluol) of the reaction of BiPhePhosNi(cod) **26** with $AlCl_3$, Ni:Al = 1:5 at room temperature. Reaction conditions: BiPhePhos **43** (23.7 mg, 0.03 mmol, 1.2 eq.) was dissolved in toluene (0.75 mL) and $Ni(cod)_2$ **25** (6.9 mg, 0.025 mmol, 1 eq.) was added. $AlCl_3$ (16.6 mg, 0.125 mmol, 5 eq.) was then added to the mixture.*

Interestingly, due to the low solubility of $AlCl_3$ in toluene, a sediment forms, which turns yellow quickly. After only 10 minutes, catalyst deactivation is almost complete, and precipitate formation increases.

Furthermore, in literature, most hydrocyanation reactions are set up in a glovebox, where the ligand, $Ni(cod)_2$ **25**, and $AlCl_3$ are preformed. After a transition to a fume hood, the substrate and the HCN is added. The rapid catalyst deactivation by $AlCl_3$ found in this thesis, occurs during that transition time and is the reason for the significant drop in conversion and yield if the Ni:Al ratio exceeds 1:5.[5] The observed quantitative styrene **28** conversion[5] can be explained styrene polymerization making it nondetectable via GC.

Despite the rapid deactivation, the ratio is increased to 1:10 to investigate limitations (Figure 39). Even faster deactivation is expected here.

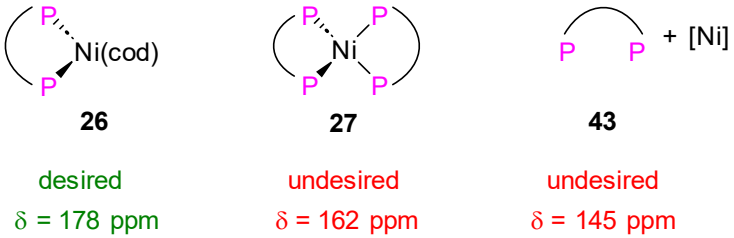

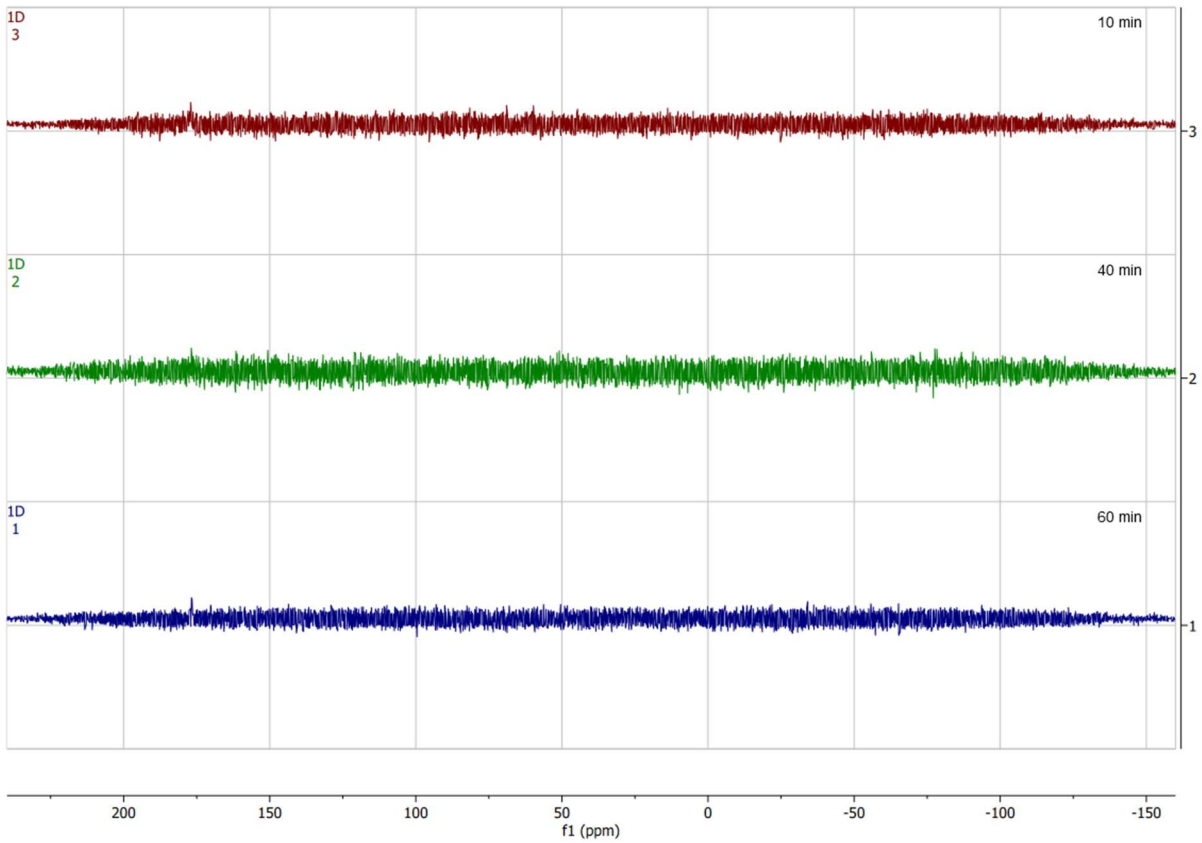

*Figure 39: $^{31}P\{^1H\}$-NMR spectra (162 MHz, Toluene) of the reaction of BiPhePhosNi(cod) **26** with $AlCl_3$, Ni:Al = 1:10 at room temperature. Reaction conditions: BiPhePhos **43** (23.7 mg, 0.03 mmol, 1.2 eq.) was dissolved in toluene (0.75 mL) and $Ni(cod)_2$ **25** (6.9 mg, 0.025 mmol, 1 eq.) was added. $AlCl_3$ (33.25 mg, 0.250 mmol, 10 eq:) was then added to the mixture.*

As expected, the catalyst deactivation proceeds immediately, and only traces of the catalytically active species BiPhePhosNi(cod) **26** can be detected after just 10 minutes. Furthermore, a white precipitate quickly appears in both reactions after adding $AlCl_3$.

The low solubility of $AlCl_3$ in toluene is common to all measurements. Yellow-brown traces were observed around the $AlCl_3$ particles. For this reason, the Lewis acid was dissolved in THF beforehand in further investigations. The aim is to obtain homogeneous reaction solutions. Due to the higher availability of Lewis acid, faster deactivation can be expected at lower Al concentrations.

3.2.4.2 Lewis acid dissolved in THF

The solubility of $AlCl_3$ in dry THF is significantly higher compared to toluene. In the following investigations, the $AlCl_3$ was pre-dissolved in THF and mixed with the BiPhePhosNi(cod) **26** solution in toluene.

Initially, a Ni:Al ratio of 1:1 was also used (Figure 40).

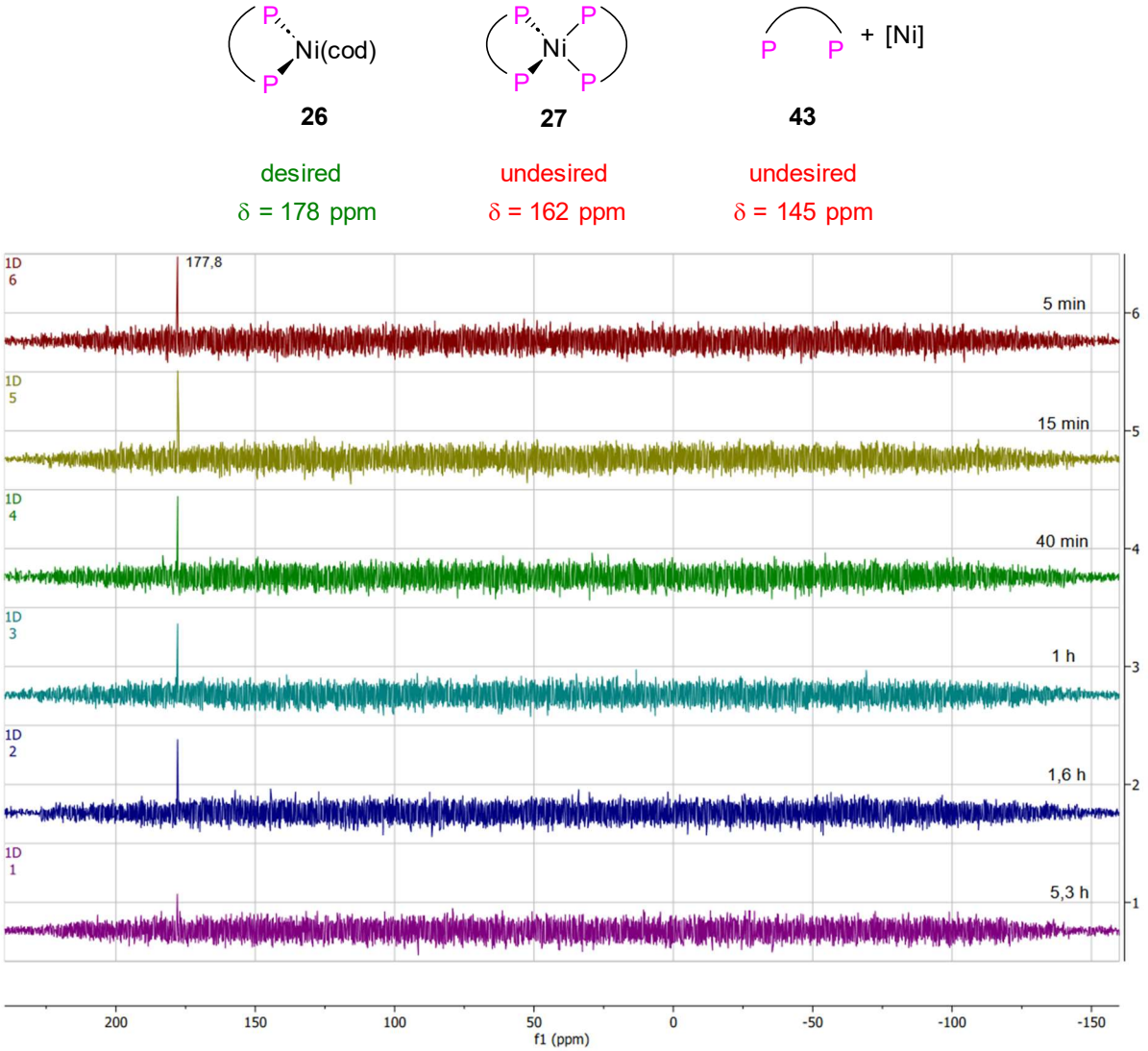

*Figure 40: $^{31}P\{^1H\}$-NMR spectra(162 MHz, toluene) of the reaction of BiPhePhosNi(cod) **26** with $AlCl_3$, Ni:Al = 1:1 at room temperature in the presence of THF. Reaction conditions: BiPhePhos **43** (47.4 mg, 0.06 mmol, 1.2 eq.) was dissolved in toluene (2.5 mL) and $Ni(cod)_2$ **25** (4.6 mg, 0.017 mmol, 1 eq.) was added. $AlCl_3$ (6.7 mg, 0.028 mmol, 1 eq.) was then dissolved in THF (0.5 mL) and added to the mixture.*

Interestingly, a light yellow coloration quickly appeared in all reaction solutions. Furthermore, the active species can be detected over a long period of time. Contrary to the assumption of faster decomposition, stabilization was observed. No precipitation was observed.

With these results, the Al:Ni-ratio was increased to 1:5 (Figure 41).

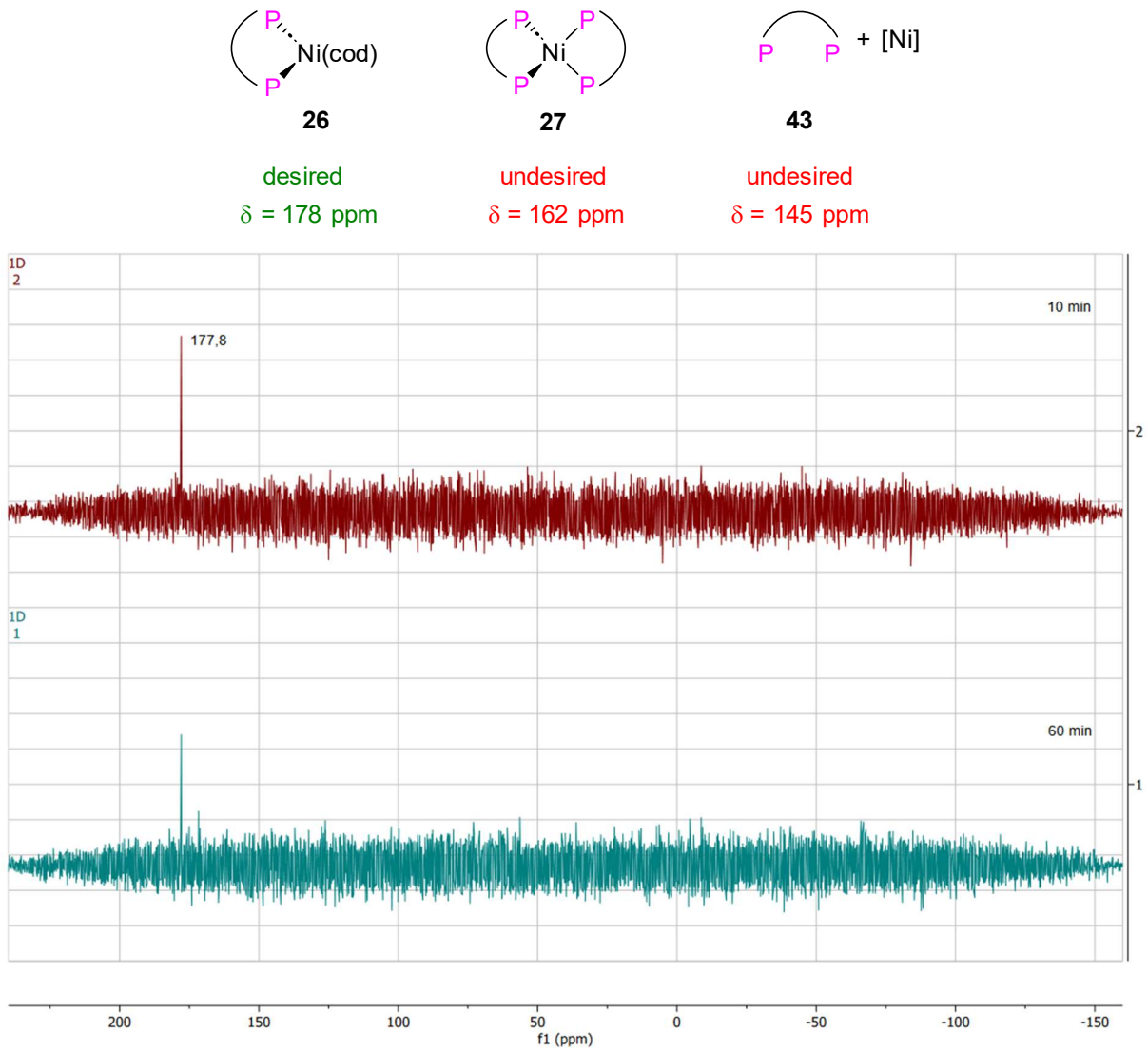

*Figure 41: $^{31}P\{^{1}H\}$-NMR (162 MHz, toluene) of the reaction of BiPhePhosNi(cod) **26** with $AlCl_3$, Ni:Al = 1:5 at room temperature in the presence of THF. Reaction conditions: BiPhePhos **43** (47.4 mg, 0.06 mmol, 1.2 eq.) was dissolved in toluene (2.5 mL) and $Ni(cod)_2$ **25** (13.8 mg, 0.05 mmol, 1 eq.) was added. Subsequently, $AlCl_3$ (33.5 mg, 0.25 mmol, 5 eq.) was dissolved in THF (0.5 mL) and added to the mixture.*

Here, too, significant quantities of the active species could still be detected after 1 hour. Unfortunately, a slight precipitate formed again, which indicates catalyst deactivation, which is also represented by an increase in the signal-to-noise ratio.

Finally, tests were carried out with a ratio of 1:20 (Figure 42).

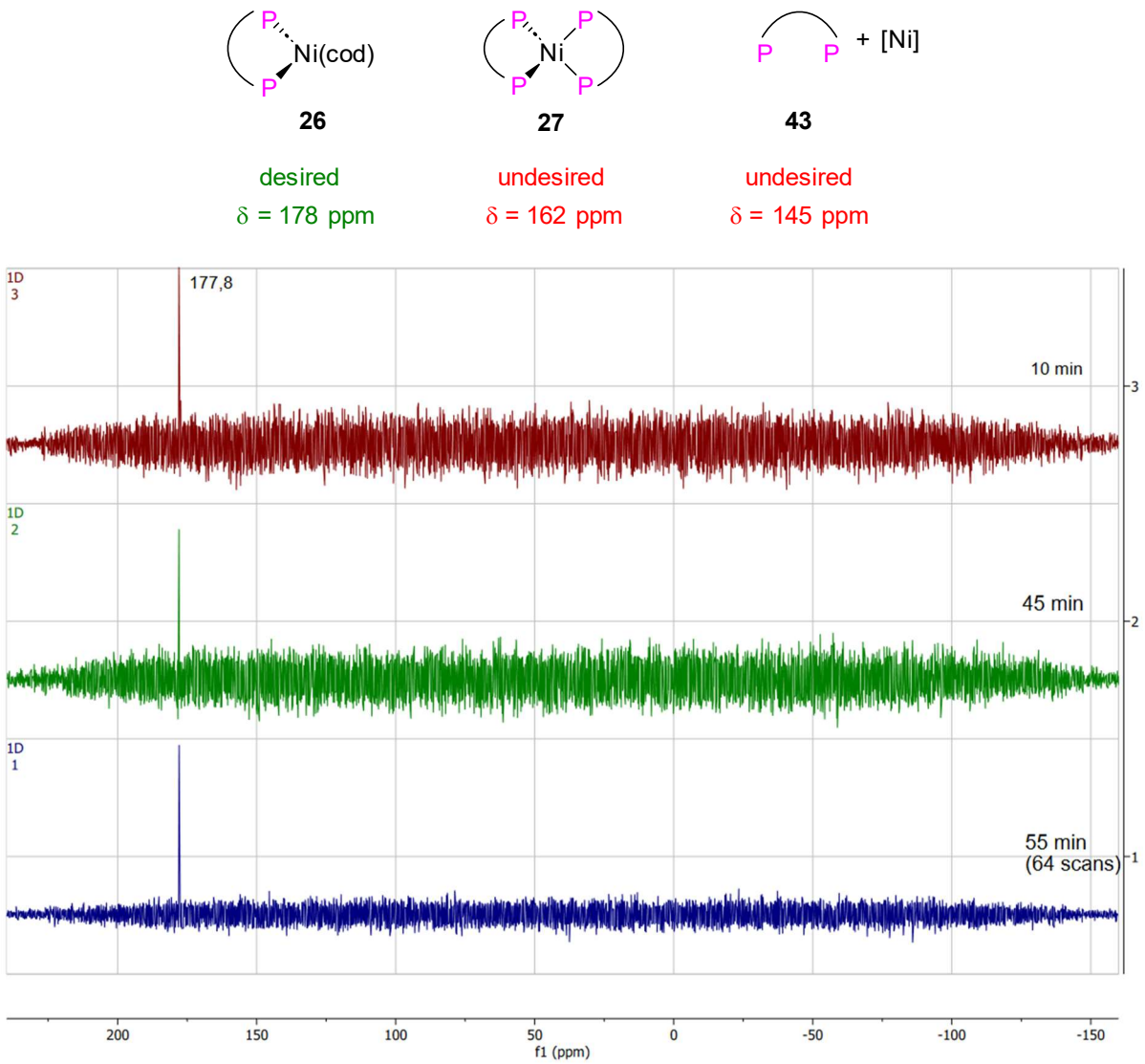

*Figure 42: $^{31}P\{^1H\}$-NMR spectra (162 MHz, toluene) of the reaction of BiPhePhosNi(cod) **26** with $AlCl_3$, Ni:Al = 1:20 at room temperature in the presence of THF Reaction conditions: BiPhePhos **43** (47.4 mg, 0.06 mmol, 1.2 eq.) was dissolved in toluene (2.5 mL) and $Ni(cod)_2$ **25** (13.8 mg, 0.05 mmol, 1 eq.) was added. Subsequently, $AlCl_3$ (134 mg, 1 mmol, 20 eq.) was dissolved in THF (0.5 mL) and added to the mixture.*

No catalyst deactivation can be detected here, either. Due to the already mentioned limitations of the NMR-studies presented here, further investigations focus on converting styrene **28** to the nitrile products as an indirect prove of the catalytic active species.

3.2.4.3 Analysis through styrene hydrocyanation

Experiments were carried out using styrene **28** as this has already proven to show excellent conversion and yield in absence of a Lewis acid (Table 24, entry 1 and 3. Catalyst loadings of 1 mol% and 0.5 mol% are selected. $AlCl_3$ is added as a solution in dry, degassed THF (Table 24, entries 2 and 4).

*Table 24: Styrene **28** hydrocyanation in presence of dissolved $AlCl_3$.*

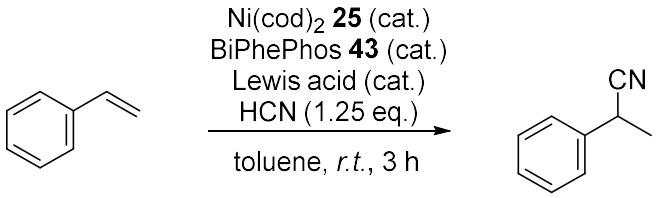

28 **29b**

entry	Lewis acid	*eq.* Ni(cod)$_2$ [mol%]	Ni:HCN ratio	*X*[a)] [%]	*Y*[a), b)] [%]	*S*[c)] [%]
1[d)]	-	1	125	98	99	> 99
2[e)]	$AlCl_3$	1	125	20	11	53
3[d)]	-	0.5	250	> 99	99	> 99
4[e)]	$AlCl_3$	0.5	250	< 1	0	< 1

*a): Based on GC analysis with n-decane as an internal standard. b): Yield of the branched product. c): Selectivity to product nitriles. d): Reaction conditions: BiPhePhos **43** was dissolved in toluene (2 mL) and Ni(cod)$_2$ **25** was added. Styrene **28** (104 mg, 1 mmol, 1 eq.) is then added. HCN (50 µL, 1.25 mmol, 1.25 eq.) was dissolved in cold toluene (1 mL) in a separate flask and injected into the reaction vessel. After the reaction time of 3 h, n-decane was added as internal standard. e): Reaction conditions: BiPhePhos **43** was dissolved in toluene (1.5 mL) and Ni(cod)$_2$ **25** was added. $AlCl_3$ was added as a solution in THF (0.5 mL). Styrene **28** (104 mg, 1 mmol, 1 eq.) is then added. HCN (50 µL, 1.25 mmol, 1.25 eq.) was dissolved in cold toluene (1 mL) in a separate flask and injected into the reaction vessel. After the reaction time of 3 h, n-decane was added as internal standard.*

In the presence of Lewis acid conversion, yield and selectivity are significantly reduced. When using 1 mol% nickel-catalyst/Lewis acid, a conversion only reaches 20%, whereas the yield of the branched product is only 11% (entry 2). No conversion can be observed if the catalyst or Lewis acid concentration is further reduced to 0.5 mol% (entry 4). In comparison, if no $AlCl_3$ is added, a quantitative conversion with a 99% yield is achieved (entries 1 and 3). This clearly

shows that the Lewis acid $AlCl_3$ has a catalyst-deactivating effect, especially at higher Ni:$AlCl_3$:HCN- ratios, in addition to its selectivity-reversing effect described in literature.[5]

Furthermore, since the interaction of the $AlCl_3$ with the nickel-catalyst leads to the formation of the linear nitrile product **29l**, the formation of only the branched product **29b** indicates that the $AlCl_3$ is not interacting with the HCN or CN-containing catalyst. This can be explained by the THF coordination to the $AlCl_3$ and, therefore, disfavoring coordination to the nitrile-/cyanide group. This could lead to the formation of HCl or the release of chloride, which has a catalyst-deactivating effect. To prevent HCl formation and free chloride-ions, chloride-free aluminum salts are applied alternatively in styrene **28** hydrocyanation.

3.2.4.4 Chloride-free Lewis acids

In the present studies, in addition to the chloride-free $Al(OTf)_3$ and $Al_2(SO_4)_3$, $Al(OEt)_3$ and $Al(acac)_3$ are applied, which are readily soluble in organic solvents. Furthermore, to determine possible limitations in application of chloride free lewis acids, different catalyst loadings and Nickel:Lewis acid-ratios are applied. The achieved yield and conversion are used as a measure of catalyst stability, whereas the *l:b*-ratio of the products provides information on the aluminum participation in the catalytic cycle.

*Table 25: Styrene **28** hydrocyanation in the presence of aluminum acetylacetonate.*

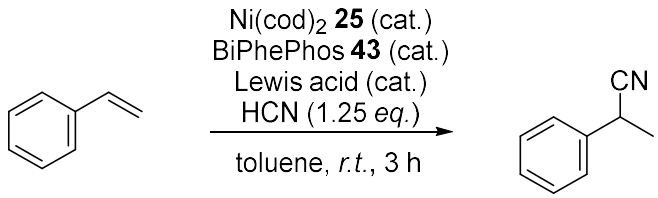

28 **29b**

entry	Al salt	*eq.* Ni(cod)$_2$ [mol%]	*X*[a)] [%]	*Y*[a), b)] [%]	*S*[c)] [%]
1	$Al(acac)_3$	2.5	> 99	99:0	> 99
2	$Al(acac)_3$	1	> 99	99:0	> 99
3	$Al(acac)_3$[d)]	0.5	> 99	99:0	> 99
4	$AlCl_3$[e)]	1	20	11:0	53

*Reaction conditions: BiPhePhos **43** was dissolved in toluene (2 mL) and Ni(cod)$_2$ **25** was added. The Lewis acid and styrene **28** (104 mg, 1 mmol, 1 eq.) are then added. HCN (50 µL, 1.25 mmol, 1.25 eq.)*

was dissolved in cold toluene (1 mL) in a separate flask and injected into the reaction vessel. After the reaction time of 3 h, n-decane was added as internal standard. a): Based on GC analysis with n-decane as internal standard, b): Yield to branched:linear product c) Selectivity to product nitriles., d): Ni:L:Al = 1:1.2:5. e): $AlCl_3$ was added as a solution in THF.

When $Al(acac)_3$ is applied, quantitative styrene **28** conversion and only the branched product is observed with excellent selectivity (entries 1–3). Therefore, it can be concluded that adding $Al(acac)_3$ does not lead to a deactivation of the catalyst, as is the case with $AlCl_3$ (entry 4). Unexpectedly, only the branched product 2-phenylpropionitrile **29b** was formed. This suggests that $Al(acac)_3$ addition does not affect the hydrocyanation reaction. A potential reason is the octahedral coordination of the aluminum atom by the three bidentate acetylacetonate ligands. Therefore, other aluminum salts with less strongly coordinating character anions will be used in the following. These include $Al(OTf)_3$, $Al_2(SO_4)_3$, or $Al(OEt)_3$ (Table 26).

*Table 26: Styrene **28** hydrocyanation in the presence of different aluminum salts.*

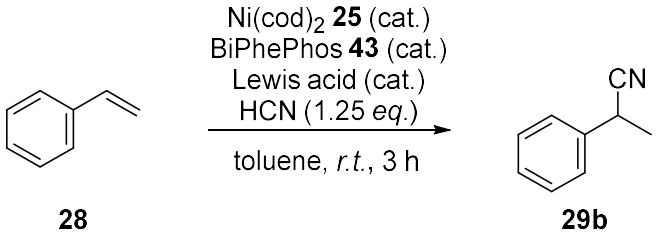

28 **29b**

entry	Al-salt	$X^{a)}$ [%]	$Y^{a), b)}$ [%]	$S^{c)}$ [%]
1	-	> 99	99:0	99
2	$Al(OEt)_3$	> 99	99:0	99
3	$Al_2(SO_4)_3$	> 99	99:0	99
4	$Al(OTf)_3$	81	86:0	> 99

*Reaction conditions: BiPhePhos **43** was dissolved in toluene (2 mL) and $Ni(cod)_2$ **25** was added. The Lewis acid is added. Styrene **28** (104 mg, 1 mmol, 1 eq.) is then added. HCN (50 µL, 1.25 mmol, 1.25 eq.) was dissolved in cold toluene (1 mL) in a separate flask and injected into the reaction vessel. After the reaction time of 3 h, n-decane was added as internal standard. a): Based on GC analysis with n-decane as internal standard, b): Yield to branched:linear product c) Selectivity to product nitriles. d) $AlCl_3$ was added as a solution in THF.*

In the presence of $Al(OEt)_3$ (entry 2) and $Al_2(SO_4)_3$ (entry 3), styrene **28** was quantitatively converted to the branched product **29b**. These findings can be attributed to the strong coordination of the corresponding anion ($Al(OEt)_3$) or the poor solubility ($Al_2(SO_4)_3$). This

shows that chloride free Lewis acids do not deactivate the nickel catalyst and that the deactivation is likely caused by *in-situ* formed HCl. Due to the exclusive formation of the branched product, a selectivity-determining intervention in the reaction mechanism analogous to $AlCl_3$ can also be excluded. The presence of $Al(OTf)_3$ also does not interfere with the reaction mechanism in a selectivity-determining manner, but also slightly deactivates the catalyst, albeit to a lesser extent than $AlCl_3$ (entry 4).

In summary, chloride-free aluminum salts do not, in case of $Al(acac)_3$, $Al(OEt)_3$, and $Al_2(SO_4)_3$ or hardly, like $Al(OTf)_3$, interfere with the nickel-catalyzed hydrocyanation reaction.

3.2.5 Activity of Hydrocyanation catalysts

A catalyst featuring a high catalytic activity, enabling high space time yields, is crucial for industrial application. Due to the catalyst deactivation by $AlCl_3$ (section 3.2.4), that severely reduces the catalytic activity, the catalysts activity in styrene **28** hydrocyanation is investigated in the absence of $AlCl_3$.

3.2.5.1 Activity with BiPhePhos application

To protect the sensitive catalyst against deactivation via oxygen contamination, for further investigation the reaction procedure includes the following: In two-thirds of the solvent, the preforming (coordination of $Ni(cod)_2$ **25** by BiPhePhos **43**) is carried out in a glovebox. In a fume hood, styrene **28** is added to the preformed BiPhePhosNi(cod) **26** solution through a septum via syringe. In a separate Schlenk tube, the required stoichiometric amount of HCN is added to one-third of the solvent in the cold, where the HCN freezes out immediately. The HCN-solution is then slowly heated to the melting point of HCN (-15 °C) before being drawn into a syringe. To start the reaction, the cold HCN-solution is injected into the reaction vessel at room temperature via the septum.

From this procedure, a temperature profile can be expected potentially impacting the catalytic activity, since reaction rates are generally temperature dependent. This makes investigations of the temperature profile necessary, which was recorded using an internal thermometer (Figure 43).

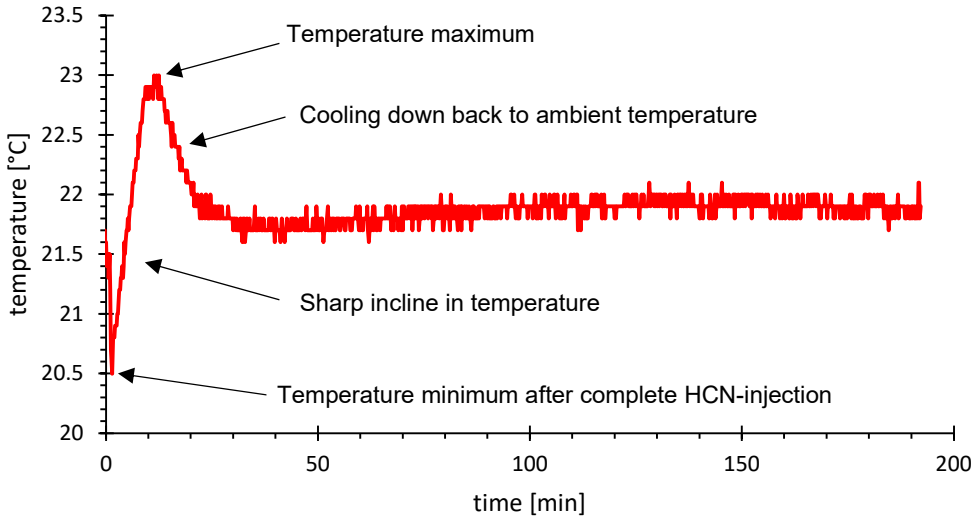

*Figure 43: Temperature profile of styrene **28** hydrocyanation with pre-cooling of the HCN. Reaction conditions: BiPhePhos **43** (4.7 mg, 0.006 mmol, 0.006 eq.) was dissolved in toluene (2 mL) and $Ni(cod)_2$ **25** (1.4 mg, 0.005 mmol, 0.005 eq.) was added. Styrene **28** (104 mg, 1 mmol, 1 eq.) was then added. HCN (50 µL, 1.25 mmol, 1.25 eq.) was dissolved in cold toluene (1 mL) in a separate flask and injected into the reaction vessel. After the reaction time of 3 h at room temperature, n-decane was added as an internal standard.*

Following the addition of the cold hydrogen cyanide (HCN) solution to the catalyst/styrene **28** mixture, an immediate temperature drop of 1.3 °C below 22 °C (21.8 °C) is observed. Subsequently, a rapid temperature rise to a 23 °C occurs within 11 minutes, attributed to the exothermic nature of the hydrocyanation reaction. After 11 minutes the exothermic hydrocyanation is (almost) finished, allowing the reaction mixture to cool back down to ambient temperature.

Surprisingly, the reaction displays only a minimal temperature profile between 20.5 and 23 °C, which can be attributed to the use of a syringe with a cannula. This configuration exposes the HCN solution in the cannula to a high surface-to-volume ratio, enabling an efficient heat exchange.

However, repeating the experiment without pre-cooling the toluene eliminates the 1.5 °C temperature drop. If the toluene is kept at room temperature, a slight gas formation can be seen immediately after the addition of HCN, consisting of vaporizing HCN (Figure 44).

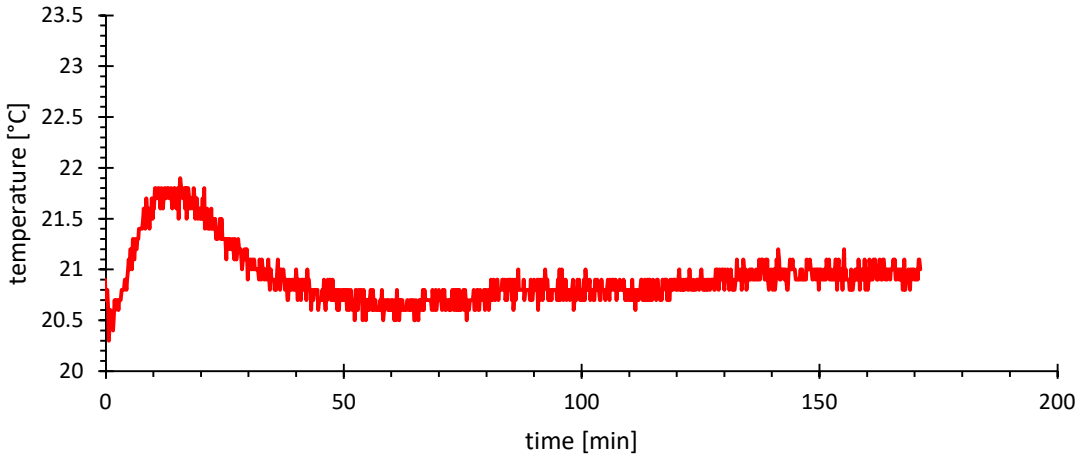

*Figure 44:. Temperature profile of styrene **28** hydrocyanation without pre-cooling of the HCN. Reaction conditions: BiPhePhos **43** (4.7 mg, 0.006 mmol, 0.006 eq.) was dissolved in toluene (2 mL) and Ni(cod)$_2$ **25** (1.4 mg, 0.005 mmol, 0.005 eq.) was added. Styrene **28** (104 mg, 1 mmol, 1 eq.) was then added. HCN (50 µL, 1.25 mmol, 1.25 eq.) was dissolved in cold toluene (1 mL) in a separate flask and injected into the reaction vessel. After the reaction time of 3 h at room temperature, n-decane was added as an internal standard.*

Considering the minor impact on the reaction temperature profile, cooling of the HCN was maintained to ensure precise stoichiometry and compliance with safety parameters, thus ensuring controlled and safe execution of the reaction protocol.

The minimal temperature changes derived from the operational procedure can be neglected, as the impact on the reaction rates is only minimal. These findings allow for studies on the catalytic activity at distinct temperatures leading to reproducible and comparable results.

The reaction progress was monitored by GC analysis of the samples withdrawn from the reaction mixture. For this study, a catalyst concentration of 0.5 mol% was selected.

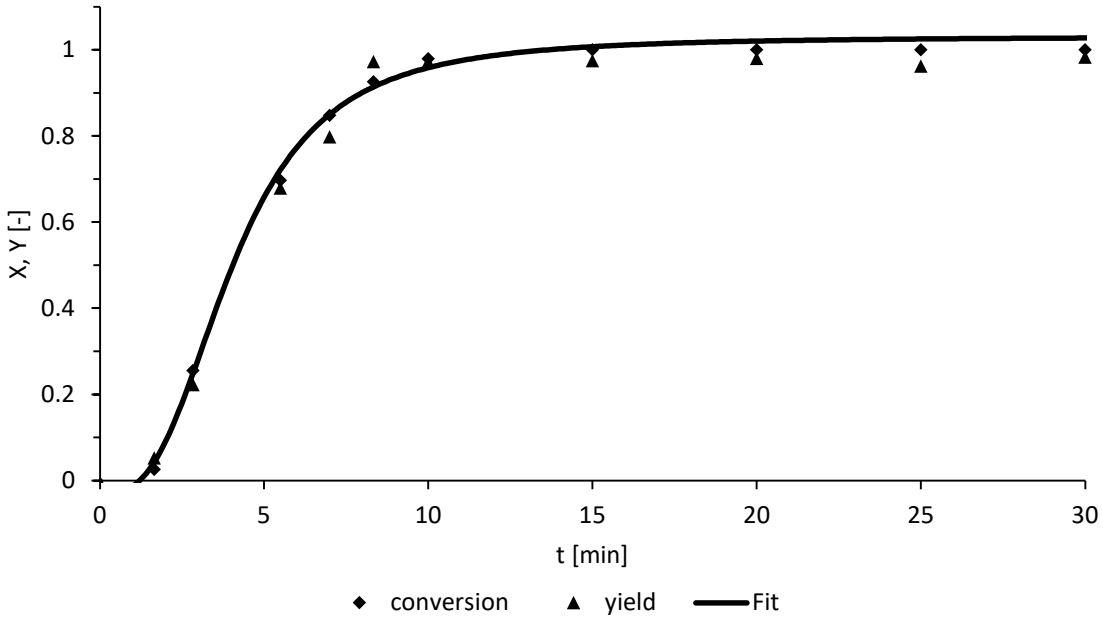

*Figure 45: Reaction profile of styrene **28** hydrocyanation: Reaction conditions: BiPhePhos **43** (11.8 mg, 0.015 mmol, 0.006 eq.) is dissolved in toluene (5 mL) and Ni(cod)$_2$ **25** (3.4 mg, 0.013 mmol, 0.005 eq.) is added. Styrene **28** (260.5 mg, 2.5 mmol, 1 eq.) and di-n-butyl ether are then added as internal GC standard. HCN (125 µL, 3.125 mmol, 1.25 eq.) is dissolved in cold toluene (2.5 mL) in a separate flask and injected into the reaction vessel.*

The investigation revealed a remarkably fast reaction, achieving total styrene **28** conversion in just 10 minutes. Notably, 20% conversion was observed already after 2.5 minutes, resulting in a turnover frequency (TOF_{20}) of 817 h^{-1}.

This activity can likely be further increased by reducing the solvent amount, as validated by stepwise solvent reduction from 3 mL (Table 27, entry 1) to 0.5 mL (Table 27, entry 4).

*Table 27: Styrene **28** hydrocyanation with reduced solvent amount.*

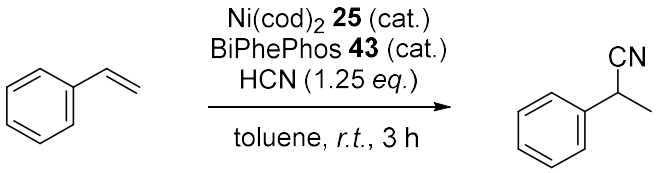

28 **29b**

entry	c(styrene) [mol/L]	Total solvent amount [mL]	$X^{a)}$ [%]	$Y^{a), b)}$ [%]	$S^{c)}$ [%]
1	0.32	3[e)]	> 99	> 99	> 99
2	0.54	1.7	94	99	> 99
3	0.79	1.1	93	98	> 99
4	1.51	0.5[d)]	> 99	> 99	> 99

*Reaction conditions: BiPhePhos **43** (4.7 mg, 0.006 mmol, 0.006 eq.) is dissolved in toluene (0.2 mL), and Ni(cod)$_2$ **25** (1.4 mg, 0.005 mmol, 0.005 eq.) is added. Additional toluene is added if necessary, and styrene **28** (104 mg, 1 mmol, 1 eq.) is added. HCN (50 µL, 1.25 mmol, 1.25 eq.) is dissolved in cold toluene (0.5 mL) in a separate flask and injected into the reaction vessel. After the reaction time of 3 h, n-decane is added as an internal standard. a): Based on GC analysis with n-decane as an internal standard. b): Yield of the branched product. c): Selectivity to product nitriles. d): HCN dissolved in 1 mL toluene. e): Addition of HCN dissolved in 0.3 mL toluene.*

Under all reaction conditions, the conversion and yield exceeded 90%, which excludes the possibility of catalyst deactivation due to an increased HCN concentration. Another reaction profile was recorded for the minimum amount of solvent (entry 4), reducing the total reaction volume from 8.1 mL to 1.4 mL (Figure 46).

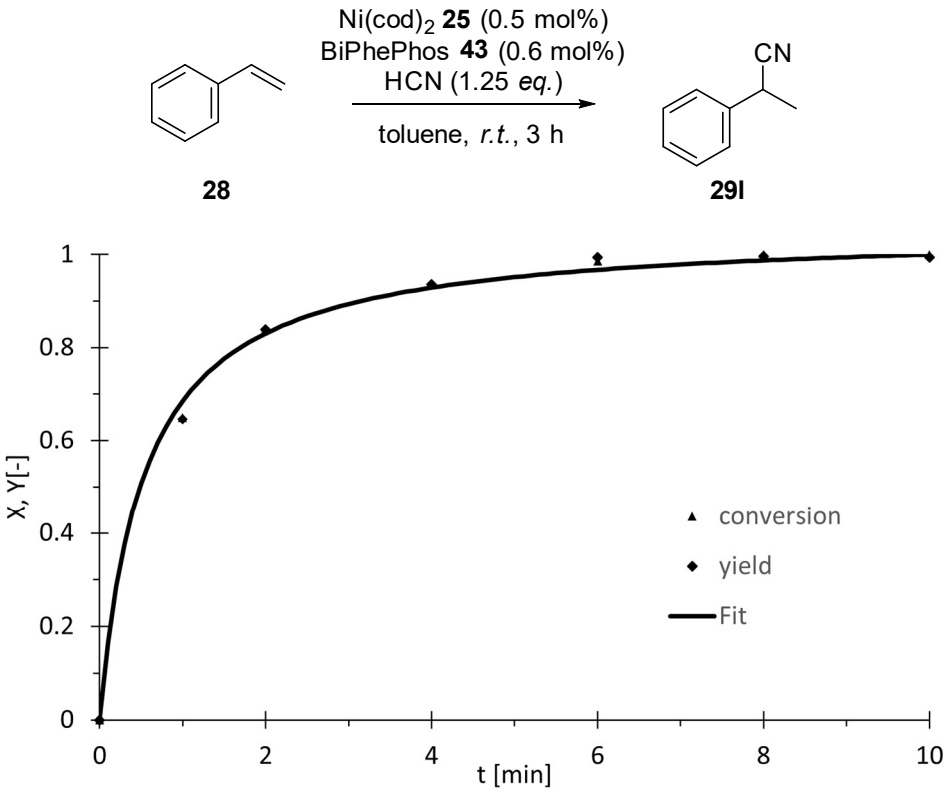

*Figure 46: Reaction profile for styrene **28** hydrocyanation with reduced amount of solvent. Reaction conditions: BiPhePhos **43** (11.8 mg, 0.015 mmol 0.006 eq.) is dissolved in toluene (0.5 mL), and Ni(cod)$_2$ **25** (3.4 mg, 0.0125 mmol, 0.005 eq.) is added. Styrene **28** (260.5 mg, 2.5 mmol, 1 eq.) and di-n-butyl ether as an internal GC standard are added. HCN (125 µL, 3.125 mmol, 1.25 eq.) is dissolved in cold toluene (0.75 mL) in a separate flask and injected into the reaction vessel. Conversion and yield based on GC analysis with DBE as internal standard. Fit: X(t) = (1.05375t)/(0.5381627 + t).*

It turns out that complete conversion is reached after 6 minutes, at which point no remaining styrene **28** is detected (Figure 46). A yield of 70% is achieved after just one minute, which can be interpolated to 20% conversion within approximately 7.5 s, relating to a TOF_{20} of 19 000 h^{-1}. Compared to the previous experiment, this remarkable increase in performance exceeds all values previously documented in the scientific literature. Further reducing the quantity of solvent employed in the experiment appears impractical due to the limited solubility of BiPhePhos **43**. Alternatively, reducing the solvent amount for dilution of the highly volatile HCN risks inaccurate stoichiometry. By increasing the temperature during activity studies, the balance between deactivation and activity is investigated. The slower, gradual deactivation of the catalyst might still allow the completion of the hydrocyanation reaction before complete catalyst deactivation. At 60 °C, TOF_{20} increases to 191,000 h^{-1}, more than ten times the results at 22 °C (Table 28, entries 1 and 2). Further raising the temperature to 90 °C boosts activity even further to 309 000 h^{-1} (Table 28, entry 3).

*Table 28: Nickel/BiPhePhos **43** catalyst activity in styrene **28** hydrocyanation at 22, 60, and 90 °C.*

entry	*T* [°C]	TOF_{20} [x 10^3 h^{-1}]
1	22	19
2	60	191
3	90	309

*Reaction conditions: BiPhePhos **43** (11.8 mg, 0.015 mmol, 0.006 eq.) is dissolved in toluene (0.5 mL), and $Ni(cod)_2$ **25** (3.4 mg, 0.0125 mmol, 0.005 eq.) is added. Styrene **28** (260.5 mg, 2.5 mmol, 1 eq.) and di-n-butyl ether as an internal GC standard are then added. HCN (125 µL, 3.125 mmol, 1.25 eq.) is dissolved in cold toluene (0.75 mL) in a separate flask and injected into the reaction vessel.*

It can be concluded that the hydrocyanation reaction rate shows a higher temperature dependency compared to catalyst deactivation by bischelate formation.

3.2.5.2 Comparison to other ligands

To assess the catalytic potential of the diphosphite BiPhePhos **43**, the diphosphanes Xantphos **35** and DPEPhos **31** will be used. The results obtained will be compared in terms of yield and conversion. First, some preliminary tests will be carried out.

*Table 29: Styrene **28** hydrocyanation with other ligands.*

entry	ligand	*X*[a)] [%]	*Y*[a), b)] [%]	*S*[c)] [%]
1	BiPhePhos **43**	>100	99	99
2	Xantphos **35**	32	32	> 99
3	DPEPhos **31**	11	4	40

*Reaction conditions: Ligand (0.006 mmol, 0.006 eq.) is dissolved in toluene (2 mL) and $Ni(cod)_2$ **25** (1.4 mg, 0.005 mmol, 0.005 eq.) is added. Styrene **28** (104 mg, 1 mmol, 1 eq.) is then added. HCN (50 µL, 1.25 mmol, 1.25 eq.) was dissolved in cold toluene (1 mL) in a separate flask and injected into the reaction vessel. After the reaction time of 2 h at room temperature, n-decane was added as an internal standard. a): Based on GC analysis with n-decane as an internal standard. b): Yield of the branched product. c): Selectivity to product nitriles.*

When using Xantphos **35** or DPEPhos **31**, reduced turnovers of 32 and 11%, respectively, can be observed. The yields are also reduced to 32 and 4%, respectively (Table 29, Entry 2

and 3). In the case of DPEPhos **31**, the low selectivity of 40% could be explained by styrene **28** oligomerization. This does not occur when Xantphos **35** is used. A direct comparison with BiPhePhos **43** shows that the chemical performance of both diphosphanes lags considerably behind that of BiPhePhos **43**. A yield of 99% can be achieved with the latter (Table 29, entry 1).

Due to the low yields with Xantphos **35** and DPEPhos **31**, preparing reaction profiles at room temperature was not suitable. Increasing the temperature comparable to the procedure with BiPhePhos **43** was not carried out due to time limitations of this project.

3.2.5.3 Scale-up and HCN dosage

A notable constraint within the present reaction setup is the required minimum catalyst concentration of 0.5 mol% to achieve complete conversion and yield (Table 30, entry 1). Lowering the catalyst concentration to 0.1 mol% only yields 8% of the 2-phenyl propionitrile (Table 30, entry 2). Despite extreme care when working in the inert atmosphere, one potential reason again is traces of oxygen contamination leading to catalyst deactivation, considering the low amount of catalyst, 0.001 mmol, applied in the reaction. Although the reaction protocol has been optimized, impurities may occur during the production of the HCN solution. In this case, running the reaction at a larger scale is expected to minimize that risk.

The reaction (Table 30, entry 3) was scaled up by a factor of 5, maintaining the total catalyst amount (0.005 mmol $Ni(cod)_2$ **25**) used in entry 1. The result is a conversion and yield exceeding 99% (Table 30, entry 3).

Another experiment analogous to entry 2 was performed, but this time, HCN was added slowly over 5 minutes. A conversion of 59% instead of 8% was achieved at > 99% selectivity (Table 30, entry 4). Both observations can be attributed to catalyst deactivation by traces of oxygen present in the hydrogen cyanide solution. If applied sufficiently, i.e., exceeding the amount of the traces of oxygen, the remaining catalyst stays active and results in product formation. In the case of the fivefold preparation (Table 30, entry 3), where 0.005 mmol of $Ni(cod)_2$ **25** are present (similar to the entry 1 conditions), this catalyst amount appears sufficient to achieve quantitative conversion and yield despite partial deactivation by oxygen. In entry 4, assuming the same total amount of contaminant in the HCN solution as in entry 2, the catalyst deactivation is sustained due to the slow addition. Ultimately, however, when the total amount of solution has been added, complete catalyst de-activation occurs, preventing full styrene **28** conversion.

Excessive HCN concentrations are another potential cause of catalyst deactivation, as well. In this case, the dosage experiment (Table 30, entry 4) would have been expected to show

total conversion/yield due to the HCN concentration being kept low. Furthermore, the fivefold preparation (Table 30, entry 3) would have been expected to show only minimal reactivity, maintaining the same Ni:HCN ratio from entry 2, but neither could be observed. This suggests that traces of oxygen are still the leading cause for the low conversion/yields in entry 2.

Table 30: Scale-up and HCN dosing.

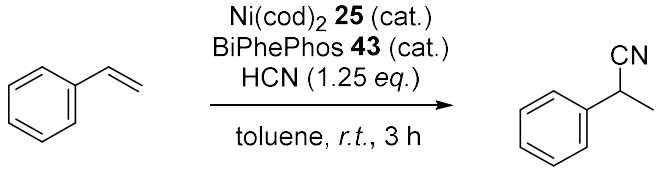

28 **29b**

entry	Batch size (styrene) [mmol]	*eq.* Ni(cod)$_2$ [mol%]	Time of dosage [min]	*X*[a)] [%]	*Y*[a), b)] [%]	*S*[c)] [%]
1	1	0.5	0	> 99	> 99	> 99
2	1	0.1	0	8	< 1	4
3	5	0.1	0	> 99	> 99	> 99
4	1	0.1	5	59	59	> 99
5	20[d)]	0.025	0	22	21	96

*Reaction conditions: BiPhePhos **43** is dissolved in toluene, and Ni(cod)$_2$ **25** is added. HCN is dissolved in cold toluene in a separate flask and injected into the reaction vessel. After the reaction time of 3 h at 22 °C, n-decane is added as an internal standard. a): Based on GC analysis with n-decane as an internal standard. b): Yield of the branched product. c): Selectivity to product nitriles. d): Half solvent amount (0.5 mL toluene per 1 mmol Styrene **28**).*

To push the limits further, an experiment at a 20 mmol scale and with a reduced catalyst amount of 0.025 mol% was performed, maintaining the total catalyst amount of 0.005 mmol (entry 5). Under these conditions, 23% conversion and 94% selectivity 21% were observed. This indicates the potential for further improvement by scaling up the batch size, a possibility not explored further in this study.

3.2.5.4 Ligand mixtures

As explained above (section 2.8), there are various types of ligands, such as phosphines and phosphites. These two classes enable different coordination chemistry at the metal center. In combination with the varying electronic effects, this results in different catalytic properties.

Nickel shows different levels of affinity for the corresponding ligand classes depending on the oxidation state. Nickel(0) shows a very high affinity for phosphites, whereas nickel(II) has a high affinity for the less electron-withdrawing phosphines. These different affinities have been used by the application of phosphine-phosphite ligands, like ligand **15,** in the literature (section 2.6, Figure 5) which might prevent catalyst deactivation effectively.[28] By using a ligand mixture consisting of a phosphite- and a phosphine-ligand, a mixed complex is generated *in-situ*. That way, the entry barrier towards combining phosphites and phosphines is drastically lowered as the synthesis of mixed ligands, like **15,** requires a multiple steps synthesis.

In hydrocyanation a Ni^{0}/Ni^{+II} cycle is utilized resulting in both high affinity towards both ligand classes. Thus, a possible deactivation of the BiPhePhos/nickel catalyst system could occur via the dissociation of one of the BiPhePhos **43** donor atoms, during a Ni^{+II}-state (Figure 48).

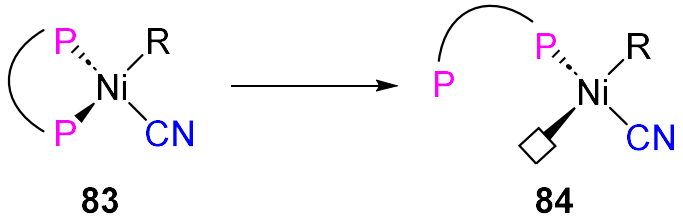

Figure 47: Dissociation of a donor atom from the nickel center.

The freed-up coordination site (**84**) is then available for deactivation by HCN or even oxygen resulting in low catalytic activity. To tackle this challenge, a mixture of triphenylphosphine, preferred for coordination by Ni^{+II}-complexes, and BiPhePhos **43**, preferred for coordination by Ni^{0}-complexes, is applied. Such ligand mixtures have never been reported in the nickel catalyzed hydrocyanation. Hence, stabilization of species **84** via PPh_3 results in formation of the phosphine-phosphite complex **85** (Figure 48).

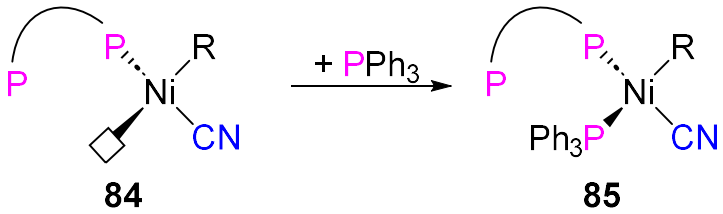

Figure 48: Association of a triphenylphosphine ligand.

At the end of the catalytic cycle, the reductive elimination of the nitrile product (Figure 7) with the associated transition of the nickel^{+II} back to 0, the PPh_3 can be dissociated again, and the second phosphorus atom of the BiPhePhos **43** ligand can be reassociated. Due to kinetic reasons, it is assumed that the reductive elimination proceeds fast enough to prevent a complete dissociation of the BiPhePhos **43** ligand from the nickel center. In case of complete BiPhePhos **43** dissociation, it is likely that another PPh_3 molecule associates, and deactivation in the form of $(Ph_3)_2Ni(CN)_2$ occurs very quickly.

To verify the consideration of stability enhancing by this ligand mixture, in this thesis, hydrocyanation experiments are carried out using styrene **28** as a model substrate. A Ni:BiPhePhos **43**:PPh_3 ratio of 1:1.2:1.2 is selected (Table 31).

*Table 31: Styrene **28** hydrocyanation in presence of a ligand mixture.*

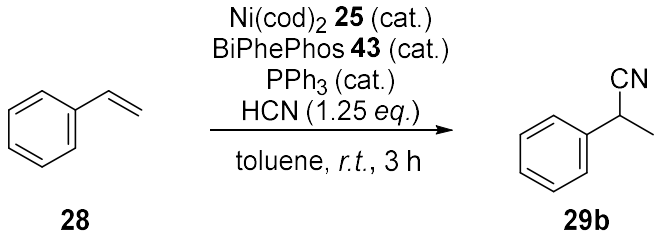

entry	*eq.* $Ni(cod)_2$ [mol%]	*eq.* (BiPhePhos) [mol%]	*eq.* (PPh_3) [mol%]	*X*[a)] [%]	*Y*[a), b)] [%]	*S*[c)] [%]
1	1	1.2	1.2	14	6	43
2	0.5	0.6	0.6	7	6	78
3	0.1	0.2	0.12	8	2	18

*Reaction conditions: BiPhePhos **43** is dissolved in toluene (2 mL) and $Ni(cod)_2$ **25** and PPh_3 are added. Styrene **28** (104 mg, 1 mmol, 1 eq.) is then added. HCN (50 µL, 1.25 mmol, 1.25 eq.) was dissolved in cold toluene (1 mL) in a separate flask and injected into the reaction vessel. After the reaction time of 3 h at room temperature, n-decane was added as internal standard. a): Based on GC analysis with n-decane as an internal standard. b): Yield of the branched product. c): Selectivity to product nitriles.*

Different catalyst loadings were chosen, to investigate limitations in catalytic longevity. Due to the shallow conversions and yields, no positive influence of PPh_3 on the nickel-catalyzed hydrocyanation can be determined.

Due to stoichiometric reasons the monodentate PPh_3, can only deactivate 60% of the nickel catalyst in the form of $(PPh_3)_2Ni(CN)_2$, as the ratio of Ni:BiPhePhos:PPh_3 is 1:1.2:1.2. The

remaining 40% of the nickel/BiPhePhos catalyst should be able to effectively catalyze the hydrocyanation of styrene **28**. Interestingly, this cannot be observed. Future investigations should therefore focus on NMR-based studies of the nickel-coordination chemistry in the simultaneous presence of phosphites and phosphines.

Another potential reason for the catalyst deactivation is insufficient PPh_3 purity, as the catalytic system is overall extremely sensitive. However, a precise characterization of the nickel species formed could not be carried out due to time constraints.

3.2.6 Chapter II: Conclusions and outlook

In this work, the experimental protocol for the Ni-catalyzed hydrocyanation of styrene **28** as a model substrate was systematically refined. The addition of HCN as a solution at the reaction temperature was found to be critical for achieving a high catalytic activity and required stringent precautions to protect the oxygen-sensitive catalyst. When following the optimized reaction protocol, quantitative styrene **28** conversion to 2-phenyle propionitrile **29b** can be achieved with a catalyst loading of only 0.1 mol%. This corresponds to a TON of 1000 proving great potential for industrial application of the hydrocyanation reaction. Furthermore, the ambient temperature, of the reaction protocol prevents bischelate formation effectively enabling hydrocyanation with high catalytic activity.

The catalytic activity was found out to be exceptionally high reaching a TOF_{20} up to 19 000 h^{-1} at ambient temperature. At ambient temperatures, diphosphine ligands like Xantphos **35** or DPEPhos **31** cannot achieve this activity. When applying BiPhePhos **43**, raising the reaction temperature to 90 °C boosts activity even further to 309 000 h^{-1}. Despite its long-time deactivating potential on the catalyst, the bischelate formation is overcompensated by the extreme increase in the reaction rate. To further improve the catalytic activity a reaction carried out neat at ambient temperature may increase the reaction rate even further. Long-term studies to balance stability, deactivation, and overall productivity are crucial for practical applications in large-scale processes.

Since bischelate formation reduces the catalytic activity, disfavoring the bischelate formation results in a more active catalyst over time. For this purpose, it is promising to increase the steric demand of both biphenole-groups of the BiPhePhos ligand making bischelate formation difficult. This is expected to result in a long-term high temperature stable hydrocyanation catalyst. The steric demand of the biphenole-groups can be increased by substituting the positions 9, 9', 11, and 11' with methyl groups. Furthermore, with regard to ligand **53** (Figure 16), a more rigid ligand backbone appears suitable for increasing the *l:b*-ratio in hydrocyanation of non-activated alkenes, like 1-octene **51**. This can be done by further adding two methyl groups in the 6 and 6’ positions, resulting in a Decamethyl-BiPhePhos **82** (Figure 49).

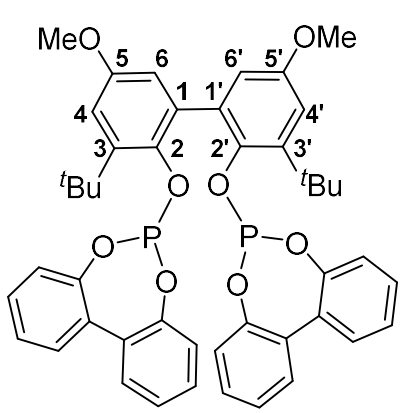

BiPhePhos **43**

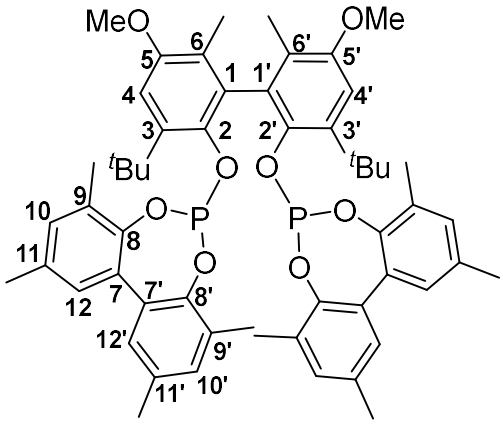

Decamethyl-BiPhePhos **82**

*Figure 49: Chemical structure of BiPhePhos **43** and Decamethyl-BiPhePhos **82** as a high-temperature stable ligand for hydrocyanation of a non-activated alkene with high l:b-*ratio.

Unfortunately, this ligand in not commercially available and needs to be synthesized accordingly in future studies.

The studies presented also demonstrate that the catalysts stability cannot be improved by the new concept of applying a ligand mixture consisting of BiPhePhos **43** and PPh_3 in styrene **28** hydrocyanation is not suitable. Still, due to low conversions and yields, there is a lot of potential for future developments based on this particularly interesting concept. More sophisticatedly designed ligands, which are better matched to each other, are promising for better utilization of the respective coordination preferences without deactivating the catalyst.

Furthermore, in these studies, it was shown that adding the Lewis acid $AlCl_3$ deactivates the catalyst over time and thus significantly reduces the catalytic activity. This might be due to *the in-situ* formation of hydrogen chloride. Consequently, when chloride-free alternatives like $Al(OEt)_3$, $Al(acac)_3$, $Al_2(SO_4)_3$, or $Al(OTf)_3$ are used, this deactivation does not occur. However, using these Aluminum salts leads to the exclusive formation of the branched nitrile product **29b** indicating no interaction with the catalyst. In conclusion, $AlCl_3$ cannot be replaced by chloride free aluminum salts.

In future studies, the optimized methodology should be transferred to different substrates especially to those based on renewable resources. This takes an important step towards a sustainable production of nitriles as platform chemicals and is therefore conducted in the next chapter.

3.3 Chapter III: β-myrcene hydrocyanation

3.3.1 Research gap and general aspects

The nickel-catalyzed hydrocyanation offers key advantages in sustainable nitrile synthesis. Pushing this sustainability even further, a transfer to renewable resources is a step that should be taken to establish nitriles as platform chemicals in future industrial processes. 1,3-diene structures are widely represented in the nature like terpenes. Based on nickel-catalyzed hydrocyanations showing high activity towards 1,3-dienes, it makes sense to use terpenes as a starting material for nitriles production through hydrocyanation. For this purpose, especially monoterpenes are promising starting materials as they often feature 1,3-diene structures. The renewable C10 1,3-diene β-myrcene **59** is almost ideal for this purpose making it an interesting substrate for hydrocyanation, which provides access to structurally attractive C11 nitriles. Surprisingly, the catalytic conversion of β-myrcene **59** in hydrocyanation has not yet been described in literature to date.

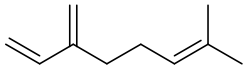

59

*Figure 50: β-myrcene **59**.*

Therefore, in this chapter, detailed studies regarding β-myrcene **59** conversion, nitrile yield and selectivity, are conducted. It is expected that different ligand classes like phosphites and phosphines have an impact on the reaction outcome by enabling slightly different reaction pathways. That way, due to the lack of symmetry of the conjugated double bonds, several different nitrile products are accessible. Consequently, the ligand influence on product distribution is studied in this thesis. For this purpose, the phosphite BiPhePhos **43** as well as the phosphines Xantphos **35** and DPEPhos **31** will be used in these studies, as they are well established in the literature on hydrocyanation. Since Lewis acids can influence the product formation in favor of linear products formation via σ-complexes, it will be included here.

To fully unleash the great potential of this reaction, a high catalytic activity is mandatory for industrial application. Therefore, the catalytic activity will be studied in this chapter focusing on BiPhePhos **43**, as its use already enabled high activity hydrocyanation in this thesis.

3.3.2 Mechanistic considerations

First, it makes sense to identify several reaction outcomes based on the reaction mechanism. The primary focus here is on the two conjugated double bonds (orange and green), as these are typically particularly reactive. The isolated tertiary double bond (grey) is expected to only plays a subordinate role here. Due to the lack of symmetry of the conjugated double bonds, several different nitrile products are accessible. The reaction scheme of all possible regioisomers is shown in Figure 51. First, the more probable reaction pathway is discussed on the left-hand side of the illustration. On the contrary, due to steric hindrance and therefore kinetic reasons, an association of the secondary double bond (orange) appears much less favorable and is shown on the right side of Figure 51.

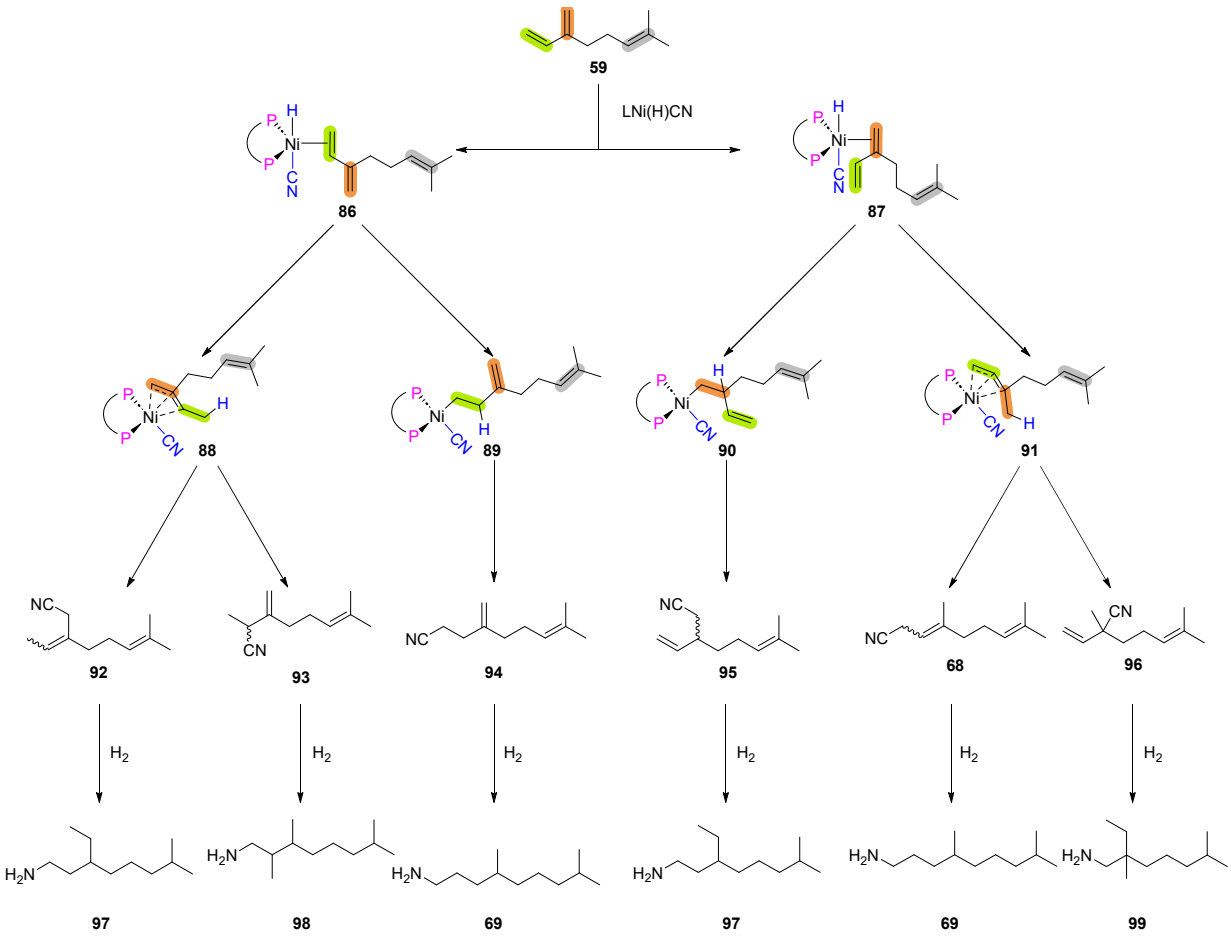

*Figure 51: Hydrocyanation of β-myrcene **59** to the products **68** and **92** to **96** and theoretical subsequent hydrogenation to the amines 69, and **97** to **99**.*

Initially, an association of the terminal double bond (green, **86**) with subsequent migratory insertion into the Ni–H bond is assumed. Since it is generally preferred for 1,3-dienes and vinyl arenes,[8] it is likely that a π-complex (**88**) is formed. After reductive elimination, the two possible

products, **92** and **93**, can emerge from this complex. In the case of the σ-complex formation (**89**), only product **94** can be formed.

As previously mentioned, the association of the secondary double bond (orange; right side of Figure 51) is less favorable. Forming the π-complex **91** is expected to be preferred, which can lead to products **68** and **96** after reductive elimination. It is to be expected that nitrile **68** is preferentially formed over the highly branched **96** for steric reasons. **95** is accessible through the formation of the σ-complex **90**.

In summary, it can be stated that the formation of six different single hydrocyanation products **68**, **92-96** is possible, which may also have the respective E/Z isomers (compounds **68** and **92**, Figure 51). A possible useful follow-up conversion in an industrial environment is the hydrogenation of the resulting nitriles to saturated amines. However, only four products are possible here (**97** - **99**), as the nitriles **92** and **95**, as well as **68** and **94**, would be hydrogenated to the same amine product **69**. Such C11-amines could be used for the production of surfactants, for example (Figure 19).

To access this synthetic potential, an efficient and effective β-myrcene hydrocyanation is of key importance and will be investigated in the following paragraphs.

3.3.3 Application of BiPhePhos

Due to its ideal characteristics, the electron withdrawing π-acceptor ligand BiPhePhos **43** has already proven advantageous in previous studies on styrene **28** and 1-octene **51**. It is expected that a sufficient nitrile yield, and selectivity is achievable in β-myrcene **59** hydrocyanation as well. Therefore, it is used under the reaction conditions optimized for styrene **28** but with an increased catalyst loading of 5 mol% $Ni(cod)_2$ **25** and 6 mol% BiPhePhos **43**.

Complete conversion was observed after just 2 h at 22 °C (Table 30, entry 1). The two main products **94** and **93** were formed and identified by 1D- and 2D-NMR analysis due to their high yields (Figure 52).

94 **93**

*Figure 52: Products **94** (left) and **93** (right).*

Product **94** was formed with a yield of 13%, and product **93** with 83%. Traces of another product can be detected. The trace-product was later identified as **92** within ongoing studies by 1D- and 2D-NMR (section 3.3.4).

From the chemical structure of the products formed, it can be concluded that the initial coordination of the β-myrcene **59** takes place via the primary double bond (orange)—the formation of the linear product **94** proceeds accordingly via the σ-complex **89**. In contrast, the favored product **93** is formed via the π-complex **88**, which is generally preferred in the absence of a Lewis acid for 1,3-dienes.[8]

Using 5 mol% $Ni(cod)_2$ **25**, results in quantitative conversion and yield, but the catalytic productivity is limited to a mere TON of 20. To increase this productivity, the catalyst loading was reduced stepwise to 0.5 mol% (Table 32).

*Table 32: β-myrcene **59** hydrocyanation using BiPhePhos **43** as a ligand.*

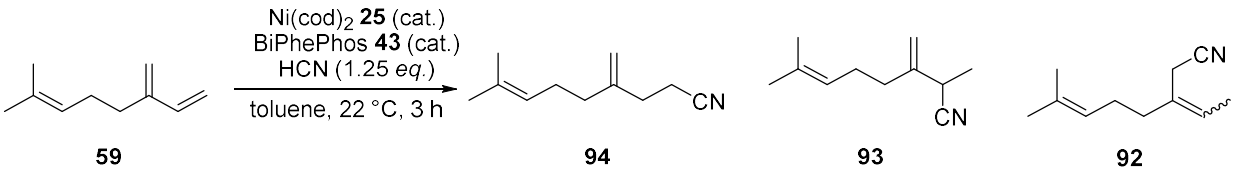

59 94 93 92

entry	*eq.* Ni(cod)$_2$ [mol%]	*X*[a)] [%]	*Y*[a)] (94) [%]	*Y*[a)] (93) [%]	*Y*[a)] (92) [%]	*S*[b)] [%]
1	5	> 99	13	83	4	> 99
2	2.5	63	10	57	3	> 99
3	1	24	4	22	traces	> 99
4	0.5	7	1	7	traces	> 99

*Reaction conditions: BiPhePhos **43** is dissolved in toluene (2 mL) and Ni(cod)$_2$ **25** is added. Subsequently, β-myrcene **59** (136 mg, 1 mmol, 1 eq.) is added. HCN (50 µL, 1.25 mmol, 1.25 eq.) was dissolved in cold toluene (1 mL) in a separate flask and injected into the reaction vessel. After the reaction time of 2 h at 22 °C, di-n-butyl ether was added as an internal standard. a): based on GC-*analysis with di-n-butyl ether as an internal standard. *b): Selectivity to nitrile products.*

Unfortunately, reducing the amount of catalyst results in a considerable reduction in conversion and yield. The **94**:**93**-ratio of the two main products, is consistently around 15:85. One potential reason for the reduced catalytic productivity is the insufficient purity of the used β-myrcene **59**, resulting in deactivation of major parts of the catalyst upon substrate addition, despite its purification by Al_2O_3 filtration, P_2O_5 drying, vacuum distillation, and degassing.

Furthermore, as this favors a reaction process via the σ-complex[5,8] (section 2.8.3.1), an attempt was made to achieve a change in selectivity by adding a Lewis acid—the selectivity is expected to be shifted in favor of product **94**. For better solubility, the reaction was carried out in the presence of THF.

*Table 33: β-myrcene **59** hydrocyanation in the presence of a Lewis acid.*

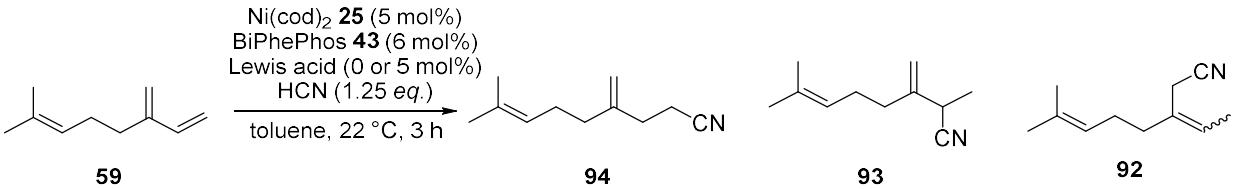

59 94 93 92

entry	Lewis acid	*X*[a] [%]	*Y*[a] (94) [%]	*Y*[a] (93) [%]	*Y*[a] (92) [%]	*S*[b] [%]
1	$AlCl_3$	24	13	5	-	75
2	$ZnCl_2$	70	20	49	-	99
3	-	> 99	13	83	4	> 99

*Reaction conditions: BiPhePhos **43** (47 mg, 0.06 mmol, 0.06 eq) is dissolved in a mixture of toluene (1.5 mL) and THF (1.5 mL). Ni(cod)$_2$ **25** (13.8 mg, 0.05 mmol, 0.05 eq) and the Lewis acid (0.05 mmol, 0.05 eq.) were added. Subsequently, in a well-ventilated fume hood, β-myrcene **59** (136 mg, 1 mmol, 1 eq.) is added via syringe through the septum lid. HCN (50 µL, 1.25 mmol, 1.25 eq.) was dissolved in cold toluene (1 mL) in a separate flask and injected into the reaction vessel. After the reaction time of 2 h at room temperature, di-n-butyl ether was added as an internal standard. a): based on GC-analysis with di-n-butyl ether as an internal standard. b): Selectivity to nitrile products.*

A strong influence on the selectivity was observed with $AlCl_3$ (Table 33, entry 1). Here, the selectivity towards product **94** was significantly reversed to 72:28. This is remarkable, as, in the absence of Lewis acid, the selectivity is around 15:85. However, a major disadvantage is that conversion and yield are drastically reduced. The use of $ZnCl_2$ reduces the conversion and yield to a lesser extent, but the **94**:**93**-ratio is only 30:70 (Table 33, entry 2). Accordingly, neither applying $AlCl_3$ nor $ZnCl_2$ in combination with BiPhePhos **43** is a sensible option. Due to catalyst deactivation via bischelate formation at higher temperatures, increasing the temperature is not suitable when diphosphites are applied (see above). Therefore, other ligands are applied in β-myrcene **59** hydrocyanation.

3.3.4 Variation of ligands

Due to different steric and electronic properties of diphonsphine ligands, a major impact on conversion, yield and selectivity are expected. Therefore, to investigate a possible selectivity-determining effect of the ligand in β-myrcene **59** hydrocyanation, Xantphos **35**, and DPEPhos **31** were applied. In addition, the monodentate triphenylphosphite $P(OPh)_3$ is applied, as it is well established in the literature. The reaction conditions were adopted from previous studies with BiPhePhos **43**. These include 5 mol% $Ni(cod)_2$ **25**, 6 mol% ligand, 22 °C reaction temperature and a 2 h reaction time. (Table 34).

*Table 34: β-myrcene **59** hydrocyanation using different ligands.*

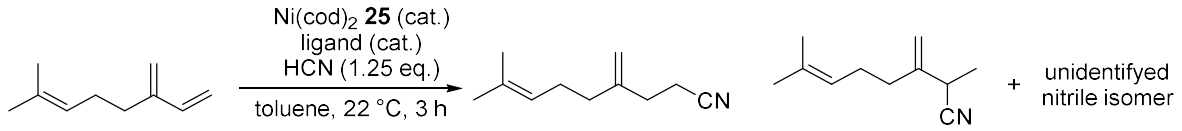

59 94 93

entry	*eq.* (Ni) [mol%]	ligand	T [°C]	*X*[a)] [%]	*Y*[a)] (94) [%]	*Y*[a)] (93) [%]	*Y*[a)] (92) [%]	*S*[b)] [%]
1	5	$P(OPh)_3$[c)]	22	3	-	-	-	-
2	5	Xantphos **35**	22	10	traces	9	traces	91
3	5	DPEPhos **31**	22	3	-	-	-	-
4	5	BiPhePhos **43**	22	> 99	13	83	4	> 99

*Reaction conditions: Ligand (0.06 mmol, 0.06 eq.) is dissolved in toluene (2 mL) and $Ni(cod)_2$ **25** is added. Subsequently, β-myrcene **59** (136 mg, 1 mmol, 1 eq.) is added. HCN (50 µL, 1.25 mmol, 1.25 eq.) was dissolved in cold toluene (1 mL) in a separate flask and injected into the reaction vessel. After the reaction time of 2 h, di-n-butyl ether was added as an internal standard. a): based on GC-analysis with di-n-butyl ether as an internal standard. b): Selectivity to nitrile products. c): 0.25 mmol, 0.25 eq, Ni:L = 1:5.*

Under the conditions selected, using $P(OPh)_3$ does not lead to the formation of any hydrocyanation products (entry 1). Furthermore, applying Xantphos **35** and DPEPhos **31** at 22 °C does not reach relevant conversion and yield. In contrast to BiPhePhos **43**, the formation of bischelates in phosphines is reversible, making phosphine ligands still usable at higher temperatures. The reaction temperature is thus increased to 60 °C and 90 °C (Table 35).

*Table 35: β-myrcene **59** hydrocyanation using diphosphines at elevated temperatures.*

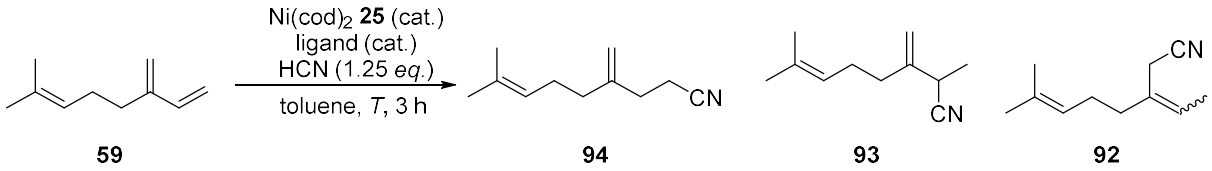

59 94 93 92

entry	*eq.* (Ni) [mol%]	ligand	T [°C]	*X*[a)] [%]	*Y*[a)] (94) [%]	*Y*[a)] (93) [%]	*Y*[a)] (92) [%]	*S*[b)] [%]
1	5	Xantphos **35**	22	10	traces	9	traces	91
2	5	DPEPhos **31**	22	3	-	-	-	-
3	5	Xantphos **35**	60	20	-	12	8	99
4	5	DPEPhos **31**	60	18	1%	7	9	99
5	5	Xantphos **35**	90	> 99	7	42	35	84
6	5	DPEPhos **31**	90	69	6	26	31	90
7	2.5[c)]	Xantphos **35**	90	58	1	32	22	94

*Reaction conditions: Ligand (0.06 mmol, 0.06 eq.) is dissolved in toluene (2 mL) and Ni(cod)$_2$ **25** (0.05 mmol, 0.05 eq.) is added. The reaction mixture is then brought to reaction temperature and β-myrcene **59** (136 mg, 1 mmol, 1 eq.) is added. HCN (50 µL, 1.25 mmol, 1.25 eq.) was dissolved in cold toluene (1 mL) in a separate flask and injected into the reaction vessel. After the reaction time of 2 h, di-n-butyl ether was added as an internal standard.* a): based on GC-analysis *with di-n-butyl ether as an internal standard*. b): Selectivity to nitrile products. c): *Ligand (0.03 mmol, 0.03 eq.) is dissolved in toluene (2 mL) and Ni(cod)$_2$ **25** (0.025 mmol, 0.025 eq.) is added.*

The yields increase significantly up to quantitative conversion with increasing temperature (entry 5). Only traces of product **94** are formed. The formation of a further product **92** is of particular interest, since it is only formed in traces in the presence of BiPhePhos **43**. Product **92** is identified by 1D and 2D NMR investigations (Figure 53).

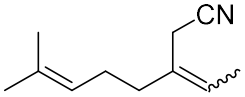

92

*Figure 53: Product **92***

Product **92** can be formed via the same π-complex from which product **93** is formed. A potential reason is the reductive elimination occurring much faster when BiPhePhos **43** is applied compared to Xantphos **35** and DPEPhos **31**. That way, the π-complex is given more time for rotation, which is necessary for product **92** formation. Due to the increased bulkiness of BiPhePhos **43**, the formation of the linear Product **94** is enabled by sterically disfavoring the π-complex formation compared to the σ-complex.

Based on the quantitative myrcene **59** conversion within entry 5, the catalyst loading was reduced to 2.5 mol% (entry 7). Unfortunately, conversion is reduced to only 58%, which is comparable to the 63% conversion reached when 2.5 mol% Ni/BiPhePhos **43** catalyst are used (Table 32, entry 2). This further emphasizes the need for an improved myrcene **59** purification method.

Interestingly, the use of DPEPhos **31** leads to higher selectivities for nitrile products at 90 °C. This could be caused by the increased flexibility of the DPEPhos **31** ligand, which could enable faster reaction rates, giving less time for side reactions such as di- and oligomerization. Some dimers/oligomers can be detected when Xantphos **35** is applied at a reaction temperature of 90 °C. Unfortunately, due to time limitations, the differences in activity between Xantphos **35** and DPEPhos **31** could not be investigated further.

Focusing on the selectivity towards linear product **94**, Xantphos **35** was used in combination with $AlCl_3$ for further investigations. The aim is to combine the high conversion achievable by applying Xantphos **35** with the selectivity-reversing potential of $AlCl_3$. This may enable the formation of product **94** with high yields (Table 36).

*Table 36: Application of Xantphos **35** and $AlCl_3$ in β-myrcene **59** hydrocyanation.*

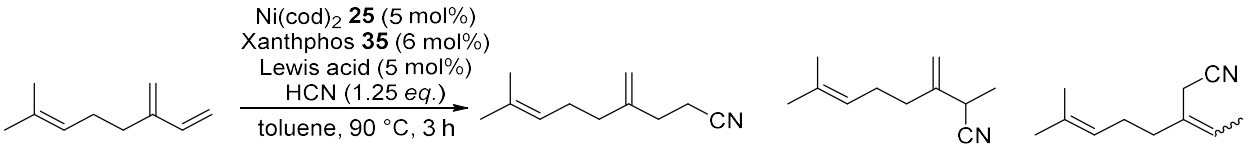

59 94 93 92

entry	Lewis acid	*X* [a] [%]	*Y* [a] (94) [%]	*Y* [a] (93) [%]	*Y* [a] (92) [%]	*S* [b] [%]
1	$AlCl_3$	11	-	2	2	40
2	-	> 99	7	42	35	84

*Reaction conditions: Xantphos **35** (34.7 mg, 0.06 mmol, 0.06 eq.) is dissolved in toluene (2 mL) and Ni(cod)₂ **25** (13.8 mg, 0.05 mmol, 0.05 eq.) is added. The reaction mixture is then brought to room*

*temperature (22 °C) and β-myrcene **59** (136 mg, 1 mmol, 1 eq.) is added. HCN (50 µL, 1.25 mmol, 1.25 eq.) was dissolved in cold toluene (1 mL) in a separate flask and injected into the reaction vessel. After the reaction time of 2 h, di-n-butyl* ether *was added as an internal standard. a): based on GC-analysis with di-n-butyl ether as an internal standard. b): Selectivity to nitrile products.*

Unfortunately, combining these was not successful, as conversion is only 11% and combined yield are 4%, indicating catalyst deactivation.

3.3.5 The catalytic activity of BiPhePhos in β-myrcene hydrocyanation

Regarding a potential application of the nickel-catalyzed β-myrcene **59** hydrocyanation, the catalytic activity is of great importance to maintain good productivity of the process.

When 5 mol% nickel/BiPhePhos-catalyst is applied at room temperature, the overall selectivity towards nitriles and the branched product **93** yield is already sufficient (Table 32). Therefore, a reaction profile is monitored using these conditions (Figure 54).

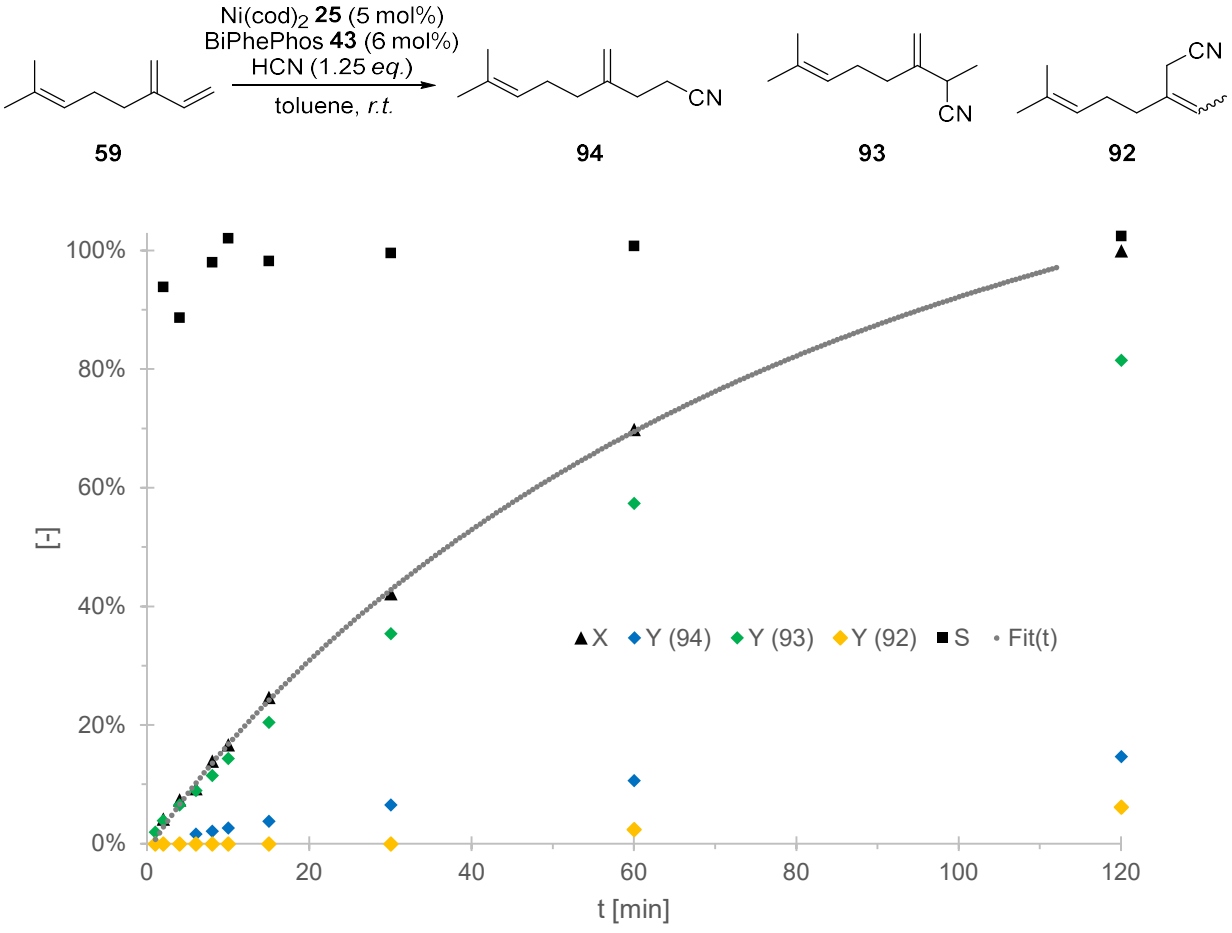

*Figure 54: Reaction profile of β-myrcene **59** hydrocyanation. Reaction conditions: BiPhePhos **43** (118.0 mg, 0.15 mmol, 0.06 eq) is dissolved in toluene (5 mL) and Ni(cod)₂ **25** (34.4 mg, 0.125 mmol,*

*0.05 eq) is added. Subsequently, β-myrcene **59** (340.6 mg, 1 mmol, 1 eq.) and di-n-butyl ether as an internal standard were added. HCN (125 µL, 3.75 mmol, 1.25 eq.) was dissolved in cold toluene (2.5 mL) in a separate flask and injected into the reaction vessel. X and Y based on GC-analysis with di-n-butyl ether as an internal standard. S: Selectivity to nitrile products.*

After a reaction time of 2 h, complete conversion with >99% selectivity towards nitriles is achieved. The yield of the main product **93**, is 82%. Fluctuating selectivities at the beginning of the reaction can be explained by low conversion and yield < 10% and, therefore, a relatively high margin of error, which does not occur with later samples of the mixtures. Based on a fit, 20% conversion is reached after 12 min. which corresponds to a TOF_{20} of only 19.9 h^{-1}. This poor catalytic activity is a strong indicator of a strong steric hindrance around the catalytic nickel center. Besides that, impurities in the substrate batch that deactivate major parts of the catalyst are also a potential explanation. Future studies may focus on a comparison of the catalytic activity of BiPhePhos **43** and the rather flexible and less sterically demanding DPEPhos **31** ligand at higher temperatures, which potentially enables a higher catalytic activity.

3.3.6 Chapter III: Conclusions and outlook

Within this work, β-myrcene **59** hydrocyanation was investigated in detail. A special focus was put on product formation as well as ligand influence on product distribution. Three hydrocyanation products can be observed using the commercially available ligands BiPhePhos **43**, Xantphos **35**, and DPEPhos **31** (Figure 55).

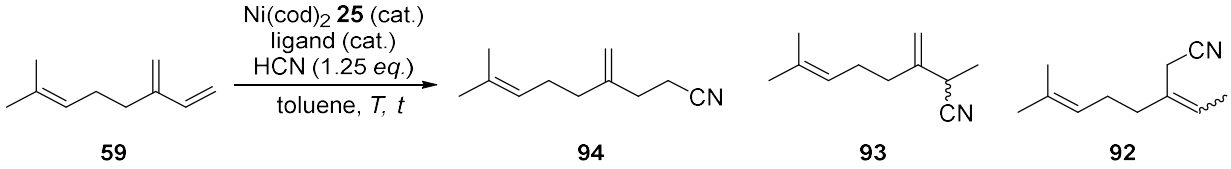

*Figure 55: β-myrcene **59** hydrocyanation.*

Applying the diphosphite BiPhePhos **43** at ambient temperatures results in 83% of product **93** via the π-complex **88** and 13% of the linear **94** via the σ-complex **89**—only traces of product **92** are formed (Table 37, entry 1). On the contrary, the diphosphine ligands Xantphos **35** and DPEPhos **31** require elevated temperatures of 90 °C and favor the formation of products **93** and **92** exclusively via the intermediately formed π-complex **88** (Table 37, entry 2 and 3).

*Table 37: β-myrcene **59** hydrocyanation with various ligands under optimized conditions.*

entry	ligand	T [°C]	*Lewis acid*	*X*[a] [%]	*Y*[a] (94) [%]	*Y*[a] (93) [%]	*Y*[a] (92) [%]	*S*[b] [%]
1	BiPhePhos **43**	22	-	> 99	13	83	4	97
2	Xantphos **35**	90	-	> 99	7	42	35	84
3	DPEPhos **31**	90	-	69	6	26	31	90
4	BiPhePhos **43**	22	$AlCl_3$	24	13	5	-	75

*Reaction conditions: Ligand is dissolved in toluene (2 mL) and Ni(cod)$_2$ **25** is added. Subsequently, β-myrcene **59** (136 mg, 1 mmol, 1 eq.) is added. HCN (50 µL, 1.25 mmol, 1.25 eq.) was dissolved in cold toluene (1 mL) in a separate flask and injected into the reaction vessel. After the reaction time of 2 h at room temperature, di-n-butyl ether was added as an internal standard. a): based on GC-analysis with di-n-butyl ether as an internal standard. b): Selectivity to nitrile products.*

Adding $AlCl_3$ as a Lewis acid to the reaction mixture inverts the selectivity towards the linear product **94**—the **94**:**93**-ratio is 72:28 then. Unfortunately, overall conversion is strongly limited to 23%. A potential reason for that is the relatively fast catalyst deactivation in presence of $AlCl_3$ compared to the relatively slow reaction rate (TOF_{20} is only 19.9 h^{-1}). Increasing the

reaction rate and selectivity to the linear product **94** remains an open challenge for future investigations. This might be achieved by an increased reaction temperature to overcompensate the catalyst deactivation by an even more substantial increase in reaction rate and should be investigated in the future. However, the deactivation behavior of BiPhePhosNi(cod) **26** in presence of $AlCl_3$ at elevated temperatures has not been investigated within this thesis.

Nevertheless, with these investigations a critical step is taken towards a more sustainable nitrile production starting from this highly interesting renewable resource. One way to boost the catalytic activity in β-myrcene **59** hydrocyanation further is to increase the β-myrcene **59** purity to protect the overly sensitive nickel-catalyst from deactivation.

4 Conclusions and Outlook

The nickel-catalyzed hydrocyanation offers economic and ecologic advantages and is therefore of great interest for industrial application. A key challenge is the lack of catalytic activity towards conversion of simple alkenes—in purely academic literature, high catalyst loadings up to 5 mol% and long reaction times up to 24 h are reported. Therefore, to tackle this challenge, in the present thesis detailed investigations on the nickel-catalyzed hydrocyanation, the practical procedure and alternative starting materials are presented.

The first goal was to increase the overall catalytic activity. Applying the commercially available electron withdrawing wide bite angle ligand BiPhePhos **43** (section 3.1.1) in styrene **28** and 1-octene **51** hydrocyanation, well-known ligands established in the literature are significantly outperformed regarding nitrile yield and selectivity. In 1-octene **51** hydrocyanation, using BiPhePhos **43** the yield was increased from 17% (DPEPhos **31**) to 87% (section 3.1.4.2). Another improvement in the field of the nickel-catalyzed hydrocyanation was achieved by applying a promotor to the reaction mixture aimed to deaggregate $AlCl_3$-oligomers. That way, using a catalytic amount of acetonitrile as the promotor, the catalytic activity is increased by an enhanced nickel/Lewis acid cooperation by almost 30% to 804 h^{-1} (section 3.1.3.5). In conclusion, this concept has never been utilized in the nickel-catalyzed hydrocyanation before and its great potential was shown. In addition, in depth NMR-based studies on the catalyst stability revealed, that strict protection of the extremely sensitive nickel-catalyst is key to maintain the catalytic activity throughout the reaction (section 3.2.2). When following the accordingly optimized protocol, an extremely high catalytic activity of up to 309 000 h^{-1} never reported before can be achieved (section 3.2.5.1). The second milestone of this thesis was to transfer the optimized conditions and experimental procedures to the renewable β-myrcene **59** as the starting material to take a first step towards a more sustainable nitrile production. It was found that, depending on the ligand choice, three major products can be obtained (section 3.3.4). At 22 °C, using BiPhePhos **43** quantitatively yields nitriles outperforming literature known diphosphine ligands, only forming traces of nitriles (section 3.3.4). Concluding, the herein for the first time reported β-myrcene **59** hydrocyanation, marks the first important step towards a sustainable production of C11-nitriles through hydrocyanation.

In the present thesis, the research gaps outlined in the preface (section 1) were investigated in detail and the results provide a significant knowledge gain in the field of the nickel-catalyzed hydrocyanation. For future large-scale applications, long term studies to balance the catalysts stability, deactivation by increased temperature and overall productivity are of great importance. Furthermore, in a large-scale process, it is important to develop a suitable recycling strategy to preserve the high-value catalyst.

5 Experimental section

5.1 General

All experiments were performed using standard Schlenk techniques. Working steps in the glovebox were performed in a Labmasterpro ECO from mBRAUN under an argon atmosphere. Hydrocyanations were performed in Schlenk tubes (height: 124.5 mm, inner diameter: 23.4 mm, glass thickness: 2.6 mm) with a GL-32 closure and Young stopcock connection.

Figure 56: Schlenk tubes used for hydrocyanation reactions.

5.2 Safety precautions when handling hydrogen cyanide

Caution: Hydrogen cyanide is highly toxic and volatile! Therefore, it must only be handled in a well-ventilated fume hood and with at least two instructed persons present. In addition to the general personal protective equipment for safe working in the laboratory (lab coat and safety goggles), an HCN gas detector (Honeywell BW™ Solo HCN) and butyl rubber gloves (Honeywell Butoject™ 898) are required. Furthermore, HCN containers must be stored in a lockable ATEX-certified freezer, located in a fume hood, and set to -26 °C which only instructed persons can access. The internal temperature is monitored via a battery-powered sensor connected to the internet. For safe handling of single containers, the volume in a single storage container should not exceed 5 mL.

5.3 Thin-layer and column chromatography

Thin-layer chromatography was carried out using mixtures of cyclohexane and ethyl acetate. Silica gel plates from Merck (60 F254 on aluminum) were used. UV-active substances were analyzed with a UV lamp at 254 nm.

Column chromatographic purifications were carried out with a BÜCHI FLASHPURE automated system using silica gel as the stationary phase and a running mixture of distilled cyclohexane and ethyl acetate as the mobile phase.

5.4 Chemicals and purification

All Chemicals were purchased from ACROS, CARL ROTH, TCI, FISHER, ABCR, SIGMA ALDRICH, MERCK, THERMO SCIENTIFIC or DEUTERO.

All chemicals were used as received without further purification, besides the ones mentioned below.

Toluene, 1-octane, tetrahydrofurane, diethyl ether, *n*-decane, di-*n*-butyl ether and were distilled over sodium under argon before usage. All liquids were degassed using the Freeze-Pump-Thaw method (three cycles).

Styrene **28** was first vacuum distilled before use with temperatures not exceeding 50 °C and further degassed using the Freeze-Pump-Thaw method (three cycles).

β-myrcene **59** was filtered through aluminum oxide to remove peroxides and was then distilled under reduced pressure. Afterwards it was degassed using the Freeze-Pump-Thaw method (three cycles).

BiPhePhos **43** was provided by EVONIK AG and used without further purification.

5.5 Experimental procedure of hydrocyanation reactions

5.5.1 V1: HCN addition at -50 °C

Ligand was added to the reaction vessel in a glovebox according to the amounts given in the script and dissolved in dry, degassed toluene. $Ni(cod)_2$ **25** was added next and the resulting solution was stirred for 30 minutes at room temperature. Afterwards the reaction vessel was transferred from the glovebox to the fume hood, connected to the Schlenk-line system. The

Substrate and *n*-decane as the GC-standard in was added in a countercurrent flowing stream of argon. After that te reaction vessel was cooled down to – 50 °C to add the HCN with quickly freezes. To start the reaction the vessel was removed from the cooling bath and was ether allowed to warm to room temperature or heated to 60 or 90 °C. Once the reaction was complete the reaction vessel was carefully opened. A light argon stream was passed through the solution to remove remaining HCN. A sample was taken to be analyzed via GC-FID.

Important: Caution when opening the reaction vessel! It may be under pressure and contains an unknown concentration of hydrogen cyanide! Wear butyl rubber gloves and use HCN warning devices.

5.5.2 V2: HCN as a solution at reaction temperature

Ligand was added to the reaction vessel in a glovebox according to the amounts given in the script and dissolved in dry, degassed toluene (2/3 of the amount of solvent). $Ni(cod)_2$ **25** was added next and the resulting solution was stirred for 30 minutes at room temperature. Afterwards the reaction vessel was removed from the glovebox and styrene **28** was added through a septum (renewed for each reaction).

Dry and degassed Toluene (1/3 of the amount of solvent) was placed in another Schlenk flask, cooled to -50 °C and then dry and degassed HCN was added using an Eppendorf pipette (HCN was only thawed to the required amount and handled close to the melting point). Upon addition, the HCN froze visibly to form a white solid. Afterwards, the mixture was carefully warmed until a homogeneous solution was formed and then added to the reaction mixture at reaction temperature using a syringe to start the reaction.

Once the reaction was complete the reaction vessel was carefully opened. A light argon stream was passed through the solution to remove remaining HCN. GC standard was added before and a sample was taken to be analyzed via GC-FID.

Important: Caution when opening the reaction vessel! It may be under pressure and contains an unknown concentration of hydrogen cyanide! Wear butyl rubber gloves and use HCN warning devices.

5.6 Procedure for conversion/time-plots

According to the previous procedure. di-*n*-butyl ether was used as an internal standard for GC-FID analysis and was added before the start of the reaction. Samples were taken with a

syringe flushed with argon. Samples are quenched using wet and air containing toluene and are degassed using a steam of argon.

Important: Extreme caution when taking samples! The flask may be under pressure and the reaction solution contains an unknown concentration of hydrogen cyanide. Wear butyl rubber gloves, use HCN warning devices, and hold the syringe and cannula firmly. When pulling out the syringe, ensure no drops are being Spilled.

5.7 Synthesis of HCN

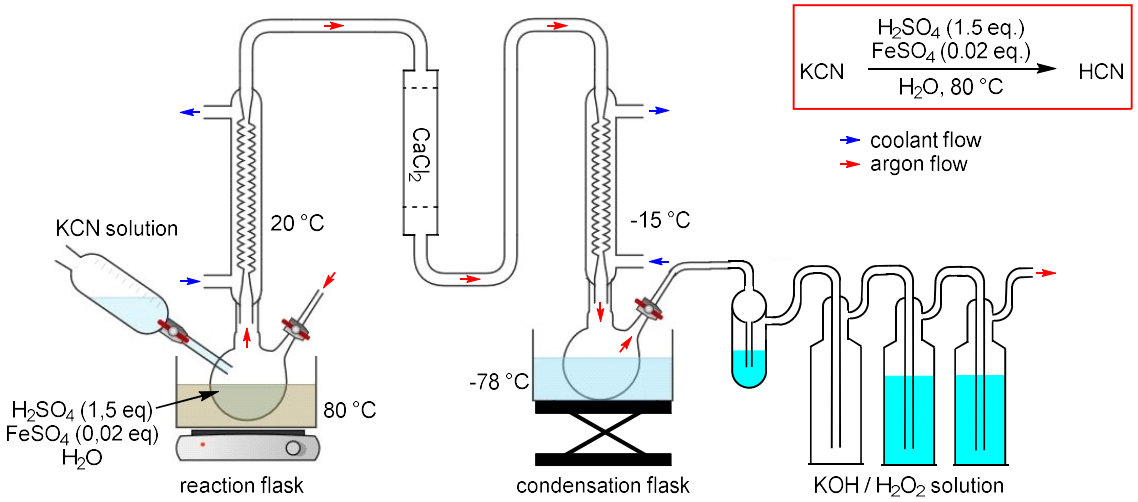

Figure 57: Apparatus for hydrogen cyanide synthesis.

The apparatus was set up as shown in Figure 57 (connections via PVC tubes) and then flushed with argon for 30 min. Water (50 mL) and concentrated sulfuric acid (102 mL, 1.91 mol, 1.5 eq) were added into the reaction flask. $FeSO_4 \cdot 7\ H_2O$ (8.2 g, 0.03 mol, 0.02 eq) was carefully dissolved as a catalyst while stirring vigorously. This solution was heated to 80 °C and KCN (82.0 g, 1.26 mmol, 1 eq) dissolved in water (150 mL) was slowly added via a dropping funnel while argon was continuously flowing through the apparatus.

The first 80 mL of solution were added within 30 min, but no condensation could be detected in the condensation flask. Therefore, the heating bath temperature was lowered to 40 °C, and the dropping rate and the argon flow were reduced to a minimum. Afterwards, a white solid condensed between the Schlenk stopcock and the ground joint of the condensation flask. This led to the stopcock becoming blocked, and the addition of the KCN had to be interrupted once to remove the cold bath briefly. Once the HCN had melted a little and sunk deeper into the flask, a gas flow could be observed again at the bubble counter and the synthesis was continued. This was done for a further 4 h (40 mL KCN solution). The apparatus was then sealed airtight, and the condensation flask was stored overnight at -26 °C under lock and key.

The next day, the apparatus was reconnected identically, and the remaining KCN solution was added. After another 5 h, this was completed and HCN (12.8 g, 0.48 mol, 38%) was obtained as a white solid in the cold. For further purification, it was additionally degassed using the Freeze-Pump-Thaw method (three cycles). Afterwards, HCN was stored at -26 °C.

The apparatus was rinsed for 30 minutes with a strong argon stream, and then all components were carefully rinsed with a KOH/H_2O_2 solution.

5.8 Purification of HCN

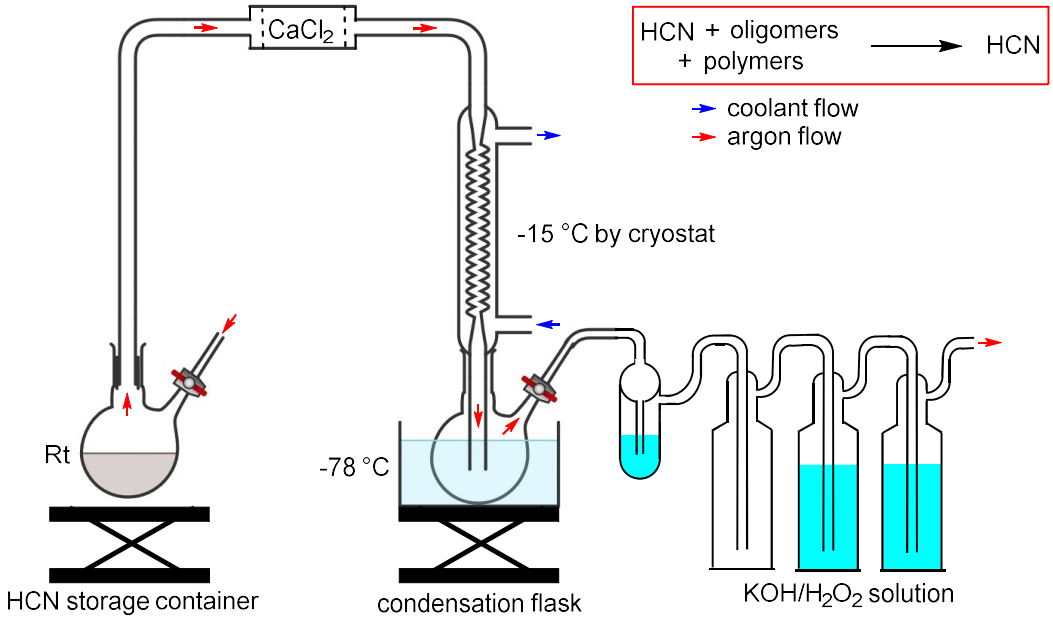

Figure 58: Apparatus for hydrogen cyanide purification.

The apparatus was set up according to Figure 58.After rinsing with argon (30 min), the HCN storage flask was connected. This was then slowly thawed to room temperature and a light flow of argon was constantly passed through the apparatus. The brown solid melted and became a brown solution, the amount of which constantly decreased. On the other side, a white solid condensed in the PVC tube, which protruded deep into the condensation flask. If this became blocked, the argon flow was stopped for this time, the condensate thawed, refrozen and the process continued. A brown/black solid residue remained in the former HCN storage flask, and pure HCN (no yield determination) could be collected in the condensation flask after 6 hours. The apparatus was then rinsed for 30 min with a strong argon stream and then with alkaline H_2O_2 solution.

Analysis of the black solid:

IR = 3306, 3282, 3222, 3176, 3160, 3120, 2204, 2185, 2170, 2157, 1651, 1559, 1541, 1508, 1473, 1396, 874 cm^{-1}.

5.9 Synthetic procedures

5.9.1 $Ni(cod)_2$

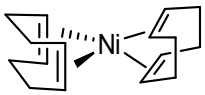

$Ni(acac)_2$ (1284.6 mg, 5 mmol, 1 eq) was added to a Schlenk flask, dried for 10 min under reduced pressure at 80 °C and then suspended in THF (4 mL) and COD (3.9 mL, 30 mmol, 6 eq). The resulting green mixture was cooled to 35 °C and $n$$Bu_2Mg$ (11 mL, 1 M in heptane, 11 mmol, 2.2 eq) was added over 10 min. The color changed from green to yellow/brown to red-black during this time. After additional 10 min time the stirring was stopped and a light-colored precipitate formed. The supernatant red-black solution was carefully removed with a filter cannula. The resulting solid was washed with degassed acetone **8** (5 x 1.5 mL) in the cold until all brown residues were removed. The light-yellow solid was dried under reduced pressure and $Ni(cod)_2$ **25** (628.7 mg, 2.29 mmol, 46%) was obtained as a fine yellow powder.

^{1}H-NMR (500 MHz, C_6D_6): δ = 4.30 (s, 8 H, (CH_2-HC=CH-CH_2)$_2$), 2.08 (s, 16 H, (CH_2-HC=CH-CH_2)$_2$) ppm.

^{13}C{^{1}H}-NMR (126 MHz, C_6D_6): δ = 89.69 (s, (CH_2-HC=CH-CH_2)$_2$), 30.89 (s, (CH_2-HC=CH-CH_2)$_2$) ppm.

*Figure 59: Yellow color of the synthesized $Ni(cod)_2$ **25** indicates high purity. (Grey or beige color indicates the presence of metallic nickel, whereas green color indicates Ni(II) complexes).*

5.9.2 2-octylmesylate

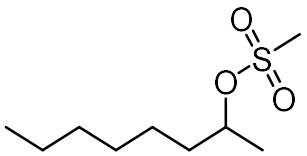

To a colorless solution of 2-octanol (4.1 mL, 25.0 mmol, 1 *eq*.) in dichloromethane (130 mL) at 0 °C were added triethylamine (21 mL, 150.0 mmol, 6 *eq*.) and methanesulfonic acid chloride (3.5 mL, 44.7 mmol, 1.8 *eq*.) were added to form a yellow suspension. After stirring the reaction solution for 1.5 hours, diethyl ether (100 mL) was then added, causing the to precipitate. After separation of the white triethylammonium chloride triethylammonium chloride by filtration, the solvent was removed from the remaining could the rotary evaporator. As a result, the reaction solution 2-octyl mesylate was obtained as a colorless liquid. It was used in the next step without further purification.

5.9.3 2-methyl-octanenitrile

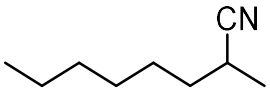

To a solution of 2-octyl mesylate (crude product from 5.9.2) in dry DMSO (50 mL), *tert*-butylammonium iodide (4 g/mol, 0.945 g, 2.51 mmol, 0.1 *eq*.) and potassium cyanide (8.121 g, 125 mmol, 5 *eq*.) were added with stirring. After the orange solution was allowed to react for 65 hours at 80 °C, the reaction solution was cooled and diluted by adding water (70 mL). The resulting mixture was transferred to a separatory funnel and diluted three times with cyclohexane (50 mL) three times. The aqueous phase was introduced into a solution of H_2O_2/KOH, whereas the combined organic phases were washed with further H_2O (3 x 30 mL) and dried with $MgSO_4$. Subsequent removal of all volatile components yielded the crude product, which was pre-purified by distillation at 250 °C and a slight vacuum. This was followed by column chromatographic purification (cyclohexane:ethyl acetate, 100:1 to 25:1) to give 2-methyl-octannitrile (1.085 g, 7.79 mmol, 31% based on 2-octanol) as a colorless liquid. Caution: If water is added to the reaction mixture, gaseous and toxic hydrocyanic acid may be formed. The synthesis must be carried out in a well-ventilated and closed fume cupboard!

^{1}H-NMR (700 MHz, $CDCl_3$): δ = 2,59-2,51 (m, 1 H, C_6H_{15}-C<u>H</u>(CN)-CH_3), 1,59-1,53 (m, 1 H, C_5H_{13}-C<u>H</u>$_2$-CH(CN)-CH_3), 1,49 (m, b a b 2H, C_4H_{11}-C<u>H</u>$_2$-C<u>H</u>$_2$-CH(CN)-CH_3), 1,41-1,34 (m, 1 H,

C_4H_{11}-C<u>H</u>$_2$-CH_2-CH(CN)-CH_3), 1,26 (m, 9 H, H_3C-C_3<u>H</u>$_6$-$(CH_2)_2$-CH(CN)-C<u>H</u>$_3$), 0,84 (m, 3 H, H_3C-C_5H_{13}-C<u>H</u>(CN)-CH_3) ppm.

^{13}C-NMR (700 MHz, $CDCl_3$): δ = 123,0 (C_6H_{15}-CH(<u>C</u>N)-CH_3), 34,0 (C_5H_{13}-<u>C</u>H_2-CH(CN)-CH_3), 31,5 (C_2H_5-<u>C</u>H_2-$(CH_2)_3$-CH(CN)-CH_3), 28,7 (C_6H_{15}-<u>C</u>H(CN)-CH_3), 26,9 (C_4H_{11}-<u>C</u>H_2-CH_2-CH(CN)-CH_3), 25,5 (C_6H_{15}-<u>C</u>H(CN)-CH_3), 22,5 (H_3C-<u>C</u>H_2-$(CH_2)_4$-CH(CN)-C<u>H</u>$_3$), 18,0 (H_3C-C_5H_{13}-CH(CN)-<u>C</u>H_3), 13,9 (H_3<u>C</u>-C_5H_{13}-CH(CN)-CH_3) ppm.

HR-MS (APCI): calculated $[M+H]^+$ = 140,1434, found $[M+H]^+$ = 140,1434.

5.9.4 8-methyl-4-methylidenenon-7-enenitrile (**94**) and 2,7-dimethyl-3-methylideneoct-6-enenitrile (**93**)

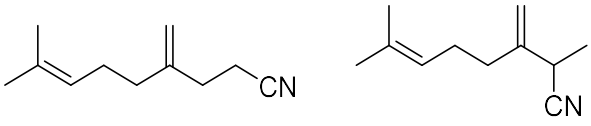

94 **93**

Procedure according to 5.5.2 using Ni(cod)$_2$ **25** (68 mg, 0.25 mmol, 0.05 eq.), BiPhePhos **43** (236 mg, 0.3 mmol, 0.06 eq.), toluene (18 mL), HCN (250 µL, 6 mol, 1.25 eq.) and β-myrcene **59** (680 mg, 5 mmol, 1 eq.). After 2 h stirring at room temperature traces of remaining HCN were removed using a steam of argon. After filtration through silica the product mixture was analyzed by 1D and 2D-NMR spectroscopy (NMR spectra in section 7.3.2).

94: ^{1}H-NMR (600 MHz, $CDCl_3$) δ = 5.67 – 5.56 (m, 1 H), 5.46 (d, J = 17.1 Hz, 1 H), 5.23 (d, J = 10.2 Hz, 1 H), 3.82 (s, 1 H), 3.02 (d, J = 24.4 Hz, 1 H), 1.32 (s, 4 H).

93: 1H-NMR (600 MHz, $CDCl_3$) δ = 5.16 (s, 1 H), 5.14 – 5.06 (m, 1 H), 5.00 (s, 1 H), 3.37 – 3.16 (m, 1 H), 2.23 – 2.04 (m, 5 H), 1.69 (s, 3 H), 1.62 (s, 3 H), 1.44 (d, J = 7.2, 3 H).

^{13}C{^{1}H}-NMR (151 MHz, $CDCl_3$) δ = 144.34, 138.30, 133.16, 132.93, 132.79, 129.72, 129.55, 129.08, 128.98, 128.86, 125.06, 124.92, 124.62, 123.22, 122.61, 122.43, 122.40, 121.50, 118.27, 115.90, 115.59, 115.31, 115.18, 112.69, 77.43, 77.22, 77.01, 55.91, 55.01, 40.76, 40.16, 35.62, 35.23, 33.67, 31.86, 30.69, 30.54, 29.99, 26.38, 26.10, 25.87, 25.84, 25.39, 24.20, 18.12, 17.95, 17.88, 17.87, 13.56.

5.9.5 3-ethylidene-7-methyloct-6-enenitrile (**92**)

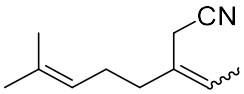

92

Procedure according to 5.5.2 using $Ni(cod)_2$ **25** (41 mg, 0.15 mmol, 0.05 eq.), Xantphos **35** (104 mg, 0.18 mmol, 0.06 eq.), toluene (9 mL), HCN (150 µL, 3.75 mol, 1.25 eq.) and *β*-myrcene **59** (408 mg, 3 mmol, 1 eq.). After 2 h stirring at 90 °C traces of remaining HCN were removed using a steam of argon. After filtration through silica the product mixture was analyzed by 1D and 2D-NMR spectroscopy (NMR spectra in section 7.3.3).

^{1}H-NMR (600 MHz, $CDCl_3$) δ = 5.57 (q, J = 6.7 Hz, 1 H), 5.13 (s, 2 H), 5.10 – 5.04 (m, 3 H), 4.97 (s, 2 H), 3.31 – 3.16 (m, 2 H), 3.01 (s, 2 H), 2.10 (d, J = 27.1 Hz, 12 H), 1.75 – 1.57 (m, 21 H), 1.41 (d, J = 7.2 Hz, 6 H).

^{13}C{^{1}H}-NMR (151 MHz, $CDCl_3$) δ = 144.18, 132.45, 128.95, 123.04, 121.24, 118.00, 112.39, 33.44, 31.60, 26.16, 25.64, 25.11, 17.88, 17.68, 13.29.

5.10 NMR

An AGILENT DD2-500 MHz, a BRUKER Avance III HD NanoBay-400 MHz, a BRUKER Avance Neo 500 MHz or a Bruker Avance III HD-600 MHz was used for NMR analysis. The investigation of the catalyst preforming and other reaction solutions using ^{31}P{^{1}H} NMR was carried out on a MAGRITEK Spinsolve 60ultra Phosphorus.

5.11 GC

GC-samples were taken after removing the remaining hydrogen cyanide by a steam of argon. *n*-decane was added as an internal standard. About 0.7 ml of the reaction mixture is filtered through a syringe filter, placed in a GC vial and diluted with toluene.

5.11.1 Device

The GC analysis was performed on an Agilent 7890A equipped with an Agilent HP-5 column and an FID detector. The calibration factors were determined experimentally using *n*-decane or di-*n*-butyl ether (di-n-butyl ether) as internal standard.

5.11.2 Method

The split ratio of the method was set to 84:1 at a split flow of 184.8 $mL \cdot min^{-1}$ and the temperature and gas flow profiles are listed in Table 1 and Table 2.

Table 1: Gas flow profile of the GC method.

	Gas flow rate	End flow / $mL \cdot min^{-1}$	Hold / min
Start	-	2.2	18.0
Ramp 1	2.0	4.4	3.0

Table 2: Temperature profile of the GC method.

	Heat rate / $°C \cdot min^{-1}$	End temperature / °C	Hold / min
Start	-	40.0	3.0
Ramp 1	7.5	140.0	0.0
Ramp 2	85.0	290.0	4.0

5.11.3 Calibrations

5.11.3.1 *n*-decane

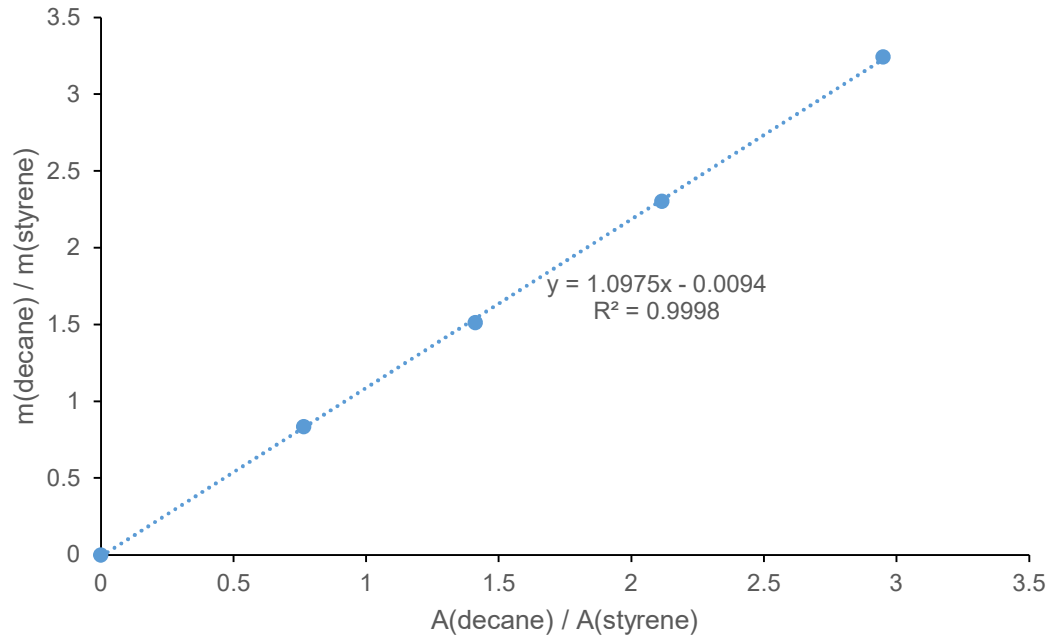

*Figure 60: GC-FID calibration of styrene **28** with n-decane as internal standard.*

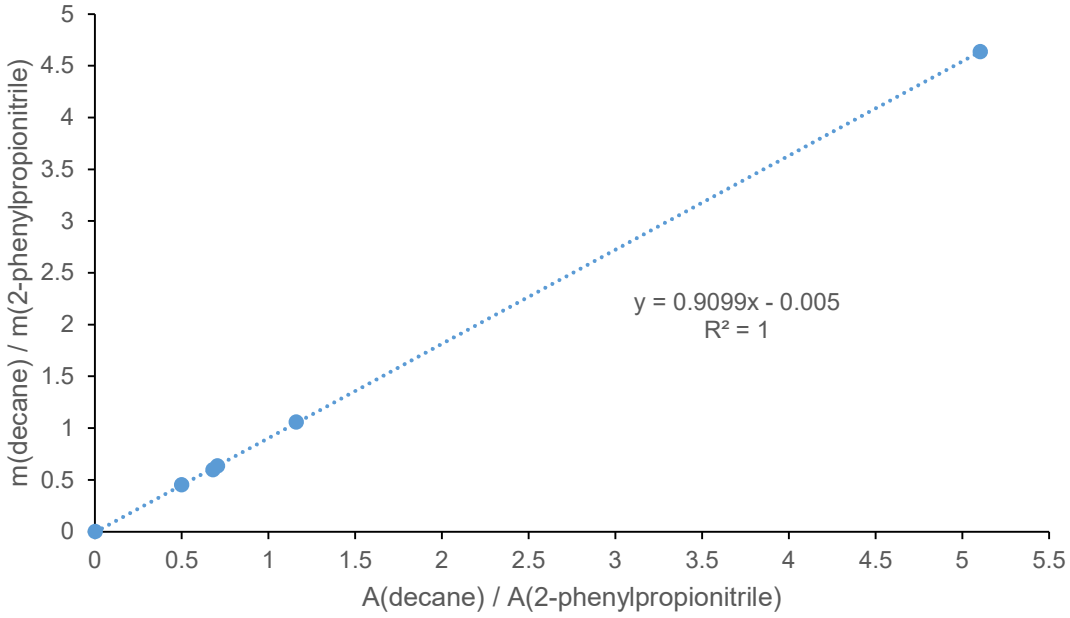

Figure 61: GC-FID calibration of 2-phenylpropionitrile with n-decane as internal standard.

5.11.3.2 di-*n*-butyl ether

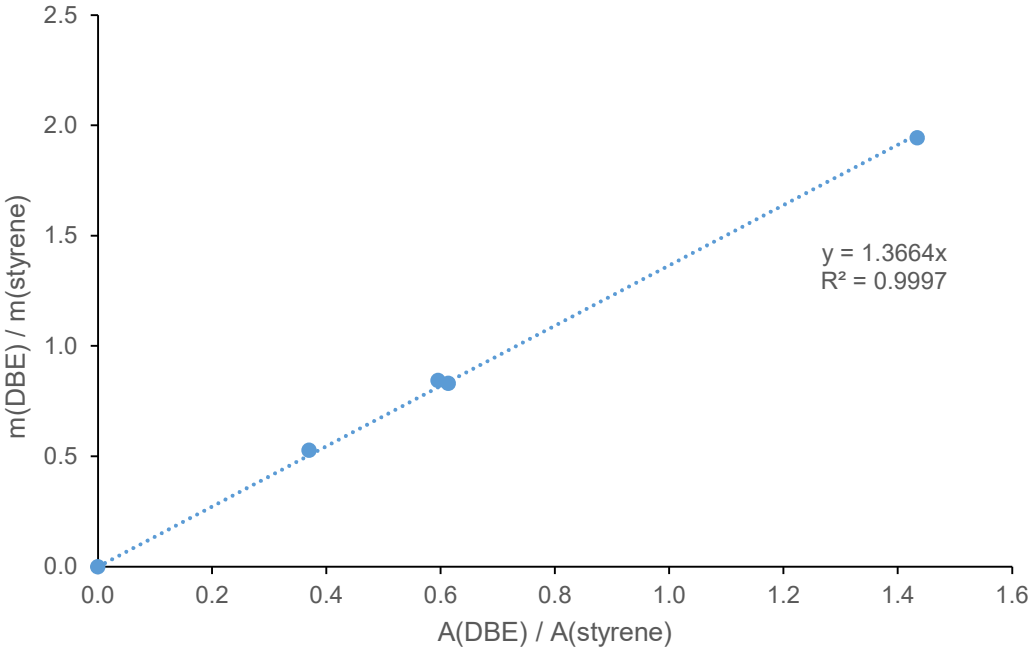

*Figure 62: GC-FID Calibration of Styrene **28** with di-n-butyl ether as internal standard.*

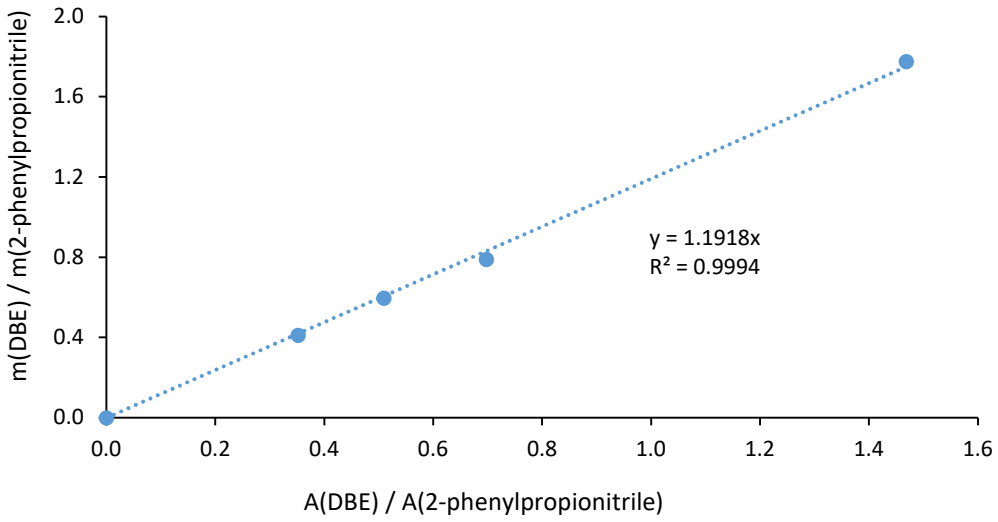

Figure 63: GC-FID Calibration of 2-phenyl propionitrile with di-n-butyl ether as internal standard

5.11.4 Calculation of conversion (*X*), yield (*Y*), and selectivity (*S*)

The mass of styrene **28** $m_{\text{styrene 28}}$ within a GC sample is calculated with the weighed mass of the
n-decane m_{decane}, the areas A of the chromatogram and the calibration factor R_f using formula (1):

$$m_{\text{styrene 28}} = \frac{m_{\text{decane}} \cdot A_{\text{styrene 28}}}{A_{\text{decane}} \cdot R_f} \quad (1)$$

The mass was then converted into the amount of substance *n* via Formula (4) to calculate conversion *X*, yield *Y,* and selectivity *S* of the hydrocyanation according to formulas (2-5):

$$n_{\text{styrene 28}} = \frac{m_{\text{styrene 28}}}{M_{\text{styrene 28}}} \quad (2)$$

$$X = \frac{n_{\text{styrene 28}}}{n_{0,\text{styrene 28}}} \quad (3)$$

$$Y = \frac{n_{\text{niriles}}}{n_{0,\text{styrene 28}}} \quad (4)$$

$$S = \frac{Y}{X} \quad (5)$$

5.11.5 Calculation of *TON*

$$TON = \frac{n_{nitrileproduct}}{n_{\text{catalyst}}} \quad (6)$$

5.11.6 Calculation of TOF_{20}

Turn-Over-Frequency was determined at a conversion of 20%. Time when conversion is exactly 20% in calculated based on a fit.

$$TOF_{20} = \frac{0.2\, n_{0,\text{styrene 28}}}{n_{\text{catalyst}} \cdot t} \quad (7)$$

6 References

1. Bini, L.; Müller, C.; Vogt, D. Ligand development in the Ni-catalyzed hydrocyanation of alkenes. *Chem. Commun.* **2010**, *46* (44), 8325–8334.
2. H. P. Latscha, U. Kazmeier, H. A. Klein. *Organische Chemie*:*Chemie-Basiswissen II*; Springer, 2008.
3. Brown, E. S.; Rick, E. A. Catalytic addition of hydrogen cyanide to non-activated olefins. *J. Chem. Soc. D* **1969** (3), 112b.
4. Taylor, B. W.; Swift, H. E. The addition of hydrogen cyanide to α-olefins catalyzed by nickel(0) complexes. *J. Catal.* **1972**, *26* (2), 254–260.
5. Bini, L.; Pidko, E. A.; Müller, C.; van Santen, R. A.; Vogt, D. Lewis acid controlled regioselectivity in styrene hydrocyanation. *Chem. Eur. J.* **2009**, *15* (35), 8768–8778.
6. Bohnet, M.; Ullmann, F., Eds. *Ullmann's encyclopedia of industrial chemistry*, 6., compl. rev. ed.; WILEY VCH, 2003.
7. van Leeuwen, P. W. N. M. *Homogeneous Catalysis*:*Understanding the Art*; Kluwer Academic Publishers, 2004.
8. Bini, L.; Müller, C.; Vogt, D. Mechanistic Studies on Hydrocyanation Reactions. *ChemCatChem* **2010**, *2* (6), 590–608.
9. Slotta, K. H. Bromcyan und wasser-freie Blausäure. *Ber. Dtsch. Chem. Ges. B* **1934**, *67* (6), 1028–1030.
10. Egekeze, J. O.; Oehme, F. W. Cyanides and their toxicity: A literature review. *Vet Q* **1980**, *2* (2), 104–114.
11. Vogel, S. N.; Sultan, T. R.; Eyck, R. P. ten. Cyanide poisoning. *Clinical Toxicology* **1981**, *18* (3), 367–383.
12. Luxon, S. *Hazards in the chemical laboratory*, 5. ed.; Royal Soc. of Chemistry, 1992.
13. B. Ballantyne. *Toxicology of cyanides*; Wright, 1987.
14. Falk, A.; Göderz, A.-L.; Schmalz, H.-G. Enantioselective nickel-catalyzed hydrocyanation of vinylarenes using chiral phosphine-phosphite ligands and TMS-CN as a source of HCN. *Angew. Chem. Int. Ed.* **2013**, *52* (5), 1576–1580.
15. Nemoto, K.; Nagafuchi, T.; Tominaga, K.; Sato, K. Efficient nickel-catalyzed hydrocyanation of alkenes using acetone cyanohydrin as a safer cyano source. *Tetrahedron Lett.* **2016**, *57* (29), 3199–3203.
16. Baker, M. J.; Harrison, K. N.; Orpen, A. G.; Pringle, P. G.; Shaw, G. Chelating diphosphite complexes of nickel(0) and platinum(0): their remarkable stability and hydrocyanation activity. *J. Chem. Soc., Chem. Commun.* **1991**, *12* (12), 803.
17. Yu, R.; Rajasekar, S.; Fang, X. Enantioselective Nickel-Catalyzed Migratory Hydrocyanation of Nonconjugated Dienes. *Angew. Chem. Int. Ed.* **2020**, *59* (48), 21436–21441.
18. Yu, R.; Xing, Y.; Fang, X. Regio-, Chemo-, and Enantioselective Ni-Catalyzed Hydrocyanation of 1,3-Dienes. *Organic letters* **2021**, *23* (3), 930–935.
19. Gao, J.; Ni, J.; Yu, R.; Cheng, G.-J.; Fang, X. Ni-Catalyzed Isomerization-Hydrocyanation Tandem Reactions: Access to Linear Nitriles from Aliphatic Internal Olefins. *Org. Lett.* **2021**, *23* (2), 486–490.
20. Gao, J.; Jiao, M.; Ni, J.; Yu, R.; Cheng, G.-J.; Fang, X. Nickel-Catalyzed Migratory Hydrocyanation of Internal Alkenes: Unexpected Diastereomeric-Ligand-Controlled Regiodivergence. *Angew. Chem. Int. Ed.* **2021**, *60* (4), 1883–1890.
21. Wang, G.; Xie, X.; Xu, W.; Liu, Y. Nickel-catalyzed highly regioselective hydrocyanation of alkenes with $Zn(CN)_2$. *Org. Chem. Front.* **2019**, *6* (12), 2037–2042.
22. Reisenbauer, J. C.; Finkelstein, P.; Ebert, M.-O.; Morandi, B. Mechanistic Investigation of the Nickel-Catalyzed Transfer Hydrocyanation of Alkynes. *ACS Catal.* **2023**, *13* (17), 11548–11555.

23. Fang, X.; Yu, P.; Morandi, B. Catalytic reversible alkene-nitrile interconversion through controllable transfer hydrocyanation. *Science* **2016**, *351* (6275), 832–836.
24. Reisenbauer, J. C.; Bhawal, B. N.; Jelmini, N.; Morandi, B. Development of an Operationally Simple, Scalable, and HCN-Free Transfer Hydrocyanation Protocol Using an Air-Stable Nickel Precatalyst. *Org. Process Res. Dev.* **2022**, *26* (4), 1165–1173.
25. Goertz, W.; Keim, W.; Vogt, D.; Englert, U.; Boele, M. D. K.; van der Veen, L. A.; Kamer, P. C. J.; van Leeuwen, P. W. N. M. Electronic effects in the nickel-catalysed hydrocyanation of styrene applying chelating phosphorus ligands with large bite angles. *J. Chem. Soc., Dalton Trans.* **1998** (18), 2981–2988.
26. A. Hewat. Zerovalent Nickel Complexes as Catalysts in the Hydrocyanation and Isomerization of functionalized Olefins. Dissertation, RWTH Aachen, Aachen, 2000.
27. Goertz, W.; Kamer, P. C. J.; van Leeuwen, P. W. N. M.; Vogt, D. Application of chelating diphosphine ligands in the nickel-catalysed hydrocyanation of alk-l-enes and ω-unsaturated fatty acid esters. *Chem. Commun.* **1997**, *16* (16), 1521–1522.
28. Falk, A.; Cavalieri, A.; Nichol, G. S.; Vogt, D.; Schmalz, H.-G. Enantioselective Nickel-Catalyzed Hydrocyanation using Chiral Phosphine-Phosphite Ligands: Recent Improvements and Insights. *Adv. Synth. Catal.* **2015**, *357* (14-15), 3317–3320.
29. Anastas, P. T.; Warner, J. C. *Green chemistry*:*Theory and practice*, 1. paperback; Oxford University Press, 2000.
30. Freixa, Z.; van Leeuwen, P. W. N. M. Bite angle effects in diphosphine metal catalysts: steric or electronic? *Dalton Trans.* **2003** (10), 1890–1901.
31. Kranenburg, M.; Kamer, P. C. J.; van Leeuwen, P. W. N. M.; Vogt, D.; Keim, W. Effect of the bite angle of diphosphine ligands on activity and selectivity in the nickel-catalysed hydrocyanation of styrene. *J. Chem. Soc., Chem. Commun.* **1995** (21), 2177–2178.
32. Göthlich, A. P. V.; Tensfeldt, M.; Rothfuss, H.; Tauchert, M. E.; Haap, D.; Rominger, F.; Hofmann, P. Novel Chelating Phosphonite Ligands: Syntheses, Structures, and Nickel-Catalyzed Hydrocyanation of Olefins. *Organometallics* **2008**, *27* (10), 2189–2200.
33. Clevenger, A. L.; Stolley, R. M.; Staudaher, N. D.; Al, N.; Rheingold, A. L.; Vanderlinden, R. T.; Louie, J. Comprehensive Study of the Reactions Between Chelating Phosphines and $Ni(cod)_2$. *Organometallics* **2018**, *37* (19), 3259–3268.
34. E. Billig; A. G. Abatjoglou; D. R. Bryant. Transition Metal Complex Catalyzed Processes. 12,329.
35. Cuny, G. D.; Buchwald, S. L. Practical, high-yield, regioselective, rhodium-catalyzed hydroformylation of functionalized α-olefins. *J. Am. Chem. Soc.* **1993**, *115* (5), 2066–2068.
36. Moasser, B.; Gladfelter, W. L.; Roe, D. C. Mechanistic Aspects of a Highly Regioselective Catalytic Alkene Hydroformylation using a Rhodium Chelating Bis(phosphite) Complex. *Organometallics* **1995**, *14* (8), 3832–3838.
37. Kiedorf, G.; Hoang, D. M.; Müller, A.; Jörke, A.; Markert, J.; Arellano-Garcia, H.; Seidel-Morgenstern, A.; Hamel, C. Kinetics of 1-dodecene hydroformylation in a thermomorphic solvent system using a rhodium-biphephos catalyst. *Chem. Eng. Sci.* **2014**, *115*, 31–48.
38. Zhang, B.; Jiao, H.; Michalik, D.; Kloß, S.; Deter, L. M.; Selent, D.; Spannenberg, A.; Franke, R.; Börner, A. Hydrolysis Stability of Bidentate Phosphites Utilized as Modifying Ligands in the Rh-Catalyzed n -Regioselective Hydroformylation of Olefins. *ACS Catal.* **2016**, *6* (11), 7554–7565.
39. Tolman, C. A.; McKinney, R. J.; Seidel, W. C.; Druliner, J. D.; Stevens, W. R. Homogeneous Nickel-Catalyzed Olefin Hydrocyanation. In *Advances in Catalysis*; Eley, D. D., Pines, H., Weisz, P. B., Eds.; Academic Press, 1985; pp 1–46.

40. Tolman, C. A.; Seidel, W. C.; Druliner, J. D.; Domaille, P. J. Catalytic hydrocyanation of olefins by nickel(0) phosphite complexes - effects of Lewis acids. *Organometallics* **1984**, *3* (1), 33–38.
41. Ding, R.; Katebzadeh, K.; Roman, L.; Bergquist, K.-E.; Lindström, U. M. Expanding the scope of Lewis acid catalysis in water: remarkable ligand acceleration of aqueous ytterbium triflate catalyzed Michael addition reactions. *J. Org. Chem.* **2006**, *71* (1), 352–355.
42. Aplander, K.; Ding, R.; Lindström, U. M.; Wennerberg, J.; Schultz, S. Alpha-amino acid induced rate acceleration in aqueous biphasic Lewis acid catalyzed Michael addition reactions. *Angew. Chem. Int. Ed.* **2007**, *46* (24), 4543–4546.
43. Yamaguchi, A.; Matsunaga, S.; Shibasaki, M. Direct catalytic asymmetric Mannich-type reactions of gamma-butenolides: effectiveness of Brønsted acid in chiral metal catalysis. *Org. Lett.* **2008**, *10* (11), 2319–2322.
44. Yoon, T. P. Photochemical Stereocontrol Using Tandem Photoredox-Chiral Lewis Acid Catalysis. *Acc. Chem. Res.* **2016**, *49* (10), 2307–2315.
45. Reich, H. J. Role of organolithium aggregates and mixed aggregates in organolithium mechanisms. *Chem. Rev.* **2013**, *113* (9), 7130–7178.
46. Bauer, W.; Schleyer, P. v. R. Mechanistic evidence for ortho-directed lithiations from one- and two-dimensional NMR spectroscopy and MNDO calculations. *J. Am. Chem. Soc.* **1989**, *111* (18), 7191–7198.
47. O. Tai, R. Hopson, P. G. Williard. Aggregation and Solvation of n-Butyllithium. *Org. Lett.* **2017**, *19*, 3966–3969.
48. Amstutz, R.; Dunitz, J. D.; Seebach, D. Crystal structure of 2-Lithio-2-phenyl-1,3-dithiane-Tetrahydrofuran-Tetramethylethylenediamine (1/1/1); Electron-Density Difference Maps for Lithio-methyl- and Lithio-phenyl-dithiane. *Angew. Chem. Int. Ed. Engl.* **1981**, *20* (5), 465–466.
49. Benn, R.; Janssen, E.; Lehmkuhl, H.; Rufínska, A. 27Al-NMR-Spektroskopie zur Charakterisierung von Organoaluminium-Verbindungen. *J. Organomet. Chem.* **1987**, *333* (2), 155–168.
50. Behr, A.; Johnen, L. Myrcene as a natural base chemical in sustainable chemistry: a critical review. *ChemSusChem* **2009**, *2* (12), 1072–1095.
51. Foca, C. M.; Barros, H. J. V.; dos Santos, E. N.; Gusevskaya, E. V.; Carles Bayón, J. Hydroformylation of myrcene: metal and ligand effects in the hydroformylation of conjugated dienes. *New J. Chem.* **2003**, *27* (3), 533.
52. Behr, A.; Johnen, L.; Neubert, P. A sustainable route from the renewable myrcene to methyl ethersvia direct hydroalkoxylation. *Catal. Sci. Technol.* **2012**, *2* (1), 88–92.
53. Kampwerth, A.; Terhorst, M.; Kampling, N.; Vogt, D.; Seidensticker, T. Synthesis of biobased amines via Pd-catalysed telomerisation of the renewable β-myrcene in a water/ethanol multiphase system: catalyst recycling enabled by a self-separating product phase. *Green Chem.* **2023**, *25* (16), 6345–6354.
54. Behr, A.; Johnen, L.; Rentmeister, N. Novel Palladium-Catalysed Hydroamination of Myrcene and Catalyst Separation by Thermomorphic Solvent Systems. *Adv. Synth. Catal.* **2010**, *352* (11-12), 2062–2072.
55. Faßbach, T. A.; Gaide, T.; Terhorst, M.; Behr, A.; Vorholt, A. J. Renewable Surfactants through the Hydroaminomethylation of Terpenes. *ChemCatChem* **2017**, *9* (8), 1359–1362.
56. Behr, A.; Johnen, L.; Vorholt, A. J. Telomerization of Myrcene and Catalyst Separation by Thermomorphic Solvent Systems. *ChemCatChem* **2010**, *2* (10), 1271–1277.
57. Behr, A.; Johnen, L.; Wintzer, A.; Gümüş Çetin, A.; Neubert, P.; Domke, L. Ruthenium-Catalyzed Cross Metathesis of β-Myrcene and its Derivatives with Methyl Acrylate. *ChemCatChem* **2016**, *8* (3), 515–522.
58. Vogelsang, D.; Dittmar, M.; Seidensticker, T.; Vorholt, A. J. Palladium-catalysed carboxytelomerisation of β-myrcene to highly branched C 21 -esters. *Catal. Sci. Technol.* **2018**, *8* (17), 4332–4337.

59. Behr, A.; Johnen, L.; Wintzer, A.; Willstumpf, A.; Dinges, M. First methoxycarbonylation of the renewable β-myrcene: high selectivity through reduced isomerisation. *Catal. Sci. Technol.* **2013**, *3* (6), 1573.
60. Kronberg, B. *Surface chemistry of surfactants and polymers*; Wiley, 2014.
61. KEIM, W. Catalytic hydrocyanation of dienes and trienes. *J. Catal.* **1982**, *78* (1), 209–216.
62. Herrmann, N.; Vogelsang, D.; Behr, A.; Seidensticker, T. Homogeneously Catalyzed 1,3-Diene Functionalization – A Success Story from Laboratory to Miniplant Scale. *ChemCatChem* **2018**, *10* (23), 5342–5365.
63. Casey, C. P.; Whiteker, G. T.; Melville, M. G.; Petrovich, L. M.; Gavney, J. A.; Powell, D. R. Diphosphines with natural bite angles near 120.degree. increase selectivity for n-aldehyde formation in rhodium-catalyzed hydroformylation. [Erratum to document cited in CA117(3):25899x]. *Journal of the American Chemical Society* **1992**, *114* (26), 10680.
64. R. Bruening; K. E. Krakowiak. Compositions And Methods For Selectively Binding Amines Or Amino Acid Enantiomers Over Their Counter-Enantiomers:International.
65. Fazekas, E. Iron and Nickel Complexes as Catalysts in CO_2/Epoxide Coupling, Radical Polymerisation and Hydrocyanation Reactions. Dissertation, The University of Edinburgh, 2018. https://era.ed.ac.uk/handle/1842/35688.
66. Hopkins, H. P.; Jahagirdar, D. V.; Moulik, P. S.; Aue, D. H.; Webb, H. M.; Davidson, W. R.; Pedley, M. D. Basicities of the 2-, 4-, 2,4-di-, and 2,6-disubstituted tert-butylpyridines in the gas phase and aqueous phase: steric effects in the solvation of tert-butyl-substituted pyridines and pyridinium cations. *J. Am. Chem. Soc.* **1984**, *106* (16), 4341–4348.
67. Khalili, F.; Henni, A.; East, A. L. L. p Ka Values of Some Piperazines at (298, 303, 313, and 323) K. *J. Chem. Eng. Data* **2009**, *54* (10), 2914–2917.
68. Sicard, A. J.; Baker, R. T. Safe and Expeditious Preparation of $Ni(cod)_2$ for Same-Day High-Throughput Screening. *Org. Process Res. Dev.* **2020**, *24* (12), 2950–2952.
69. Jezorek, R. L.; Zhang, N.; Leowanawat, P.; Bunner, M. H.; Gutsche, N.; Pesti, A. K. R.; Olsen, J. T.; Percec, V. Air-stable nickel precatalysts for fast and quantitative cross-coupling of aryl sulfamates with aryl neopentylglycolboronates at room temperature. *Org. Lett.* **2014**, *16* (24), 6326–6329.
70. Vaultier, F.; Monteil, V.; Spitz, R.; Thuilliez, J.; Boisson, C. New insights on Ni-based catalysts for stereospecific polymerization of butadiene. *Polym. Chem.* **2012**, *3* (6), 1490.

7 Appendix

7.1 Temperature profiles

Temperature profiles were recorded with an EnviroPad-TC, whose temperature probe reached into the toluene through a pierced septum. This was cooled to a temperature of 50±2 °C using a cold bath (corresponds to the addition temperature for the HCN of the reaction mixtures) and then thawed to the corresponding reaction temperature (oil bath 90 °C / above the stirring plate, temperature in the fume cupboard: 22.4 °C). The temperature was recorded every 10 s.

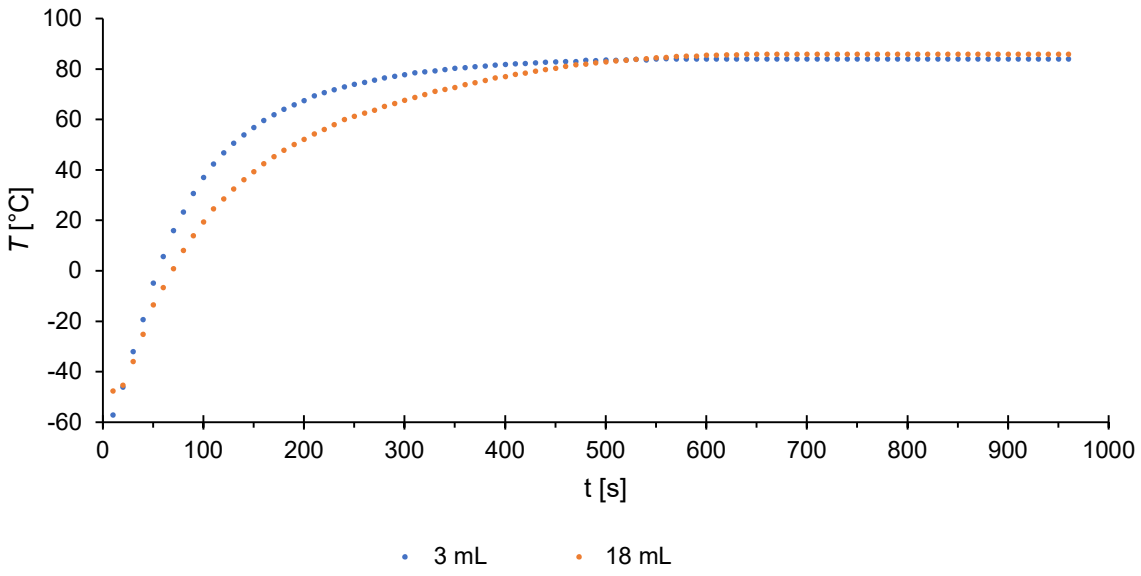

Figure 64: Heating profile of 3 mL and 18 mL batch sizes.

7.2 GC

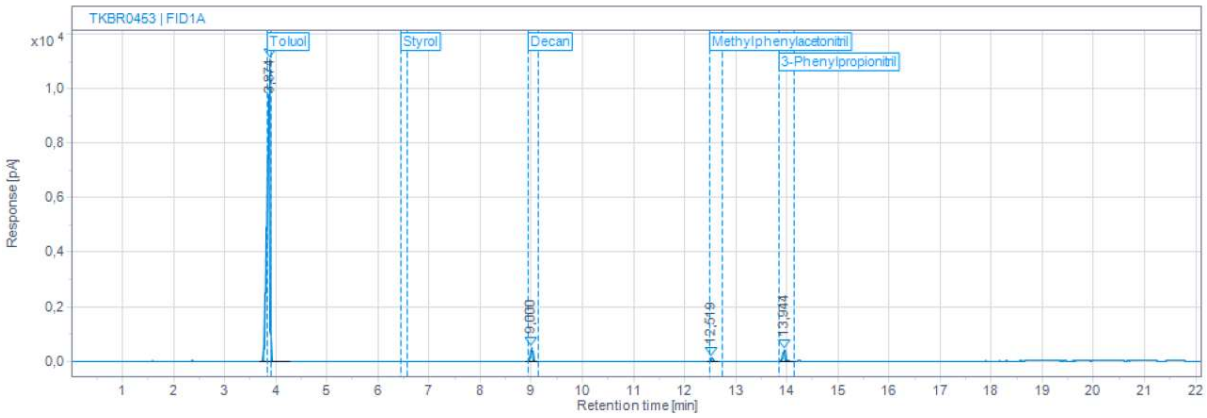

*Figure 65: Exemplary gas chromatogram of styrene **28** hydrocyanation using n-decane as the internal standard.*

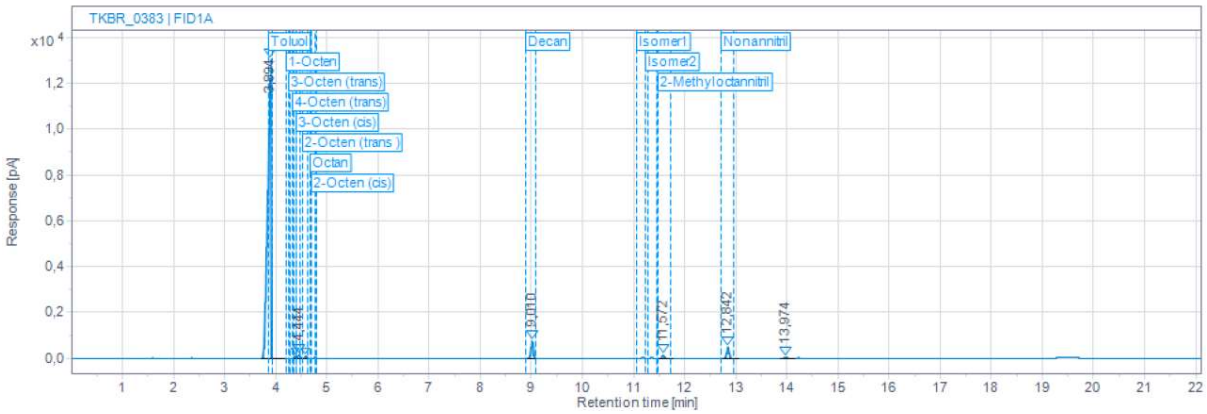

*Figure 66: Exemplary gas chromatogram of styrene **28** hydrocyanation using n-decane as the internal standard.*

7.3 NMR

7.3.1 $Ni(cod)_2$ **25**

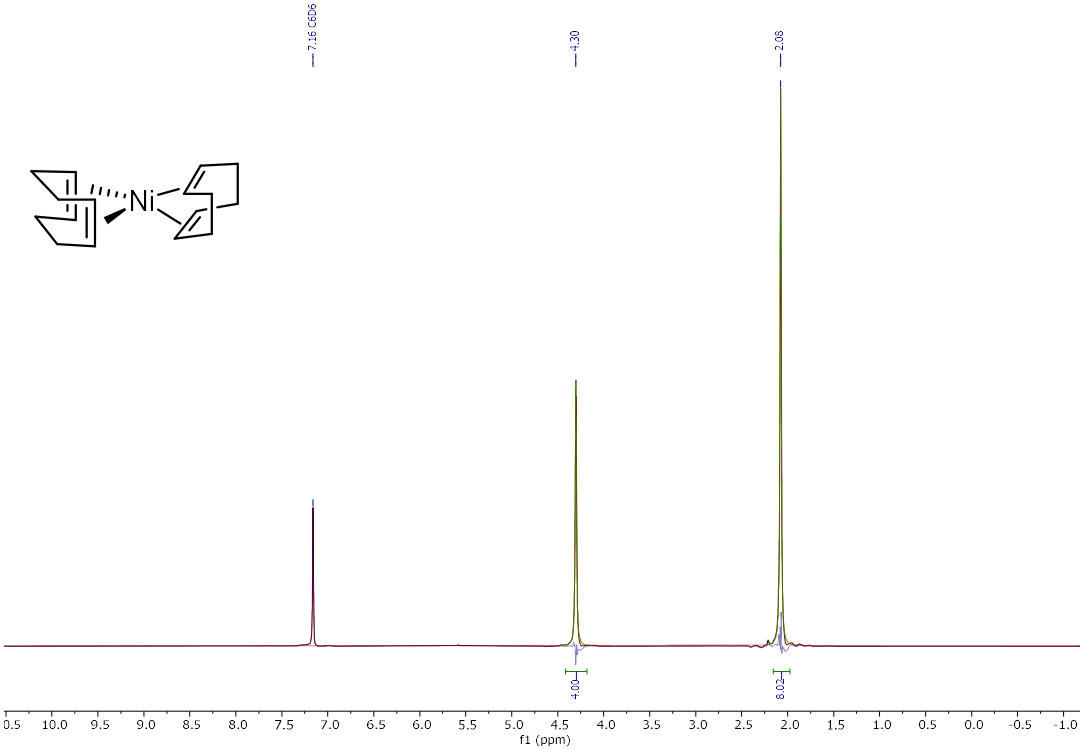

*Figure 67: ^{1}H-NMR spectrum of $Ni(cod)_2$ **25**.*

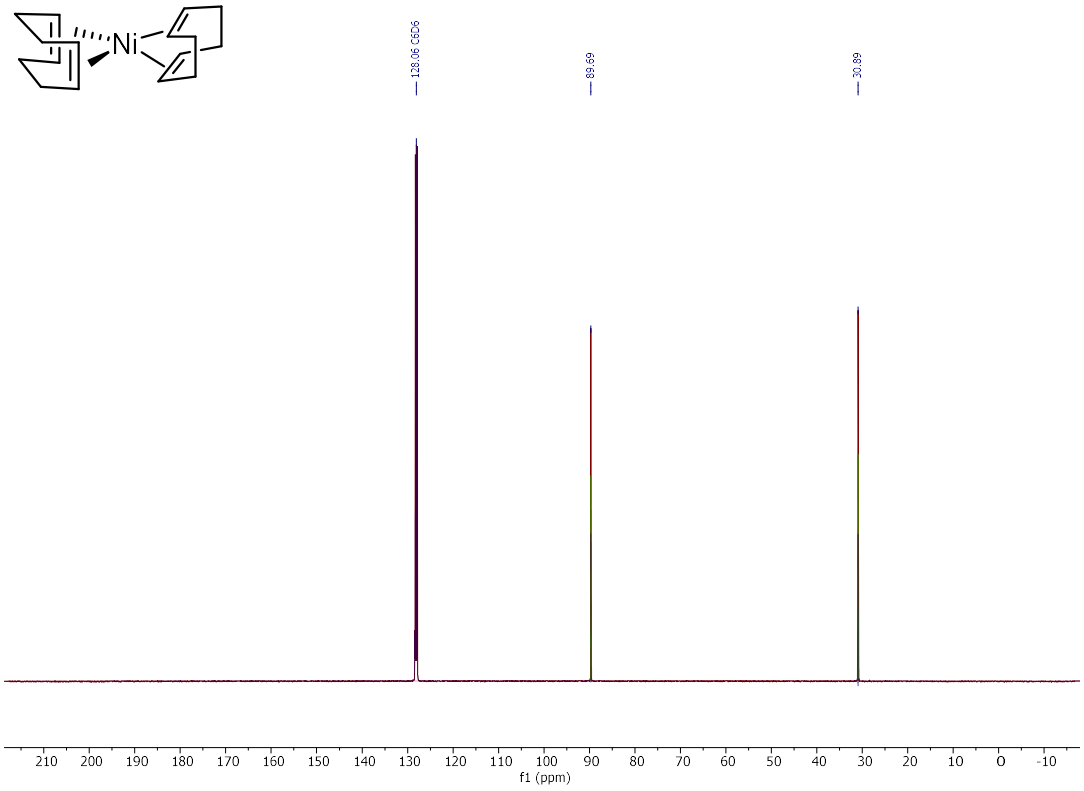

*Figure 68: ^{13}C-NMR spectrum of $Ni(cod)_2$ **25**.*

7.3.2 **94** and **93**

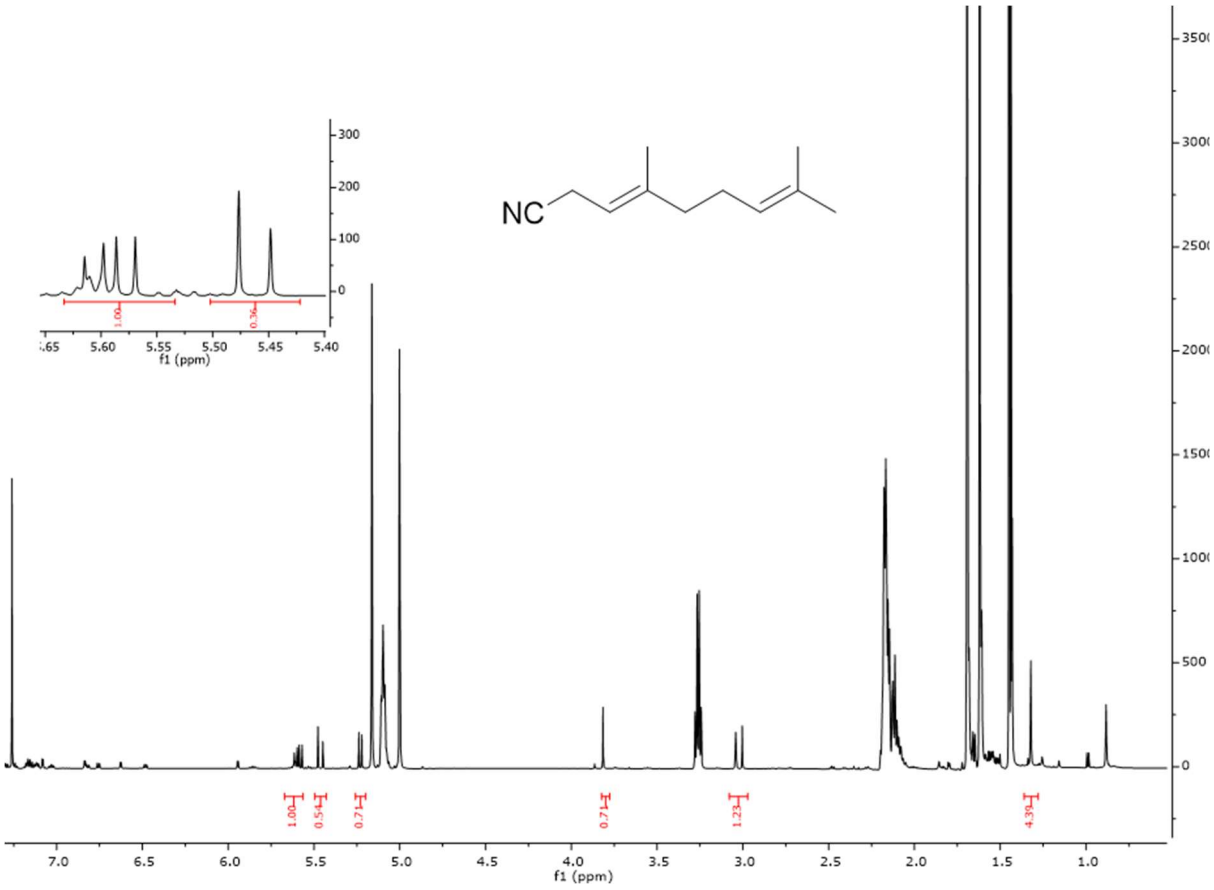

*Figure 69: ^{1}H-NMR spectrum of **94** and **93** with chemical shifts assigned to **94**.*

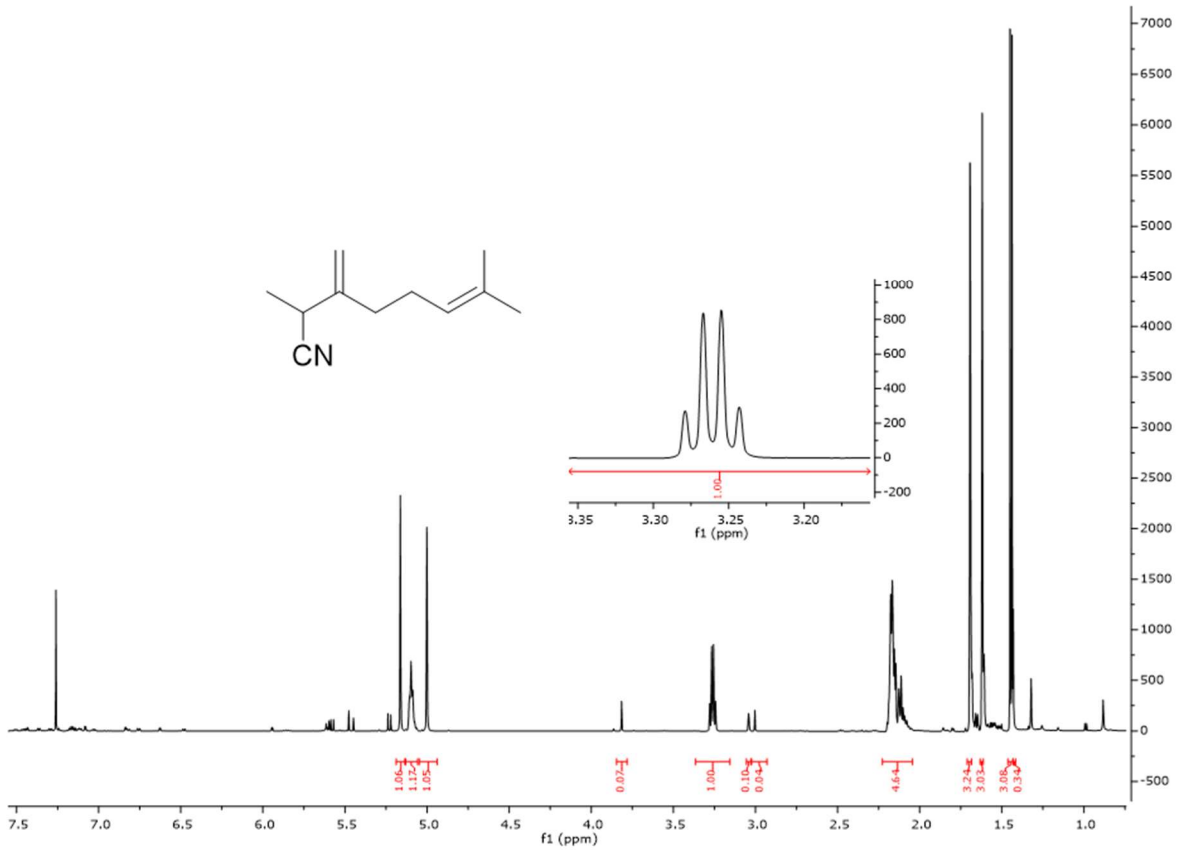

*Figure 70: ^{1}H-NMR spectrum of **94** and **93** with chemical shifts assigned to **93**.*

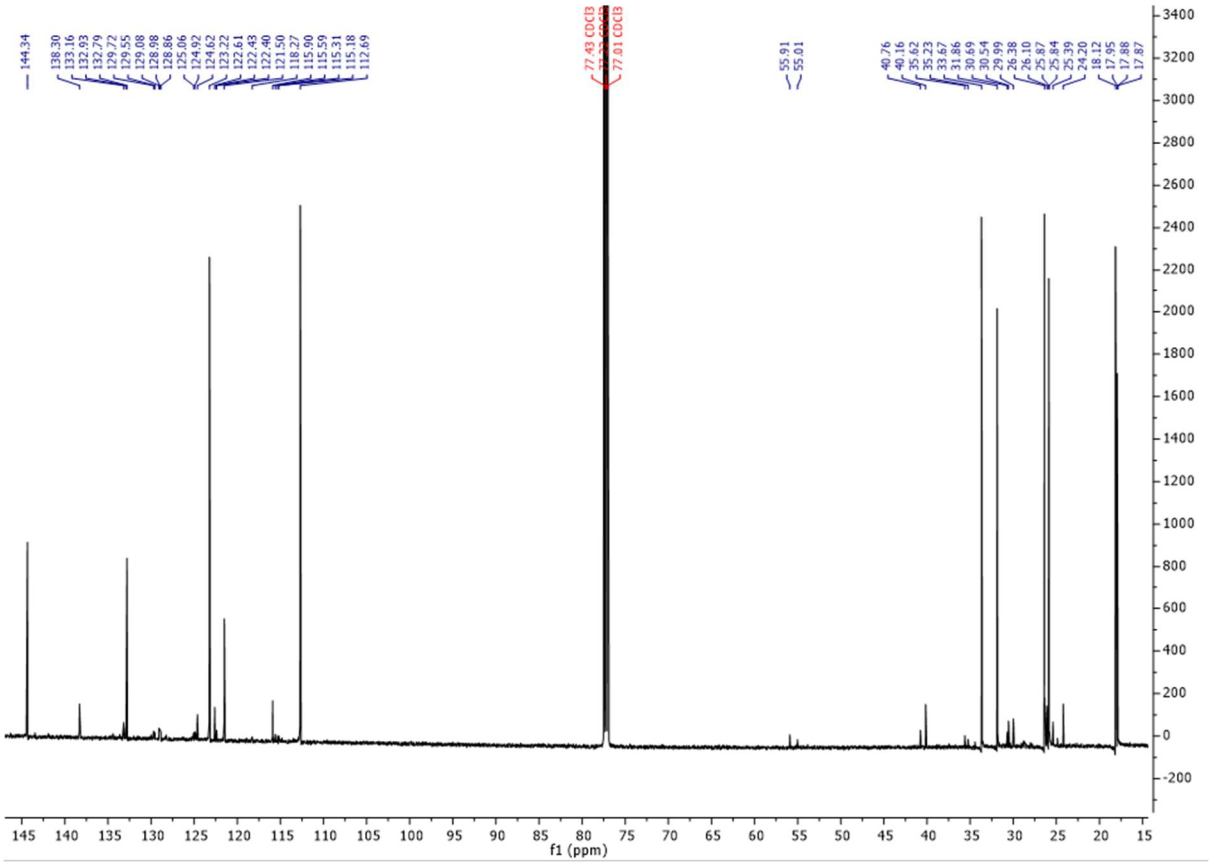

*Figure 71: ^{13}C-NMR spectrum of **94** and **93**.*

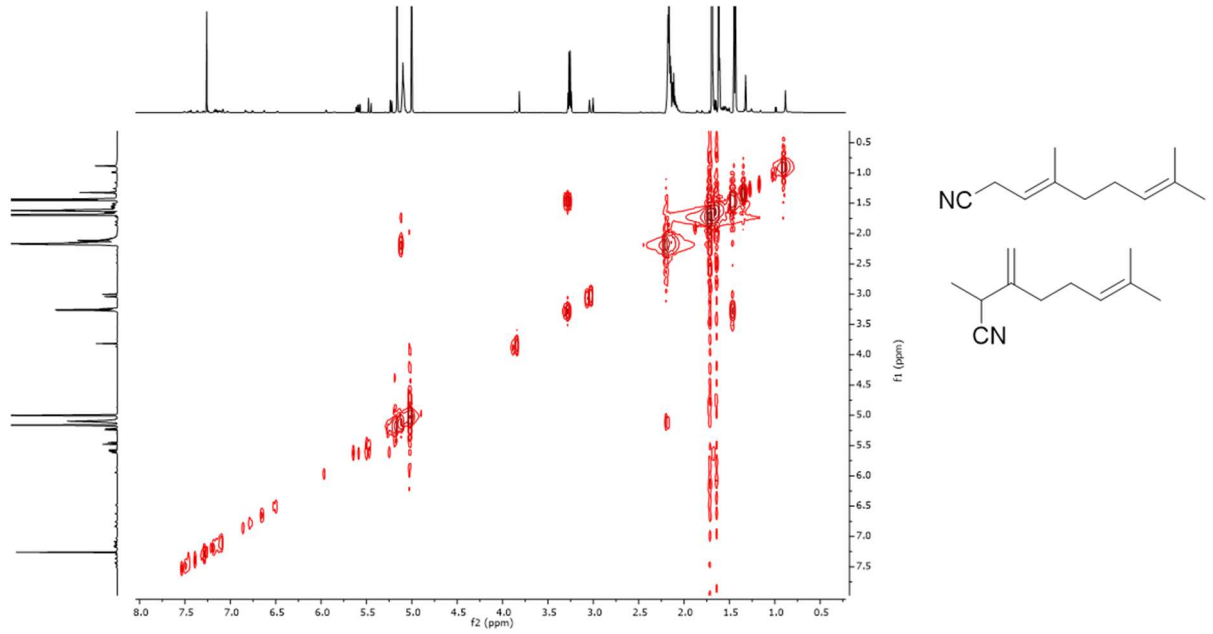

*Figure 72: COESY-NMR spectrum of **94** and **93**.*

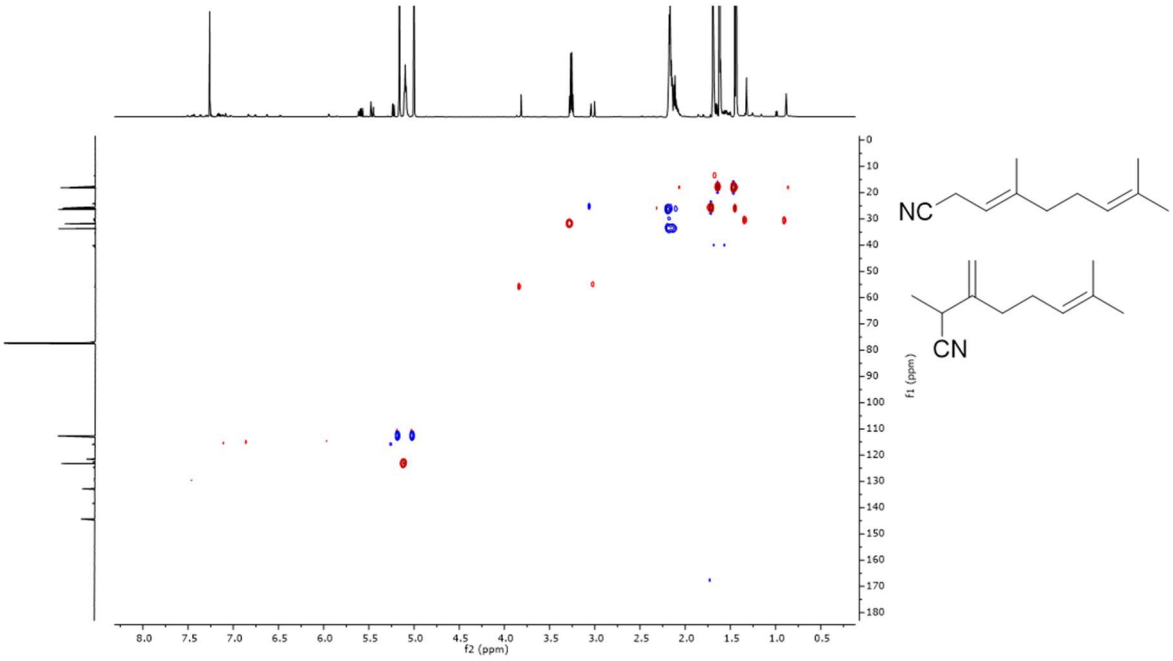

*Figure 73: HSQC-NMR spectrum of **94** and **93**.*

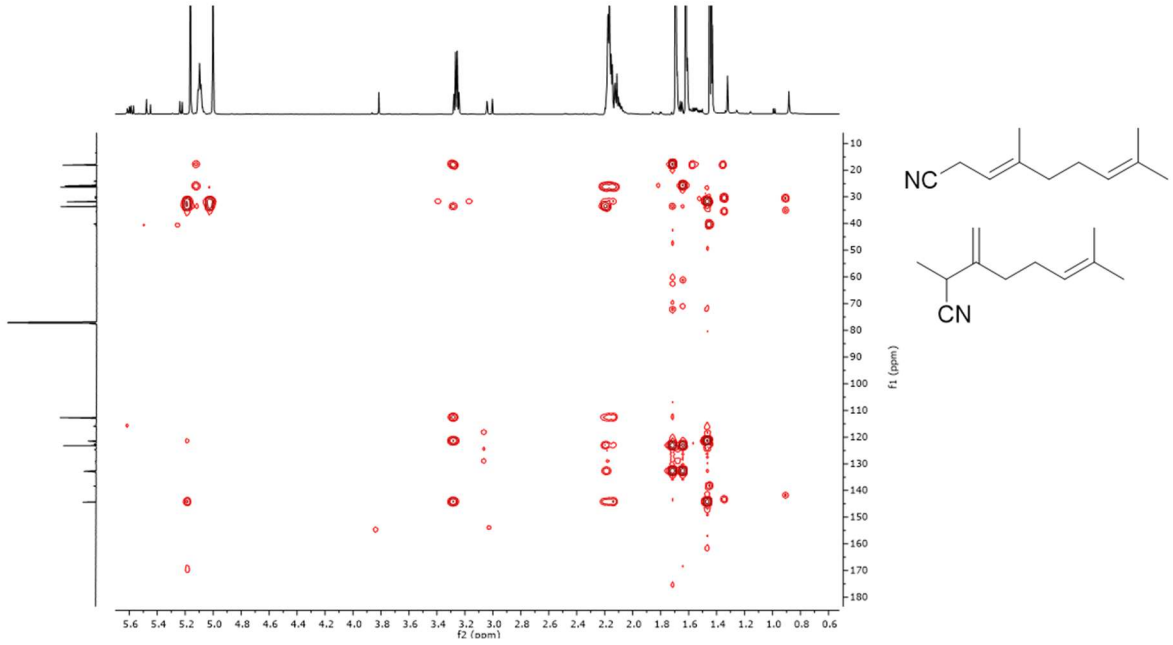

*Figure 74: HMBC-NMR spectrum of **94** and **93**.*

7.3.3 92

All signals that were already assigned to B were ignored in the following spectra.

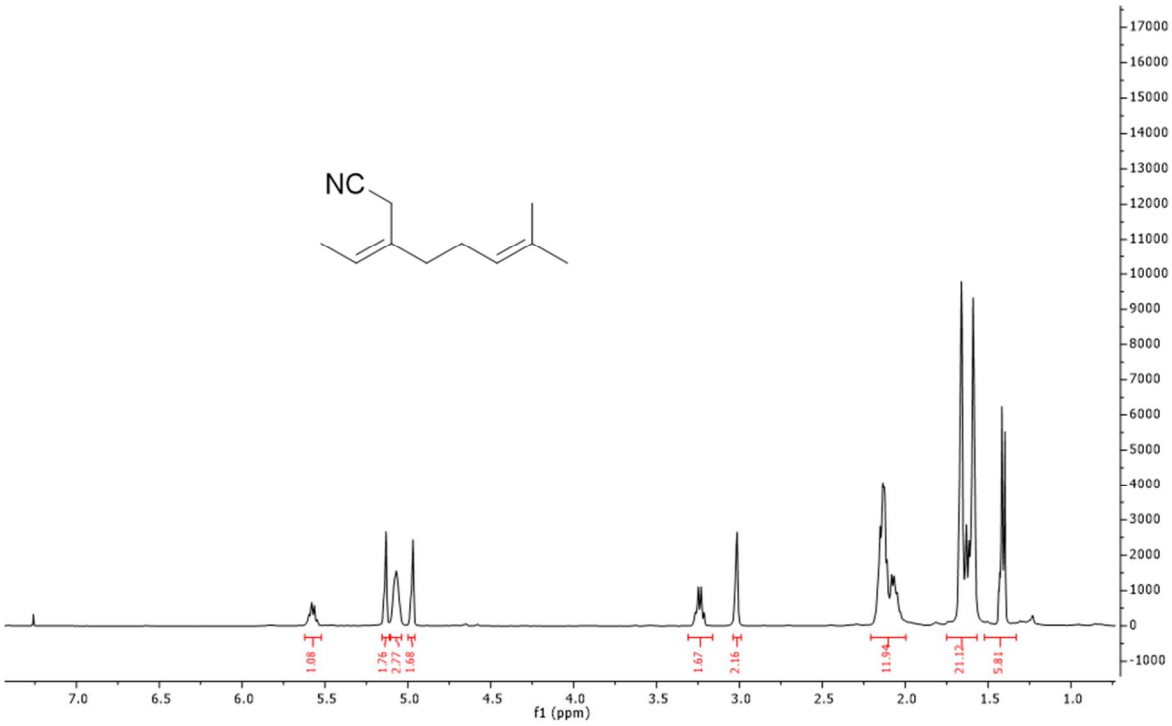

*Figure 75: [1]H-NMR spectrum of **92** with **93** present*

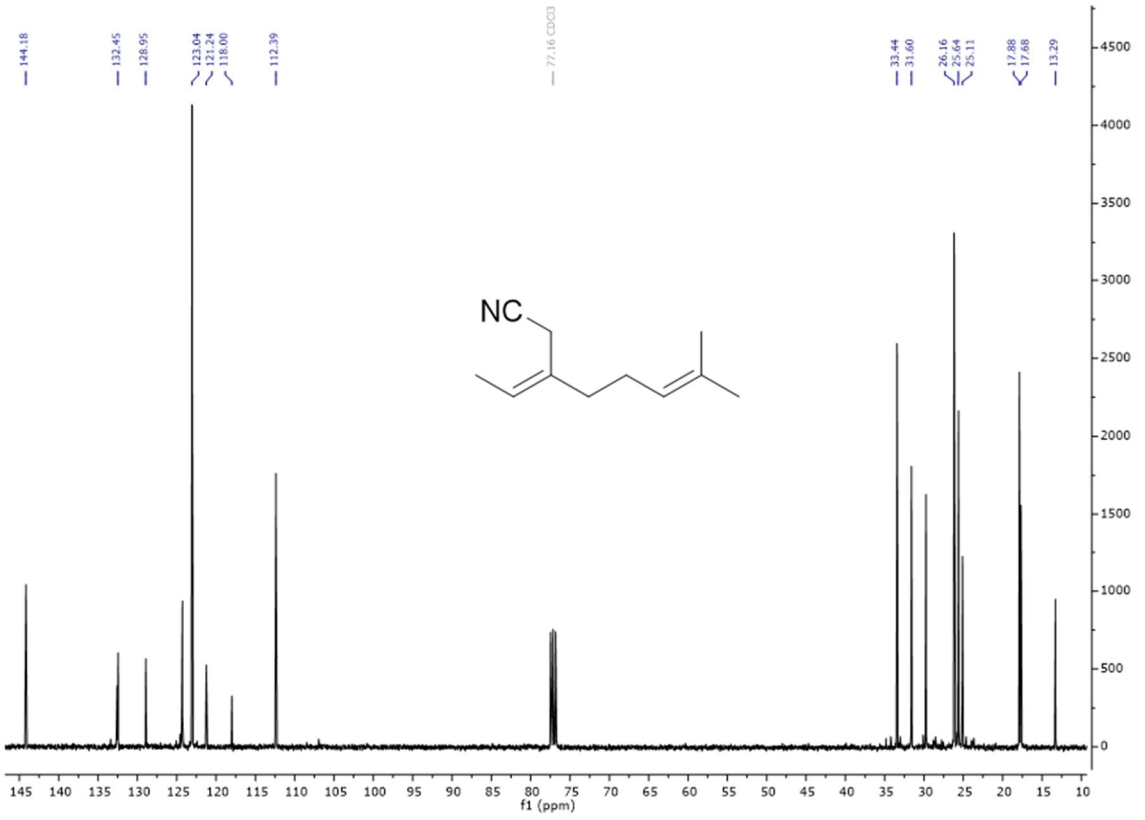

*Figure 76: [13]C-NMR spectrum of **92** with **93** present.*

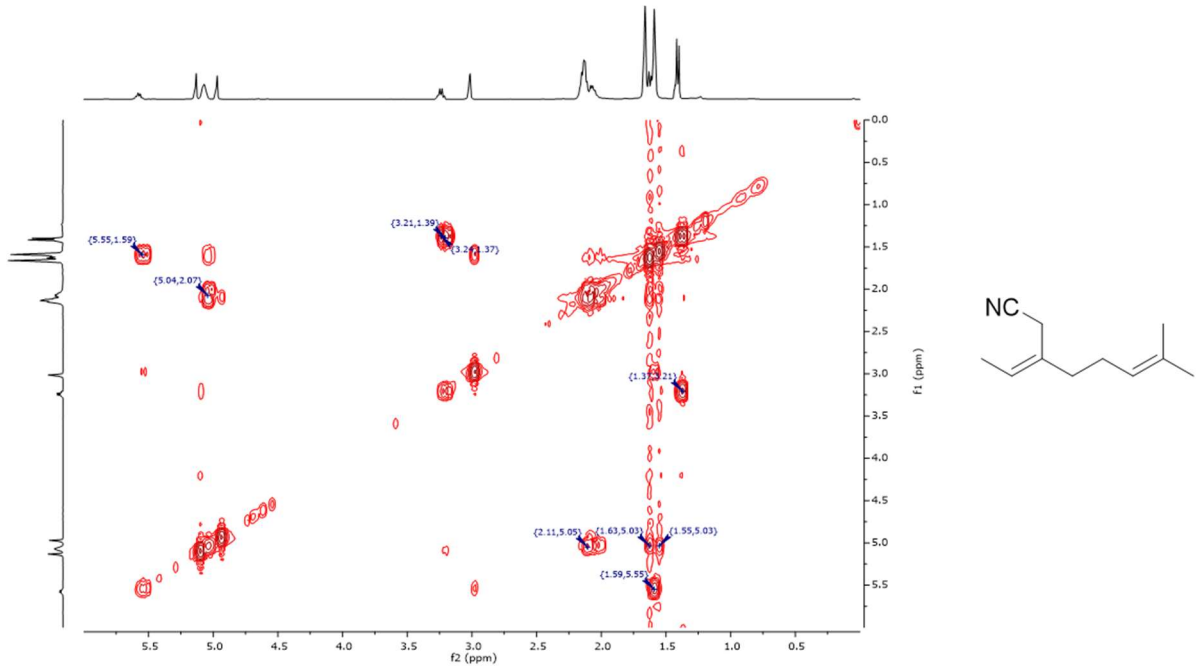

*Figure 77: COESY-NMR spectrum of **92** with **93** present.*

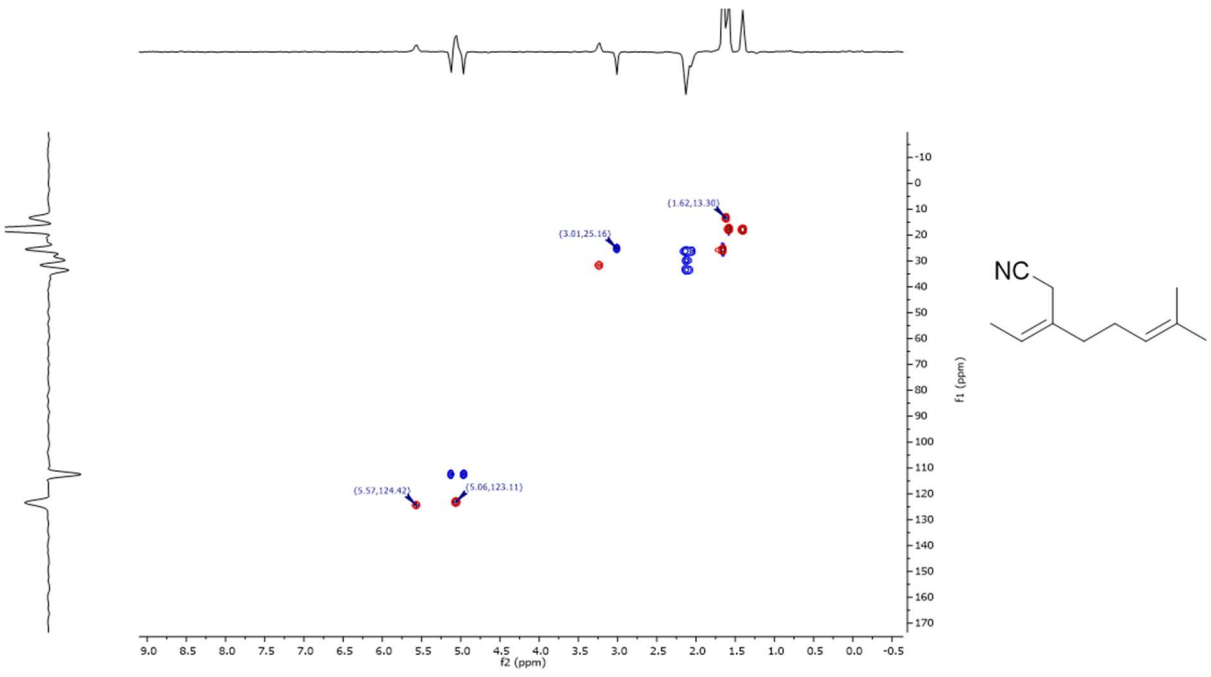

*Figure 78: HSQC-NMR spectrum of **92** with **93** present.*

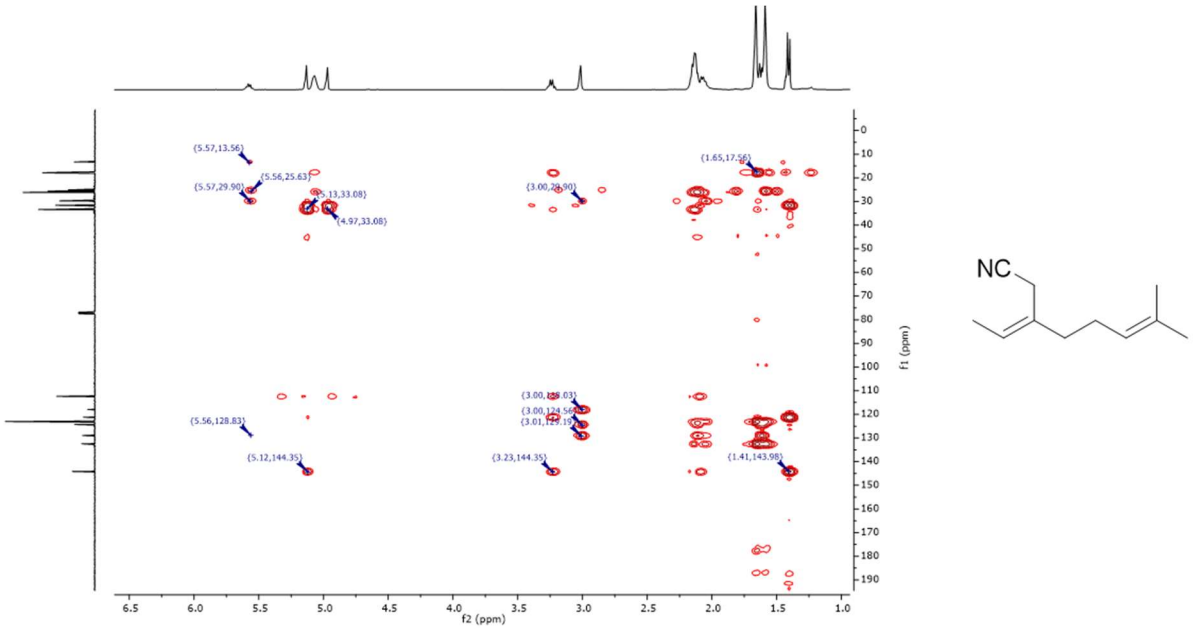

*Figure 79: HMBC-NMR spectrum of **92** with **93** present.*

7.4 List of tables

7.5 List of figures